The use of simple analytical techniques to assess surface oxidation of sulphide ores

Ayanda Sikhona Sibiya

A thesis submitted to the Faculty of Engineering and the Built Environment, University of Cape Town, in fulfilment of the requirements for the degree of Master of Science in Engineering, in Chemical Engineering

September 2022

Plagiarism declaration

I understand what plagiarism is and declare that all of the work in the document, save for that which is properly recognized, is mine. This thesis has been submitted to the Turnitin module, and I affirm that my supervisor has seen my report and that any issues raised by it have been addressed.

Signed by candidate

Ayanda Sikhona Sibiya

Acknowledgements

First and foremost, I would like to praise and thank God, the Almighty, who has given me countless blessings, wisdom, this opportunity, and guided me from the beginning of this research project till the end. I am truly grateful for His unconditional love and grace. Apart from my efforts, the success of this thesis is highly dependent on the support and guidance of many others. I would like to take this time to thank everyone who helped make this thesis a success.

- A/Prof Kirsten Corn, my primary supervisor. I can't thank you enough for your patience and support. I came into this program with a lot of doubts but because to your guidance, I've learnt to trust myself again. I appreciate your supervision, your accessibility, your concern for my welfare, and your insightful criticism. Thank you for providing a positive working environment where I can thrive and be myself.
- Dr Magreth Tadie and Ms Rešoketšwe Manenzhe, my co supervisors. Thank you very much for being incredible supervisors. Thank you for placing me on the right path and always pushing me to submit quality work. I appreciate the honesty and motivation from both of you very much. I especially appreciated Shokie's private motivational sessions when I needed them.
- I would also like to thank A/Prof Megan Becker for her assistance in making sense of some of the most important sections of my thesis.
- Thank you to everyone at the CMR, especially our laboratory manager, Shireen Govender, who made sure I had everything I needed for my work. Thank you for organizing all of the team building trips; they were quite beneficial. Thank you, Sir Monde Bekaphi, for your warm welcome and assistance with my milling curves when I first arrived. Thank you for all of the laughs and valuable conversations; I have no doubt that I was your favorite lol. Sir Kenneth Maseko, thank you for never tiring of my inexperience, even when I nearly burned down the department (over-exaggeration). Thank you, Refilwe Moalosi, for the lab training and for becoming my friend and confidant. LOL I honestly don't know what would have happened to me in that lab if it hadn't been for you. I owe you lunch.
- Thank you to my parents, Hayo and Stan, for allowing me to make such career decisions and for supporting me even when they don’t understand. I am today because you raised me to be a strong, independent woman with a healthy appetite for challenges. I am eternally grateful.
- Thank you to my brother and sister, Veli and Dido. Veli, for instilling in me as a child the belief that I can accomplish anything I set my mind to and for always wanting the best for me. You

are my oldest (and best) friend, and your help during this challenging time is greatly appreciated. Dido, thank you for being the best sister a girl could wish for. I adore our imperfect bond because I know you have my back no matter what and I have yours. I love you so much and it motivates me to know that you are proud of me.

- Thank you to my partner, Soso. Akhon'tungayaziyo Ta. Words honestly fail me. You have been a rock for me throughout this period and for the better part of my life. Thank you for the many sacrifices (big and small) that you do for me. Thank you for pushing me, even when I fought you for it. Thank you for being incredibly supportive. All I want is to be the same support structure for you.
- My fellow colleagues/peers. Guys your presence nje on its own motivated me. I wish you all the best in your respective careers.
- And finally, thank you to SAMMRI for providing financial assistance towards this research project and to my personal funding. I was comfortable throughout this period, which allowed me to focus solely on the research. Thank you to Heather Sundström for managing my finances throughout the duration of my studies at UCT.

Abstract

Surface oxidation is known to have a negative impact on the flotation performance of sulphide minerals. This is because severe oxidation makes it more difficult to process low-grade sulphide minerals, which reduces the recovery of valuable minerals during flotation. It may be possible to quantitatively correlate the rate/level of oxidation to oxidized sulphide ores using simple surface analytical techniques. This, if done well, could eliminate the need for numerous mineralogical tests, saving both time and money. This study investigated the Ethylenediaminetetraacetic acid (EDTA) Extraction Technique and Reactivity Number (RN) Technique as possible techniques to quantitatively describe oxidation levels in different ore types with different mineral compositions and grade. The aim was to determine if the changes in the surface character generated by oxidation are linked to a measurement obtained from the selected techniques. In the thesis, the techniques were validated on fresh ores of differing grades, Impala UG2 referred to as Ore A and High-grade copper ore referred to as Ore B. The two ores were ground to generate varying particle size distributions and liberation profiles to study the link between oxidation, particle size and liberation. Based on ore type and sulphide liberation, the tests attempted to provide an indicator of feed grade and surface oxidation. Flotation is used as a diagnostic tool. For Ore A, results showed that the grind size 60 % -75 μm yielded the highest Cu recovery, the coarsest grind size 40 % -75 μm yielded the second highest Cu recovery, and the grind 80 % -75 μm yielded the lowest Cu recovery. Overall, the Ore A results showed that where the grind sizes had high reactivity (high RN OCF) and high EDTA value, poor flotation recovery was observed and where the OCF and EDTA values were lower, favourable recoveries were obtained. EDTA and RN numbers therefore aided in giving an indication of the extent of oxidation that the ore had undergone, which ultimately translated to flotation recoveries. The grind size 80 % -75 μm had clearly suffered significantly more oxidation than the other grind sizes and this was indicated by the high OCF and the EDTA value and low Cu recoveries. The liberated Base Metal Sulphides (BMS) for Ore B was generally consistent throughout the three grind sizes, however, the highest Cu recovery was achieved by the grind size 80 % -75 μm (95.11 %), followed by grind sizes 60 % -75 μm and 40 % -75 μm respectively (92.25 % and 90.86 %). The recovery of this ore increases as the grind size becomes finer. Ore B demonstrated that, while the OCF and EDTA value for ore B increased as the grind size became finer, so did the recovery. It is possible that the particles that were ground to achieve particle size 80 % -75 μm were at their most hydrophobic state, owing to the increased liberation of the BMS, particularly chalcopyrite.

Glossary

CMR	Centre for Minerals Research
C1	first concentrate (with C2 being the second, C3 being the third, etc.)
DOW 200	DOW froth 200
mL	Millilitres
Mg/L	Milligrams per litre
g	grams
Cu	Copper
Ni	Nickel
Fe	Iron
BMS	Base Metal Sulphides
ICP-OES	inductively coupled plasma optical emission spectrometry
XRD	X-Ray Diffraction
QEMSCAN	Quantitative Evaluation of Minerals by Scanning Electron Microscopy
EDTA	Ethylenediaminetetraacetic acid
RN	Reactivity Number
OCF	Oxygen consumption Factor
Eh	Pulp Redox Potential
OD	Oxygen Demand
60% -75 µm	60% passing 75 µm

Contents

List of Figures

List of Tables

1. Introduction

1.1. Background

Froth flotation is a separation method based on exploiting differences in surface properties of minerals to effect separation between valuable and gangue minerals. It is used to recover both primary and secondary copper sulphides, as well as related precious metals, such as gold, from raw ores (Schulze, 1984). In recent years, froth flotation has enabled the extraction of low-grade and complex ore deposits that would have otherwise been considered uneconomic.

Various chemical and physical processes that cause alteration to the mineral surface are at work during flotation, and oxidation is one of them. Sulphide minerals oxidize when exposed to air and aqueous solutions during storage, crushing and grinding (Moimane et al., 2020). Sulphide mineral surfaces are prone to oxidation because they are semiconductors and are typically more reactive and the oxidizing impact of ambient oxygen on sulphide minerals is difficult to control (Zhao and Peng, 2012). The increased surface chemical alterations are indicated by a larger amount of oxidation products, e.g., hydroxide species, being present on mineral surfaces (Parker et al., 2015). According to Fuerstenau et. al (1991), the separation efficiency of froth flotation is determined by the degree of hydrophobicity obtained by the valuable minerals, with hydrophobicity of some minerals being determined by the adsorption of the targeted flotation reagents, such as collectors and depressants.

Researchers commonly use two qualitative phrases to characterize the stage or amount of oxidation, “moderate or mild oxidation” and “excessive oxidation”. These terms inform us whether that level is beneficial to mineral recovery or destructive to the process. For instance, “moderate or mild oxidation” is important in flotation because it alters the surface properties of sulphide minerals, increasing their hydrophobicity and the differences can then be exploited by flotation (Moimane et al., 2020). It produces a surface rich in hydrophobic polysulphides and certain metal hydroxides (Zhao and Peng, 2012).

However excessive surface oxidation, in which mineral recoveries have decreased due to the degree to which the surfaces have been oxidized, increases ore variability and complicates the processing of accessible lower-grade ores. This is because excessive oxidation produces large amounts of metal and hydrophilic sulphur oxidation products with high valency on mineral surfaces (Tolley et al., 1996). It causes certain collectors to have difficulty accessing sulphide minerals, which reduces the sensitivity of the process as well as the flotation recovery of valuable minerals. This makes oxidation one of the most serious problems confronting the minerals processing sector (Kelebek, 1993; Smart, 1991; Newell et al., 2006a; Guy and Trahar, 1985).

The properties of mineral surfaces can be determined using surface characterisation techniques (Bicak, 2019); these techniques include, but are not limited to, Scanning Auger Microscopy (SAM), Camsizer, X-ray Photoelectron Spectroscopy (XPS), Scanning Tunnelling Microscopy (STM), Atomic Force Microscopy (AFM), Scanning Electron Microscopy (SEM) and the recent application of Time-of-Flight Secondary Ion Mass Spectrometry (ToF-SIMS) (Roger et al., 2003). These techniques measure the shape, chemical, physical, and micromechanical properties, composition, and chemical states of any solid surface (Smart et al.,2007). These techniques have established their importance in several scientific fields through the characterisation of oxidation products and their statistical distribution on mineral surfaces (Bicak, 2019).

Much research has focused on the "moderate" and "excessive oxidation" terms, but few have attempted to quantify these qualitative phrases. This may be due to a variety of factors, one of which being the high cost and the inaccessibility of the techniques needed to research oxidation. Numerous studies have also used surface techniques (such as XPS) to address surface oxidation. However, there has been a lag in applying the findings and contributions that come from the studies because of complexities that are associated with using such surface characterisation techniques. This is because these techniques require complex sample preparation protocols, and the level of analysis and data interpretation requires expert knowledge. This has created a gap between research and industry because the solutions from these techniques are hard to implement in the industry. New innovative devices, as well as easy-to-do methods and affordable techniques for mineral processing, are increasingly adopted to improve performance in processing the now dominant low-grade ores (King, 2001).

As the mining sector faces the challenge to develop innovative, cost-effective, and environmentally safe methods, it is also important to improve existing techniques that are pivotal in processing sulphide minerals. One such existing technique is Reactivity Number determination (RN). RN contributes to the characterisation of minerals by measuring the reactivity of different minerals in sulphide ores. Studies such as that by Owusu et al., (2013) have demonstrated that minerals can react differently to air, or more specifically, oxygen. The technique was used in this study to quantify the different reactivities of minerals present in two different ores of differing grades by monitoring variations in their dissolved oxygen decay rates and how that can be linked to chemical and mineralogical composition. Differences in oxygen consumption of minerals can be related to the differences in their mineralogical characteristics. Their oxygen uptake can be used to quantify the reactivity number of varying ores (Becker et al., 2010).

The metal ions that arise from the oxidation of sulphides and grinding media are typically determined using the ethylenediaminetetraacetic acid (EDTA) extraction technique. EDTA is a polyamine carboxylic acid that can form complexes with the metal species of the oxidation products of sulphide minerals (e.g., hydroxides, carbonates and sulphates) without reacting with the metal sulphides (Rumball and Richmond, 1996). It can be used to selectively leach the metal oxides, away from sulphide mineral surfaces when the pH is conditioned between 7 and 11, and enough time is given for the extraction to occur (Bicak, 2019). According to Bicak (2019), the EDTA extraction technique is typically more suited and effective in plant-scale measurements than the conventional techniques stated above.

The EDTA and RN techniques were chosen for this study mainly because they do not require specialized expertise, the techniques are convenient and can be used by anyone. The EDTA and RN techniques were also chosen because they could potentially give a response that can be related to the current state of oxidation of the ore as well as the rate of oxidation should the ore be refreshed in some way, most commonly through regrinding. This would not only quantify the “moderate oxidation” and “excessive oxidation” but also eliminate numerous mineralogical tests, thus saving time and being cost effective. While some literature considers these techniques (Bicak, 2019; Owusu et al., 2013; He et al., 2006; (Becker et al., 2010); Peng et al., 2003; Goktepe and Williams, 1995), majority of the research is done on pure minerals and the techniques still need to be validated on real ores.

Therefore, this study aims to investigate the capabilities of the chosen techniques in dealing with different ore types that have different mineral compositions and grade. The study seeks to establish whether the alterations that occur on minerals caused by oxidation in various stages of mining e.g., in-situ, in the reef or post-mining can be related to a level or rate of oxidation, using such simple surface analytical techniques.

1.2. Overall scope and approach

This study aims to validate whether simple, low-cost techniques can be used to give an indication of surface oxidation for varied ore types (UG2, known as Ore A in this thesis and HG Cu known as Ore B in this thesis). The technical methods, EDTA and RN, will be used to predict the level of surface oxidation. The study will be conducted as follows:

- Two standard ore samples with varying feed grades will be considered under three different grind sizes, thus varying liberation profiles. This study will validate the two techniques to see whether they give values that makes sense using sulphide ores and the chosen techniques. This is because although EDTA and RN techniques have been validated on minerals, the techniques still need to be validated on real ores. The experiments attempt to give an

indicator of feed grade and the potential for surface oxidation based on ore type and sulphide mineral liberation.

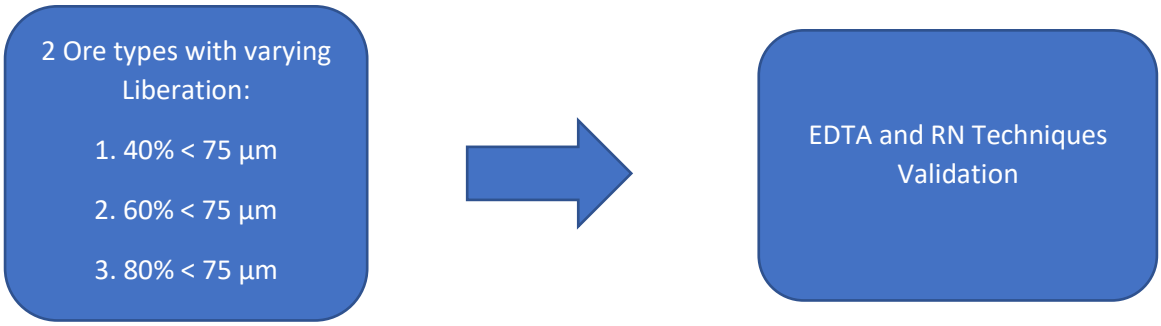

Figure 1.1: Brief experimental procedure to illustrate the structure of the investigation.

2. Literature Review

2.1. Generic Ore Oxidation (Introduction)

This chapter provides a critical synthesis of the literature relevant to the scope specified in Chapter 1. The oxidation of sulphide minerals will be thoroughly examined and related to the processes that ores go through that oxidize sulphide minerals, such as storage, crushing, grinding, and flotation. Following a general overview of the fundamentals of froth flotation, both the EDTA and RN procedures will be critically examined because the purpose of this study is to investigate the capabilities of the two techniques in dealing with different ore types (HG Cu and UG2) with varying mineral compositions and grades.

2.1.1. Stockpiling

In the mining industry, stockpiles are ore or mineral accumulations formed when demand falls or when the treatment plant or beneficiation equipment is incapable of handling the mine production; any heap of material formed to build a reserve for loading or other uses (Gruner et al., 2006). Stockpiles can also form from waste and low-grade materials that were considered invaluable when mining occurred. The grade that distinguishes between ore and waste is known as the cutoff grade (Kasmaee et al., 2018). The ore in the deposit with a grade greater than the cutoff grade is transported to the processing plant, while the material with a grade lower than the cutoff grade is transported to the waste collection (Dagdelen, 1992). However, because of the increasing metal demand and the mining industry depleting in-situ reserves, stockpiles are now considered as valuable ore reserves.

The surface properties of this material are, however, not the same as when they were discarded. It is expected that there is a level of variability as a result of temperature changes, oxidation and other processes that would, in turn, hinder their flotation response and alter the environment (Nordstrom, 2011). Re-mining from stockpile material has led to considerations regarding the characterisation of the mineral grade found in stockpiles. Over time the cut-off grades have become dynamic, implying that although the low-grade ore found in stockpiles was once uneconomic to process, it now contains metal grade that is high enough to warrant secondary mining and refining (Kasmaee et al., 2018; King, 2001).

Ore materials that consisted of a stockpile undergo weathering and oxidation over time, as a result of oxygen, water and solutes being transported within the stockpile. This results in the formation of oxidation products such as brochantite $CH_4(OH)6SO_4$ that are found on the surface of oxidised copper within the stockpile (Figure 2.1) (Nordstrom, 2011). In dry seasons the pH increases, resulting

in the precipitation of ferric iron species which gets washed off into water pathways (Garvie et al., 2008).

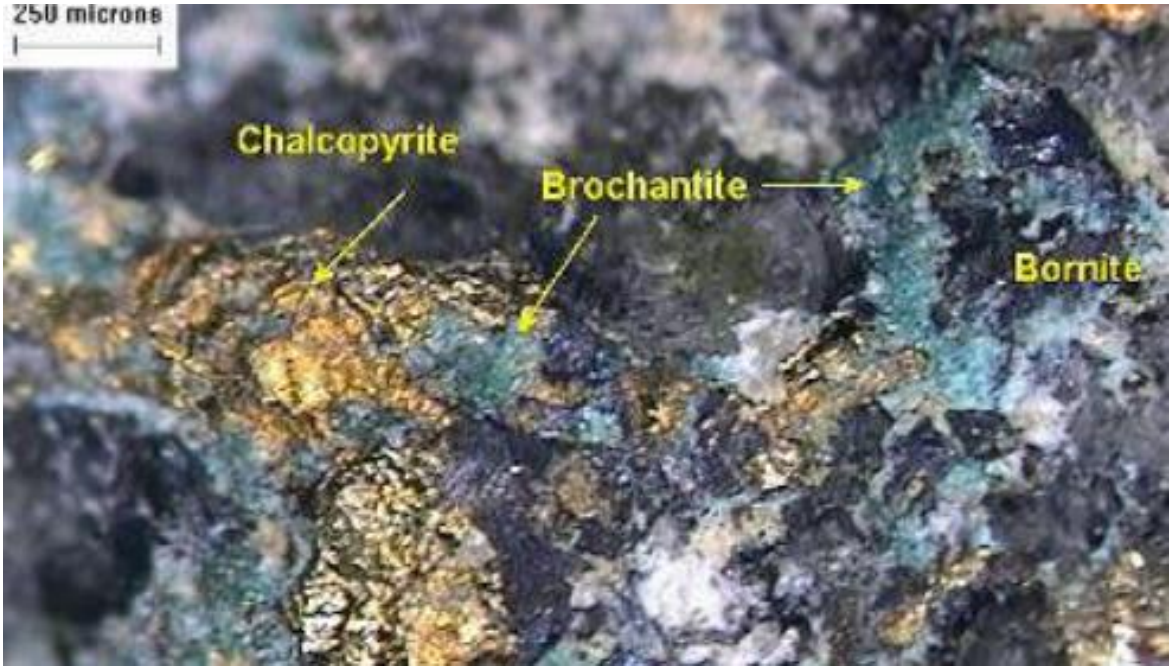

Figure 2.1: Photo taken by Garvie et al. (2008), showing Brochantite that is precipitated on the surface of chalcopyrite.

2.1.2. Water Effect on oxidation

Studies such as those by Nordstrom (2011), Mills (1985); Caruccio et al. (1989) and Winland et al. (1991) mention acid mine drainage as one of the major environmental problems linked to surface mining and sulphide mineral oxidation. This occurs when the minerals are removed from the earth's crust and brought to the surface where they are exposed to the atmosphere in the presence of water, forming drainage that is usually acidic and toxic to the environment (Nordstrom, 2011). The general term for this water is acid-rock drainage and is called acid mine drainage when it originates from mining activities (Nordstrom and Alpers, 1999). Acid-rock drainage is produced by numerous chemical and microbiological processes within a complex hydrogeological environment (Nordstrom, 2011).

The water that is affected by this process can be highly variable in its physicochemical characteristics but is typically highly acidic and has high concentrations of SO_4^{2-}, Fe and other heavy metals (Monterroso and Macias, 1998). Although a lot has been written on this topic, the oxidation of sulphides and its effect on water is a complex subject and its effects vary enormously between different sites and under different conditions.

Two factors affect the generation of acid drainage, namely high precipitation and the presence of a large surface area where streams intercept and are exposed, the two of which favour the oxidation of

sulphides (Monterroso and Macias, 1998). The production and dissemination of acidic streams in the landfill zone cause an issue for land recovery as it interferes with vegetation, resulting in the vegetation disappearing (Gil Bueno et al., 1990).

Monterroso and Macias (1998) investigated the composition of drainage water of the As Puentes lignite mine dump located in Galicia, Spain. The water analysis results showed that the Eh–pH and ionic concentrations were highly variable, and this illustrated the assorted variety of geochemical conditions in the drainage systems. The geochemical conditions also have a few attributes which contrasted notably from those of natural waters. These characteristics were said to be caused by the process of sulphide oxidation, which affects, to a greater or lesser extent, all the waters analysed.

Acid mine drainage (AMD)

AMD is a worldwide environmental issue where waste rock on the earth's surface pollutes the surface water, making the water more acidic and metal rich (Abrosimova et al., 2015). This takes place as a result of a chemical reaction that occurs between surface water and rocks containing sulphur-bearing minerals (Johnson and Hallberg, 2005). It occurs when carbonates and silicates that are contained in stockpiles and mine waste fail to neutralize the acidity produced by the sulphide oxidation (Abrosimova et al., 2015). Johnson (2003), in his study, stated that AMD is mainly caused by the accelerated oxidation of iron pyrite and other sulphide minerals that are present in a stockpile or waste rock when they are exposed to oxygen and water which often occurs during mining and mineral processing.

2.1.3. Temperature effect on oxidation

Natural temperature effect

Stockpiles can generate heat and develop temperature gradients which in turn influence the gas distribution and the oxidation rates (Garvie et al., 2008). The oxygen is naturally transported from the surface to the interior of a stockpile through diffusion and convection or advection (Garvie et al., 2008). Oxidation of ore materials in a stockpile depends on the history (time) and the rate at which oxygen and heat are transported to the various places within the stockpile. The oxidation rate depends on the characteristics of the sulphides as well as the conditions that they are subjected to e.g. oxygen concentration and temperature (Garvie et al., 2008).

Temperature effects controlled in the lab by heating.

Sulphide ores naturally oxidise over a long period. For instance, the Merensky ores oxidised over 1 billion years (Newell et al., 2006a). It is almost impossible to replicate this level of oxidation. However, there have been methods that are used by researchers such as Newell et al. (2006a) that have investigated the formation of oxidised layers within sulphide minerals within a practical

timeframe. Studies such as those by Wang et al. (2005) and Zhu et al. (2012) used isothermal conditions to oxidise pure pentlandite. They crushed and ground their samples into fine particles and then put them in a pre-heated oven that was at 700°C. The studies then followed a series of oxidation periods that ranged between 10 minutes and 24 hours, until their mineral samples were oxidised. During the oxidation of pentlandite, the iron moves to the surface of the mineral and is oxidised, forming a dense layer of oxide that surrounds the core (Zhu et al., 2012). Some studies discovered that using the "low-temperature thermal approach" gave results that were closer to natural oxidation. Forsmo (2005) artificially oxidised their magnetite sample at 130 °C over 48 hours. Newell et al. (2006a) heated their samples at 85 °C with circulated air (duration was not specified). The samples that were oxidised at lower temperatures showed results that were similar to those reported by Wang et al. (2005) and Zhu et al. (2012). Iron and sulphur (oxidation products) coated the surface of the minerals present, while within the sulphide minerals, sulphur and iron were depleted (Newell et al. (2006a). Steger (1982) studied the oxidation of sulphide minerals (particularly pyrrhotite) at temperatures ranging from 28 to 50 degrees Celsius and discovered that as the temperature increased, so did the amount of ferrous iron on mineral surface.

The effect of pre-roasting

Roasting was initially a preliminary chemical step in the treatment and extraction of copper from chalcopyrite when using the pyrometallurgical route. This route has since been eliminated in the extraction of copper and lead because faster smelting and converting are more economic processes which were developed later (Shamsuddin et al., 1990). However, it still plays a pivotal role in the extraction of nickel from pentlandite, molybdenum from molybdenite and zinc from sphalerite (Shamsuddin et al., 1990).

Roasting occurs when large amounts of air that is often enriched with oxygen is introduced to sulphide mineral concentrates at high temperatures. After the oxygen comes in contact with sulphur (from the minerals), sulphur dioxide is formed. Oxidation must occur without smelting the charge and this helps prevent the reduction of particle surface–oxidizing gas contact area. Stirring the charge in some way always means the oxidising gas is distributed to all particle surfaces. The degree of sulphur removal is controlled by regulating the roaster's air supply and by the degree of affinity of the mineral elements for sulphur or oxygen (Shamsuddin et al., 1990). Roasting has been demonstrated to be the most effective method for destroying carbonaceous materials as well as oxidizing the sulphides generally associated with the ore and is commonly used (Afenya, 1991; Fernández et al., 2000).

2.2. Oxidation of Samples

2.2.1. Introduction: History

Oxidation is (generally) the chemical process of removing electrons from an atom or a group of atoms. There are two different types of oxidation, first is the well-known oxidation that occurs during weathering where there is an addition of oxygen, and the second is oxidation during anamorphism, which involves the elimination of hydrogen. The first destroys the primary minerals and forms new ones, while the second one merely modifies existing minerals without destroying them (Winchell, 1941). This section will focus on the first type of oxidation, which is the oxidation of one or more minerals.

When sulphide ores are exposed to weathering at the Earth's surface, either through natural processes or as a result of mining activities, they react with oxygen in the air and mineral oxidation occurs (Nordstrom, 2011). The recognition of the concept of oxidation dates back to the 1930s, where Taggart et al. (1930) wrote about the formation of coatings on sulphide mineral surfaces. Taggart et al. (1930) in their explanation, implied that the presence of the oxidation products affected mineral selectivity and flotation. DeBavay (1904) also wrote about the alkaline carbonates and bicarbonates and other impurities that were found on the surface of sphalerite and how these "impurities" interfered with the process of flotation. Scientists were aware that oxidation products existed, however, because they did not have the appropriate tools and solvents, they were unable to identify the species that were in small quantities (Steger., 1982).

A name "hydroxide" (which includes metal hydroxides, oxyhydroxides, hydrous oxides, etc.) was given to refer to the mixture of oxidation products that form on the mineral surfaces as a result of oxidation (Steger, 1982). Researchers that studied hydroxides in the 1990s confirmed that the presence of these products on mineral surfaces indeed hindered the flotation of valuable minerals during mineral processing (Kant et al., 1994). Surface oxidation has become one of the most important factors that influence the flotation selectivity and recovery in the processing of copper sulphide ores. This is because surface chemical reactions determine whether the "surface film" on the sulphide mineral will render it hydrophobic or hydrophilic (Kelebek, 1993).

2.2.2. The effect of oxidation on flotation behaviour

Nickel copper ores contain pentlandite, chalcopyrite, pyrrhotite as the dominant sulphide minerals and then pyrite and other sulphides in smaller amounts. As already discussed, Sulphide minerals' surfaces are very reactive, and they begin to oxidize as soon as they come into contact with water (Fullston et.al., 1999). They are subjected to surface oxidation as a result of various mining processes and this impact could deliver various outcomes depending on the factors. The factors include the grinding media used (stainless steel generates oxidising conditions which promote the formation of

hydrophobic surface species), reagents used, flotation stage, mineralogy and susceptibility to natural activation (Gokepte and Williams, 1995; Owusu et al., 2013; Kelebek, 1993). Oxidation of these surfaces is a significant phenomenon, particularly in the flotation process, where it impacts collector attachment and may decrease valuable mineral recovery and grade (Fornasiero et al., 1994). The oxidation of sulphide minerals may be studied using a variety of surface sensitive methods. One of the most powerful ex-situ methods, X-ray photoelectron spectroscopy (XPS), has been extensively employed to analyze processes happening at the mineral surface (Fullston et al., 1999).

Kelebek (1993) argued that low redox conditions dominate during the initial stages of flotation, which is why mineral selectivity is at its peak around this time, following the grinding operations. As flotation progresses, the hydrophobicity of the valuable minerals decreases and the unwanted minerals such as pyrrhotite (that contribute to environmental problems) become harder to depress resulting in a decrease in mineral sensitivity and recovery. This is caused by an increase in surface oxidation as the flotation process progresses, which proves that the effect of oxidation in the flotation process is complex as it can be both positive, (by increasing selectivity) (the separation between wanted and unwanted minerals), and negative (by depressing valuable minerals that were meant to float) (Peng, 2003; Kelebek, 1993).

A number of chemical processes control the surface characteristics of base metal sulphides during grinding, including oxidation of minerals and media, oxygen reduction, and galvanic coupling (Grano, 2009). Grinding not only reduces particle size and liberates minerals, but it also creates differential surface properties on valuable and gangue minerals, allowing for effective separation in subsequent separation processes such as flotation, which uses the difference in surface properties on valuable and gangue minerals to separate them. (Zhao and Peng, 2012).

Zhao and Peng (2012) looked into the mechanism behind the various interactions of chalcopyrite, a main copper sulphide mineral, and chalcocite, a secondary copper sulphide mineral, with bentonite, a clay mineral, during grinding with stainless steel medium. According to the findings, chalcocite was significantly oxidized during grinding whereas chalcopyrite was only marginally oxidized, indicating that chalcocite is more electrochemically active than chalcopyrite based on zeta potential measurements (Lascelles and Finch, 2002). More EDTA extractable copper ions were identified in chalcocite than chalcopyrite using the EDTA extraction technique. This meant that when chalcocite and chalcopyrite are crushed to the same grind size, chalcocite is the one that oxidizes the most. Chalcopyrite remained negatively charged after grinding due to differing extents of mineral surface oxidation, whereas chalcocite became positively charged after grinding, resulting in distinct

interactions with bentonite particles. Bentonite particles were repelled by chalcopyrite, but chalcocite attracted them.

2.2.3. The importance of pulp potential

Controlling pulp chemistry through redox potential in flotation is a significant and recognised practice in the industry. Studies by Goktepe and Williams (1995), Owusu et al. (2013) and He et al. (2006) have investigated how flotation performance and selectivity can be improved by optimizing pulp redox potential (Eh) and oxygen demand (OD). The main factors that affect these parameters are the mineralogy, electrochemical reactivity of sulphides and grinding media (Owusu et al. 2013).

Pulp potential has also proven useful in separating sulphide minerals that occur together. Cations that are created by sulphide oxidation may react in various ways in different systems. For instance, pyrite and pyrrhotite occur together in numerous significant ores and the galvanic interactions of the two minerals, as well as their impact on their floatabilities, have been explored by Nakazawa and Iwasaki (1985). The study by Nakazawa and Iwasaki (1985) demonstrated how the galvanic contact decreased the development of sulphate, hydroxide or oxide types of iron-on pyrrhotite, though such formations were expanded on pyrite. Chalcopyrite is also normally associated with pyrite in sulphide ores. Its separation from pyrite turns out to be progressively difficult especially when pyrite reports into the copper concentrate as a result of its accidental activation by copper released from chalcopyrite during grinding or conditioning (He et al, 2006). Results from He et al. (2006) showed that at a fixed Eh of 275 mV (SHE) zinc sulphate could be used to increase mineral recovery of chalcopyrite and pyrite by selectively depressing the flotation of pyrite. Mildly alkaline pH conditions resulted in the precipitation of zinc hydroxide on the minerals present. The effect of zinc hydroxide in the flotation was found to be more selective to pyrite than chalcopyrite, which made the surface of pyrite more hydrophilic, resulting in its depression (He et al., 2006).

The control of redox conditions is convoluted not just by the galvanic interactions between the various minerals in the ore but also the interactions between the minerals and the steel grinding media (Martin et al., 1991). Grinding conditions impact the resulting flotation recovery of sulphide minerals (Peng et al., 2003). The reducing conditions at a sulphide mineral surface made by the oxidation of steel grinding media result in a galvanic interaction which can obstruct the adsorption of the collector (Wills and Napier-Munn, 2006).

A study by Learnmont and Iwasaki (1984) looked at the interaction between galena and mild steel media. The results showed that oxidation products formed on the galena surface after the interaction with the media and this decreased the floatability of galena. Peng et al. (2003) also investigated the role that is played by grinding conditions in flotation. In their study, the floatability of chalcopyrite was

similarly adversely affected by the grinding media. The authors argued that the depression of chalcopyrite can be attributed to hydroxide species on chalcopyrite surface which are closely related to anodic iron oxidation (using mild steel grinding media). This was explained using a theory that stated: *"When two materials are coupled, the oxidation rate of the more active material will increase, and the oxidation rate of the less active material will decrease"* (Owusu et al., 2013).

The authors concluded that grinding conditions significantly affected the flotation of chalcopyrite. This impact was associated with the presence of iron oxidation species and metal deficient sulphide present on the chalcopyrite surface. Iron oxidation species from the grinding media played a predominant role in depressing chalcopyrite flotation, while the presence of metal-deficient sulphide improved chalcopyrite flotation.

Studies by Chander (1988), Woods (1987) have shown the possibility of floating sulphide minerals in the absence of collectors when the pulp potential is controlled to bring out certain favourable conditions. These studies imply that an oxidising potential is required for successful collector-less flotation. Sulphide minerals oxidize through a continuum of metal-insufficient sulphides of decreasing metal substance through to elemental sulphur. These sulphur-rich metal-insufficient zones can render the mineral hydrophobic, provided that the local conditions are such that the metal oxides/hydroxides formed by the reaction are solubilised (Wills and Napier-Munn, 2006). Buckley et al. (1985) studied the surface oxidation of galena, bornite, chalcopyrite and pyrrhotite and the authors learned that flotation of the minerals could be accomplished without the aid of collectors and confirmed that collectorless flotation is effective only under oxidising conditions.

2.3. The effect of comminution on oxidation

Minerals are mined out of the ground incorporated into valueless gangue materials. These minerals need to be liberated from the gangue before the separation of the value can occur, this can be achieved by comminution (Jankovic et al., 2006). Comminution progressively reduces ore material sizes from larger particle sizes to smaller particle sizes, by blasting, crushing and grinding (Jankovic et al., 2006).

Grinding liberates the valuable minerals by reducing the particle size, preparing the particles for froth flotation (Weiss, 1985). The grinding process initiates intensive interaction between minerals and grinding media, which in turn forms a complex physical and chemical system that causes various changes in particle size, pulp chemistry and surface chemistry of minerals (Hadizadeh et.al., 2017).

Ores get fractured and when the fractures occur, some of the energy that is stored is transformed into free surface energy, which becomes the potential energy of newly produced surfaces (Wills et al., 2016). The new and increased surface energy causes new surfaces to be more chemically active and

are often more susceptible to the action of flotation reagents (Wills et al., 2016). These surfaces also undergo oxidation more readily (Wills et al., 2016).

Over the past years, research has focused on the benefits and impacts within the comminution circuit and not so much on the effect comminution has on the mineral surface chemistry. For example, Andres et al. (2001) tested an electric device that commutes ore. The outcomes of his study demonstrated improved concentrate grades; even though the mineral recovery did not improve. It was presumed that the electrically broken-down metal was more liberated with less impure influences being recuperated into the concentrate. The study, however, did not investigate the surface chemistry changes that occur as a result of electrical comminution and the fact that the reductions in recovery could be due to oxidised valuable mineral surfaces.

Parker et al. (2015) investigated the effects of electrical comminution on the mineral liberation and surface chemistry of a porphyry-copper ore. The study argued that during comminution, the heat energy that is produced results in the surfaces of the mineral grains being exposed to highly oxidative conditions which change the overall surface chemistry. Electrical, more so than mechanical, comminution improves liberation and free surface area, however, it also affects the surface chemistry of minerals (Parker et al. 2015). Parker et al. (2015) concluded that both the recoveries and concentrate grades were higher in the SELFRAG electric comminution device compared to the mechanical comminution device. This was because of the improved mineral liberation that was obtained from electrical comminution. The results indicate that the surface oxidation that resulted from the SELFRAG comminution product had very little impact on the flotation response.

2.4. Ore types used in the study

2.4.1. The Bushveld Complex

Economic concentrations of PGM occur within three distinct horizons within the Bushveld Complex, these are the Merensky Reef, the Upper Group 2 (UG2) Chromitite and the Platreef (Anglo Platinum, 2009). The BIC is the largest, geologically unique igneous intrusion within the Earth's crust and is considered unique because of its size, mineral content and its layering (Anglo Platinum, 2009). Over the years, the igneous intrusion has been tilted and exposed as a result of erosion, revealing three separate segments known as the Western, Eastern and Northern limbs respectively (Anglo Platinum, 2009). The Merensky Reef and the UG2 Reef occur around the Eastern and Western limbs of the complex, while the Platreef is found only along the eastern edge of the Northern Limb. The Merensky Reef is silicate dominated and constitutes of pyroxene, feldspar, olivine and chromite, whereas the UG2 reef is oxide dominated with the following mineralogy: chromite, pyroxene and feldspar. The last reef, which is the Platreef is silicate dominated with pyroxene, feldspar, amphibole and carbonate (Anglo Platinum, 2009).

2.4.2. The UG2 Reef

The impala UG2 is a copper and nickel ore deposit that is the second most mined source of the platinum group elements (PGEs) in the Bushveld Complex after the Merensky reef (Anglo Platinum, 2009). This reef is located next to and parallel to the Merensky Reef, as shown in *Figure 2.2*.2 (Nel et al. 2004). The UG2 reef has always been an attractive source of the PGEs, but its extraction was delayed due to metallurgical difficulties (Nel et al. 2004). The mineralogy of the UG2 reef can be divided into three main mineralisation groups which are the chromite, the aluminium silicates and the sulphides.

The chromite minerals make up approximately 50% of the UG2 plant feed, while the silicates and the sulphides constitute approximately 24% and 0,2% respectively (Nel et al., 2004). The sulphides are the least dominant and they consist mainly of chalcopyrite, pentlandite and pyrrhotite constituting approximately 10%, 35% and 50% of the sulphide portion, respectively.

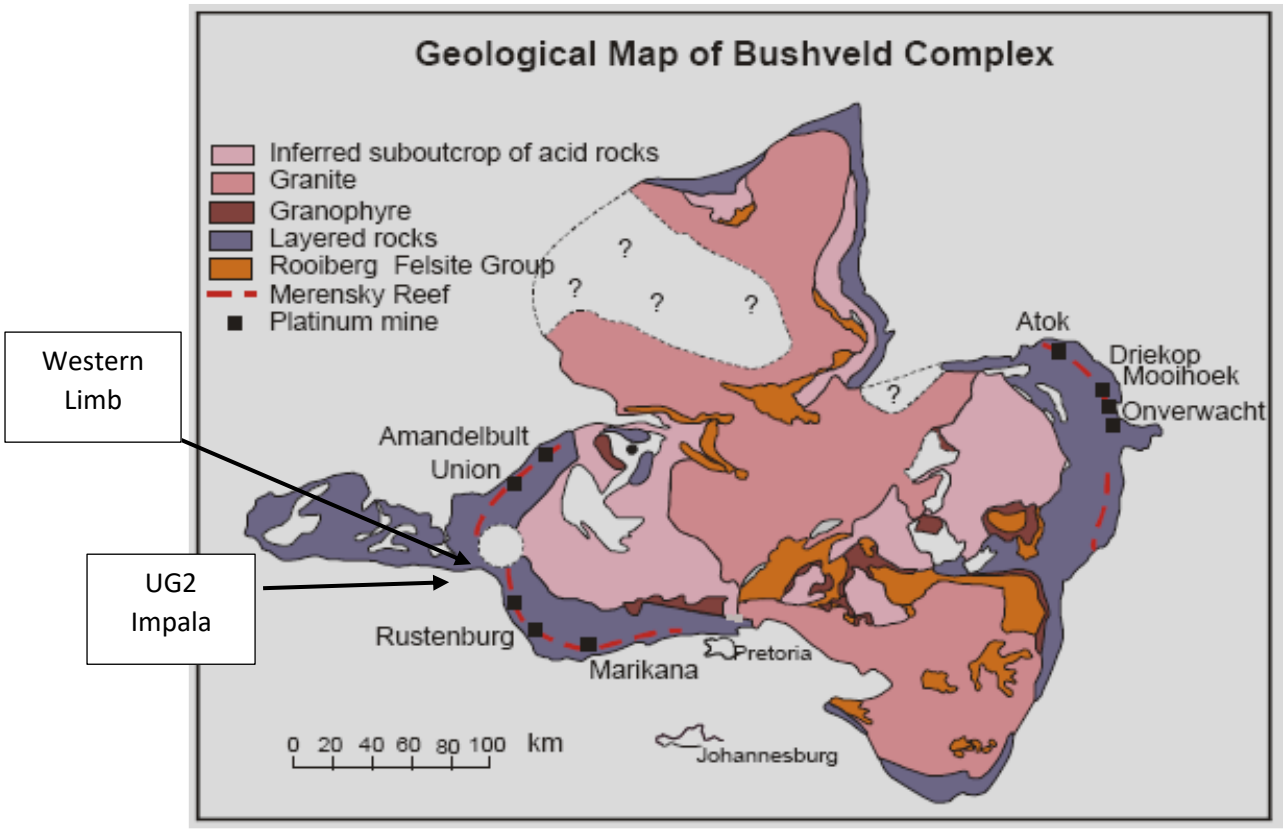

Figure 2.2: Geological map of the Bushveld Complex highlighting the location of the Impala UG2 (Taken from Cawthorn et al., 2005)

2.4.3. Kansanshi (High-grade Cu ore)

The Kansanshi copper deposit is situated in the Northwest Province of Zambia (Figure 2.3). Recent exploration studies have reported an open-pit resource of 267 million tons averaging 1.28% Cu and

0.16 g/t Au, making Kansanshi one of the biggest known Zambian copper resources outside the Copperbelt (Corin et al., 2017).

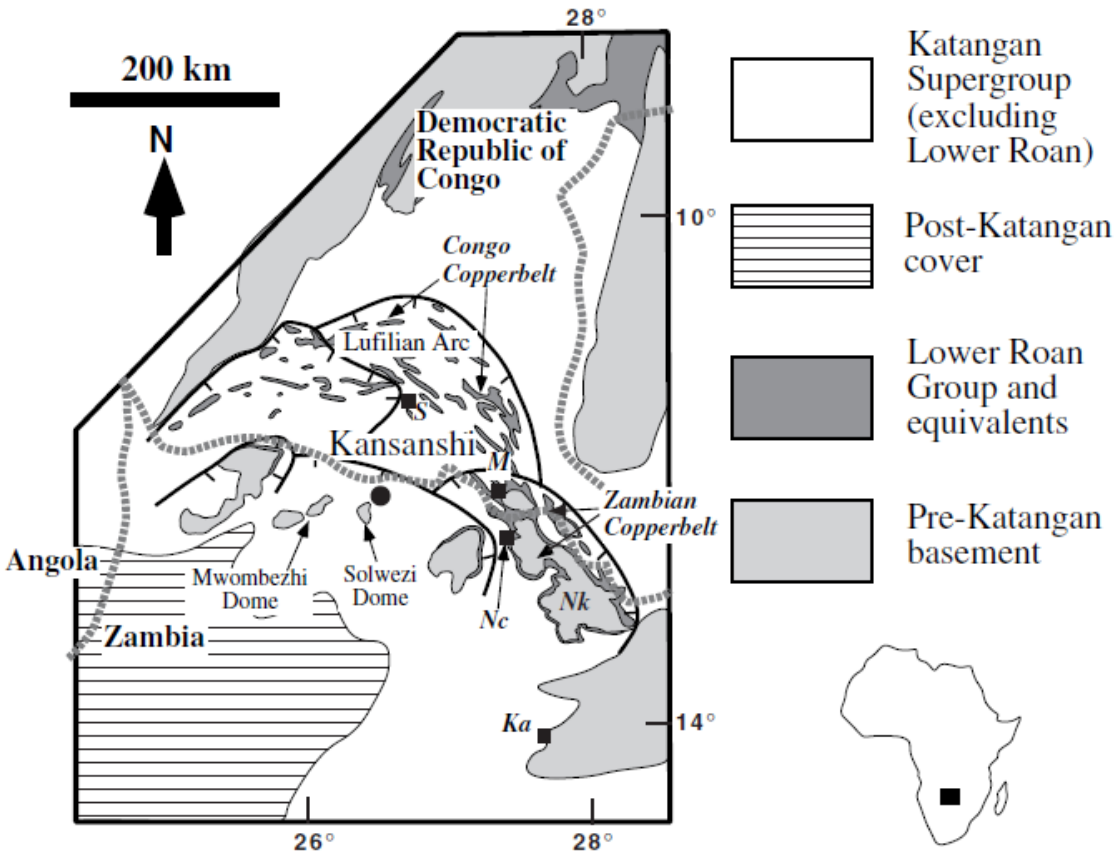

Figure 2.3: The Kansanshi Cu (-Au) deposit situated in the Central African Copperbelt taken from Kalichini, (2015).

The Kansanshi ore is classified into two groups, the high-grade ore (which consists mainly of sulphides) and the low-grade ore (which consists of oxides) (Ngulube, 2016). The high-grade ore has a total copper content of about 1%. Chalcopyrite (CuFeS2) is the deposit's primary copper-bearing mineral, with a weight fraction of 3.9 percent; secondary sulphides include chalcolite (Cu2S) and bornite (Cu5FeS4), digenite (Cu9S5), and covellite (Cu9S5) (CuS). Quartz, calcite, dolomite, pyrrhotite, and pyrite are the most common gangue minerals found in the deposit (Kribek et al., 2005). The bulk gangue minerals included mica, plagioclase-feldspar, and quartz.

Different ores show varying susceptibility to oxidation. This is because chemical and mineralogical characteristics, as well as ore grade, determine how prone the ore will be to oxidation. It is expected that oxidation will affect sulphide minerals the most because they are generally more reactive.

2.5. The fundamentals of Froth Flotation

2.5.1. Introduction

Froth flotation was originally patented in 1906 and has since become the most dominant technology that is used to process sulphide minerals (Wills and Napier-Munn 2006; Lamia and Mouhamed 2017; Li et al. 2019). Froth flotation has made the mining of low-grade and complex ore bodies, which would have otherwise been regarded uneconomic, possible (Wills, 2006). This technique was initially developed to treat the sulphides of copper, iron and zinc and is now expanded to treating platinum, nickel, gold-hosting sulphides and oxides (and oxidised minerals).

2.5.2. Principles of flotation

Flotation is a physico-chemical process that uses the differences in the surface properties of valuable minerals and the invaluable gangue materials to separate these minerals (Wills, 2006). The process occurs when crushed and liberated particles are suspended in the water in a flotation cell that is aerated (Harris, 1982). The particles are treated with reagents that make the differences in the surface properties of the particles involved more defined. The valuable minerals are usually hydrophobic (water-repellent) and they attach onto the bubbles that are formed, which make their way to the water surface where they are collected. The unwanted gangue material is hydrophilic, which means it remains suspended in the solution and is later passed on as tailings (waste) (Corozier, 1984; Sutherland and Wark, 1955).

Particle size is essential in froth flotation because the size determines whether the particles will attach to the air bubbles. The size of the particle must be compatible with the bubble size. For instance, there is a higher chance for larger particles to attach to the air bubbles than the fine particle. This is because the probability of larger particles colliding with the air bubbles is higher than that of fine particles. However, when the air bubbles rise the larger particles are often too heavy to be carried to the froth, so they often fall back into the slurry. The finer particles, on the other hand, are easily carried upwards to the froth where they are recovered (Aktas, et al., 2008).

The theory of froth flotation involves three phases (solids, water and froth) and several subprocesses and interactions which are not completely understood. The process can be summarised into three important steps:

a) Selective attachment to air bubbles (true flotation). This is the most important step that includes the valuable minerals being attached to air bubbles. The substances that attach to the bubbles represent the particles that were recovered.

b) Entrainment in the water involved in froth flotation. Entrainment is the mechanism that is responsible for recovering fine-grained gangue mineral particles in flotation. The effectiveness

of the separation between valuable materials and gangue is dependent on the degree of entrainment.

c) Physical entrapment among particles attached to the air bubbles, in a froth (See froth in *Figure 2.4*).

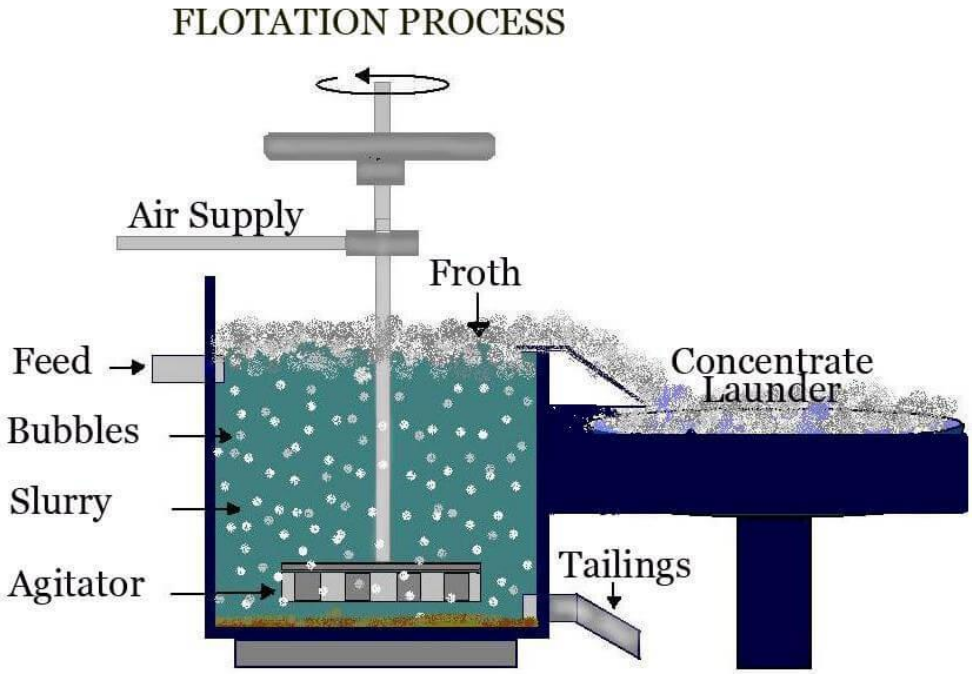

Figure 2.4: Diagram of a flotation cell (Michaud, 2013).

2.5.3. Flotation recoveries vs surface oxidation

Oxidation plays an important role in flotation as it modifies the properties of mineral surfaces, which affects the adsorption of collectors onto minerals. Studies such as Heyes and Trahar (1977) have demonstrated how “mild oxidation” can improve flotation performance by increasing the formation of hydrophobic species, which is beneficial for the adsorption of collectors.

Excessive oxidation, on the other hand, increases the precipitation of hydrophilic species such as metal hydroxides and oxides on minerals surfaces (Smart, 1991). This increases the number of minerals with hydrophilic surfaces, resulting in decreased flotation sensitivity and recovery (Moimane et al., 2020). *Figure 2.5* shows the inversely proportional relationship between surface oxidation and flotation recoveries. This is because excessive oxidation is detrimental to the effective separation of valuable minerals and gangue materials.

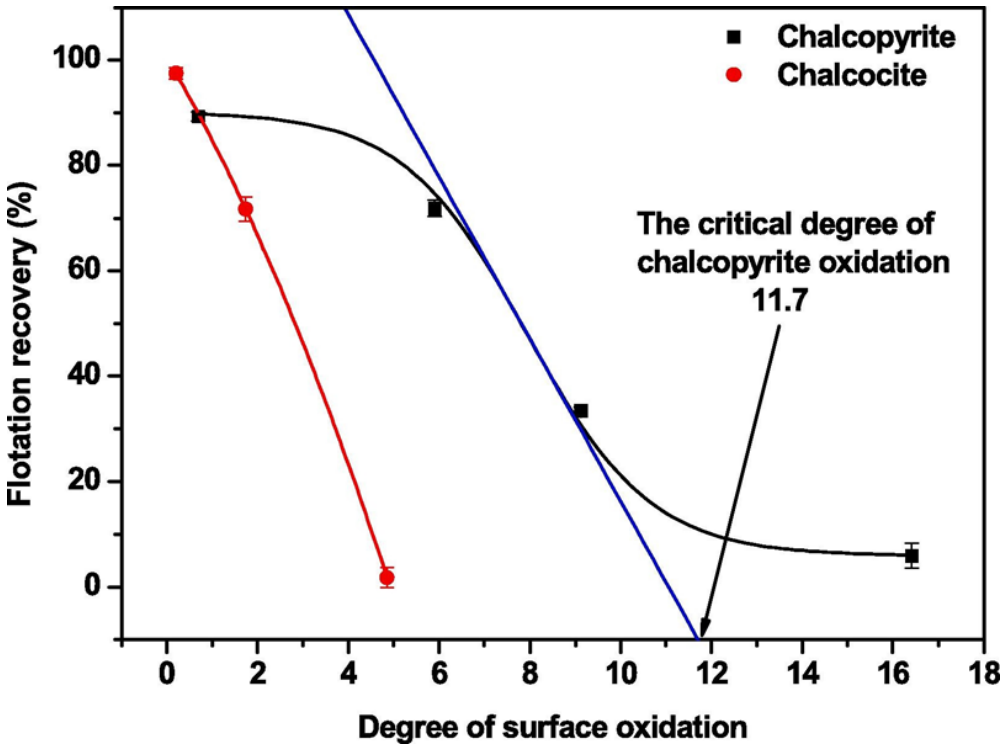

Figure 2.5: Degree of surface oxidation vs Flotation recovery (Moimane et al., 2020).

2.6. Measurements of degree of oxidation using EDTA and RN

2.6.1. Ethylenediaminetetraacetic acid (EDTA)

EDTA is a colourless amino polycarboxylic acid that is soluble in water and has become a common and widely used analytical reagent (Pribil, 1972). This acid was synthesised for the first time by I.G. Farbenindustrie in the mid-1930s and is used both for industrial and medical purposes. According to Pribil (1972), the initial findings were that the compounds formed stable, water-soluble complexes, even with calcium and magnesium, which then suggested that they would be good for use as water softeners as well and dyeing assistants. Please see the skeletal formular of EDTA in Figure 2.6.

Figure 2.6: Skeletal formula of EDTA.

In the early 1940s, EDTA was studied and proved to be a good titrant. All complexes were colourless and soluble in water, except if the metal itself was coloured. These complexes would be perfect for masking metal ions and thus preventing them from interfering with analytical procedures. Over the

years, other applications of EDTA have also progressed and have become as important as in the titration of metal ions (Pribil, 1972).

Minerals undergo oxidation when they are taken out from the ground and processed, and this generally reduces flotation sensitivity and recovery (Smart, 1991). EDTA can form complexes with oxidation products without reacting with the metal sulphides. It selectively leaches the metal oxides, carbonates, and sulphates away from sulphide minerals when the pH is adjusted from 7 to 11 and enough time is given for the extraction process.

EDTA is said to be more effective in plant scale measurements for oxidation products on mineral surfaces compared to other surface characterisation techniques like the X-ray fluorescence spectrometers (XPF), which struggle to deal with ore variability (Bicak, 2019). It could also be used as a proxy to estimate ore surface chemistry variability. Bicak (2019) used EDTA to investigate ore variability that is caused by surface oxidation. Ninety tests, that were representative of the spatial distribution of the ore types used, were conducted. Her results showed a large variation in EDTA values, which she explained was due to ore differences in mineralogy and surface oxidation. Her results also explained how extensive oxidation was detrimental to flotation performance.

2.6.2. Reactivity Number (RN)

Minerals react differently with air. This is because the way different minerals consume oxygen and their rate of oxygen consumption can be related to their unique chemical composition as well as electrochemical and mineralogical characteristics (Owusu et al., 2013). The two studies by Becker et. al., (2010) and Owusu et al. (2013) recognised the significance of RN in determining the electrochemical reactivities of sulphide ores with varying properties such as chemical and mineralogical compositions, grade, etc. Becker et. al., (2010) demonstrated how RN can be used to investigate the relationship between mineralogy and flotation performance. The study used 4 pyrrhotite samples from different ore deposits and their behaviour was tested using oxygen uptake and micro flotation tests. The different pyrrhotites (magnetic and non-magnetic pyrrhotites) were all compared in terms of the effect of pH, mineral chemistry, mineral association, crystallography, collector addition and mineralogy.

The level of mineral reactivity was estimated in reactivity numbers, where higher reactivity numbers (60-110) demonstrated more prominent reactivities. Results showed that under the conditions where pyrrhotite had a high reactivity number for oxidation, poor flotation recovery was observed. The samples that had a low reactivity number (6-8) and had not experienced excessive oxidation and showed a good flotation performance, while the samples that were already oxidised showed a poor flotation performance. Becker et. al., (2010) concluded that pyrrhotite conduct (behaviour in flotation)

can't essentially be clarified by just the mineralogical factor, but that it is a blend of mineralogical attributes overseeing its reactivity and flotation performance.

Owusu et al. (2013) showed how this method can be used to determine the electrochemical reactivity of low-grade and high-grade sulphide minerals. The study specifically looked at and tested the reactivity of two pyrite minerals, high-grade pyrite (Py-A) and low-grade pyrite (Py-B). The two minerals were put into an airtight vessel and the same amount of air was put into both experiments. The results showed that the amount of oxygen in the pulp with Py-B pyrite was greater than that of Py-A which indicated that Py-A reacted with all the oxygen present in the vessel, although the same amount of air was put into both experiments (*Figure 2.7*). This showed that Py-A was more reactive than Py-B and that the shortcomings of Py-B were related to its mineralogical and chemical composition. However, when the grain size particles of Py-B were further ground to a smaller distribution size, and its oxygen consumption rate increased. Further grinding to smaller particles increased the surface area which exposed more sites for reactions to occur.

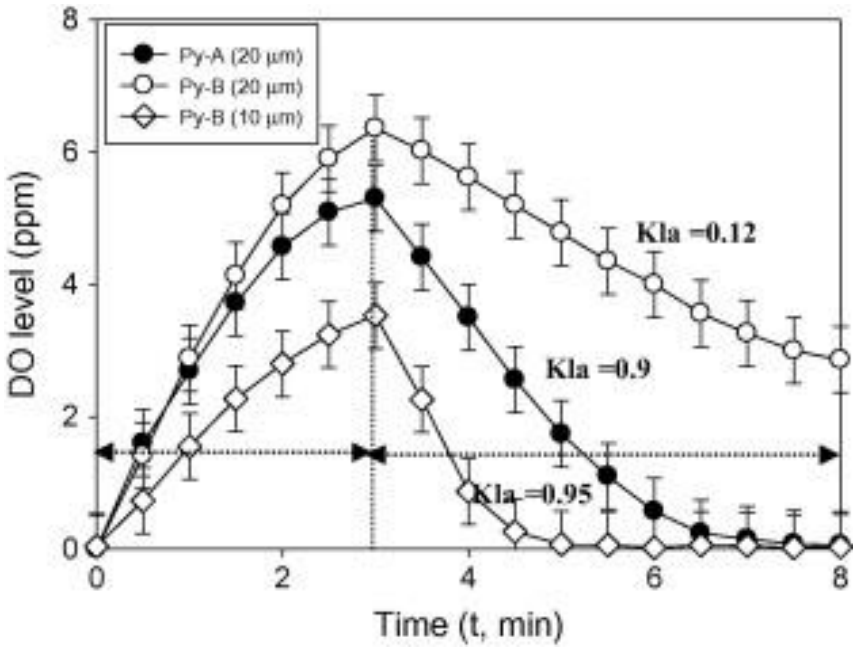

Figure 2.7: Dissolved oxygen levels of Py-A and Py-B (Owusu et al., 2013).

Owusu et al. (2013) and Becker et. al., (2010) concluded that the differences in the oxygen consumption rate or reactivity of the two pyrites can be related to their chemical and mineralogical composition characteristics. These differences impacted the pulp chemistry and the flotation response, where the flotation behaviour of chalcopyrite was depressed in the presence of pyrite. Chalcopyrite was more depressed in the presence of Py-A, the more reactive mineral, than Py-B.

2.7. Summary of Literature

The flotation of sulphide minerals is well documented, and numerous studies have focused on the significance of oxidation in the flotation of sulphide minerals (Kelebek, 1993). Oxidation alters the surface properties of sulphide minerals, increasing or decreasing their hydrophobicity, and these surface mineral changes subsequently influence the flotation process (Moimane et al., 2020). Kelebek (1995) addressed the effect of oxidation on flotation behaviour of nickel-copper ores. The study also claims that the oxidation taking place during the processing of nickel-copper ores influences the flotation sensitivity. The outcomes differ based on factors such as grinding media type, reagent dose, flotation stage, mineralogy, and natural activation susceptibility.

Previous work has also shown that there is a good relationship between floatability and pulp potential for pure sulphide minerals. Studies such as Owusu et al. (2013) showed that controlling pulp chemistry can be essential for improving mineral grade and recovery for sulphide minerals. Controlling pulp chemistry can significantly increase the selectivity of sulphide minerals as well as improve their recovery and grade (He et al.,2006). These parameters are known to be generally influenced by the ore mineralogy, chemical composition, the electrochemical reactivity of sulphide minerals and grinding media (Goktepe and Williams, 1995).

Peng et al. (2003) studied the effects of grinding conditions on chalcopyrite flotation and chalcopyrite separation from pyrite. Two types of grinding media were used, mild steel grinding media and 30 wt. % chromium grinding medium. The results confirmed that chalcopyrite recoveries increased when the chromium grinding media was used compared to the mild steel medium. The 30 wt. % chromium grinding medium creates a reducing grinding environment, lowering mineral oxidation (Peng and Grano, 2009). When sulphide minerals come into contact with grinding media, they can cause galvanic coupling, which causes electrons to flow from the less noble to the nobler elements. As a result, the 30 wt. % chromium grinding media corrodes more quickly, resulting in a decrease in dissolved oxygen at the mineral–water interface (Peng et al., 2003).

2.8. Gap in knowledge:

Grinding not only reduces particle size to liberate precious minerals, but it also creates differential surface characteristics on the surface of valuable and gangue minerals (Zhao and Peng, 2012). The liberation of precious minerals is directly linked to oxidation, which is one of the processes that cause mineral alteration. The more liberated the valuable minerals are, the more likely they are to oxidise. The oxidation products are indicated by hydrophilic metal hydroxides and oxides that precipitate on mineral surfaces. A certain quantity of these oxidation products on mineral surfaces allows for successful separation in separation processes like flotation.

However, in some instances, the extent of oxidation negatively affects flotation recoveries. This occurs when large quantities of hydrophilic metal hydroxides and oxides precipitate on mineral surfaces, increasing the hydrophilicity of the mineral surfaces, rendering the minerals unfloatable, and resulting in reduced mineral recoveries. Mineral processing would benefit from techniques that are not only less expensive and maintain overall economic variable capabilities, but also ones that will help us understand the level of oxidation indicated by the quantity of oxidation products present on the mineral surface.

The EDTA and RN techniques may be able to assist us connect the notion of valuable mineral liberation with the level of oxidation the particles have experienced while being liberated, thus being able to predict the value that is in the particle before it can be floated. By assessing the quantity of oxidation that the particle has undergone, the techniques might help us obtain a measurable estimate of value in the liberated particle, and this measurement could be used to predict how the particle would float.

There is a gap in industry for techniques that are not only less expensive and maintain overall economic variable capabilities, but also ones that will help us understand the level of oxidation indicated by the quantity of oxidation products present on the mineral surface. This study will show that these simple, cost-effective techniques would be able to indicate surface oxidation which imply the likelihood of flotation performance based on how much the surfaces have oxidized. As a result, they will act as a guideline to assist flotation plants in managing oxidized ores better in order to potentially prevent losses in recoveries as well as to investigate alternative solutions that may be adapted to the flotation of ores with differing degrees of oxidation.

3. Research key Questions and Hypotheses

In accordance with the highlighted gaps in the literature, the EDTA and RN techniques were chosen for this study since they may provide responses relevant to the ore's current state of oxidation as well as the rate of oxidation, should the ore be refreshed in some way. This might remove the need for several complex mineralogical tests, saving both time and money. While some literature considers these techniques, they must be confirmed on real ores.

3.1. Aim and Objectives

The aim of the study is to investigate the capabilities of the chosen techniques in dealing with different ore types that have different mineral compositions, liberation profiles and grades. This will be done by:

- Validating the use of the EDTA technique to determine the level and/or rate of oxidation of the selected ores.
- Validating the use of the RN technique to determine the level and/or rate of oxidation of the selected ores.
- Studying the relationship between oxidation of the minerals contained in the ore.
- Correlating the level and/or rate of oxidation with the original mineralogy and/or liberation of the ore samples.

3.2. Key Questions

Oxidation vs Mineral Liberation experiments will address the following questions:

- What are the changes in surface chemistry that occur as a result of increased mineral liberation?
- How does mineral liberation affect the EDTA and RN numbers?

Oxidation vs Ore type experiments will address the following questions:

- How will the EDTA and RN numbers change based on the ore types?
- How will the changes in liberation and oxidation relate to the flotation performance of Ore A and Ore B?
- Will EDTA and RN results, and the flotation process, give an indicator of the level of oxidation and how will that relate to the mineralogy?

3.3. Hypotheses

a) Although grinding finer particles will improve mineral liberation, it will also cause significant chemical changes. The oxidation rate (as measured by either EDTA or RN) will increase. This is because as the grind becomes finer, the surface area increases, thus more active sites are made available for chemical reactions to occur.

b) The EDTA values will vary between the different ores. This will be mainly influenced by the differences in the chemical and mineralogical composition of the ores. There will be variations in the degree of surface chemistry that the sulphide minerals present in the ore will experience. Some minerals will have a higher degree of surface oxidation than others. The EDTA values will vary between different ores depending on the properties of the minerals present.

c) The RN values will vary between the different ores. This will be mainly influenced by the differences in the chemical and mineralogical composition of the ores. Some minerals are known to be influenced by their elemental stoichiometry. Vacancies created by the variations from the stoichiometric composition and impurities may act as contributors or acceptors of electrons, affecting both conductivity and the reactivity of the minerals.

3.4. Research Sustainability Goals

Figure 3.1: Research sustainability goals.

This project addresses sustainability goals 8 and 9 (Figure 3.1). It enhances the growing scientific knowledge by investigating more cost-effective techniques in mineral processing. It investigates how using EDTA together with RN could potentially give the necessary information needed to indicate in-situ mineralogy, eliminating several expensive mineralogical tests and steps. The project will attempt to upgrade the technological capabilities of these techniques that are already known and apply them in a way that they have not been applied before. When applied together, these techniques will allow persons to carry out analysis on-site with minimal instructions and solvents.

4. Experimental Details

4.1. Background

The Experiments were aimed at addressing the alterations that occurred on mineral surfaces caused by oxidation, using the Ethylenediaminetetraacetic acid (EDTA) extraction technique and the Reactivity Number (RN) technique. All the experiments used three different grind sizes (40% -75 µm, 60% -75 µm, and 80% -75 µm) to investigate the relationship between oxidation and liberation using EDTA and RN techniques. The techniques were tested on two different ores (HG Cu and UG2) to consider the impact of grade.

The experiments intended to give an indicator of feed grade and the potential for surface oxidation based on ore type and sulphide liberation. The experiments validated the EDTA and the RN technique to determine data that can be linked to literature data when sulphide ores were used instead of minerals. This chapter explains the materials that were used and the procedures that were followed to conduct the tests. The flotation procedures are explained, as well as the ore preparation, assay, and mineralogy techniques used.

4.2. Ore Sampling and Preparation

A bulk UG2 ore (Ore A) was sourced from the Bushveld Igneous Complex (BIC) of South Africa. A bulk high-grade Copper ore (Ore B) was obtained from the Zambian Copperbelt.

The samples were crushed using a terminator jaw crusher, and screened to achieve size fractions of 100% - 6 mm for Ore A and 1 cm for Ore B. The crushed particles were then divided into 1 kg portions using the rotary riffle splitter and stored in airtight sealable plastic bags at ambient temperature.

4.3. Ore Minerology

X-Ray Diffraction (XRD) and Quantitative Evaluation of Minerals by Scanning Electron Microscopy (QEMSCAN) were used to conduct a mineralogical study of the two ores. 100 g portions of milled ores were weighed and wet screened at screen mesh sizes of 53 and 25 µm to prepare the samples for mineralogy. The sample preparation process for XRD and QEMSCAN is summarised in *Figure 4.1*.

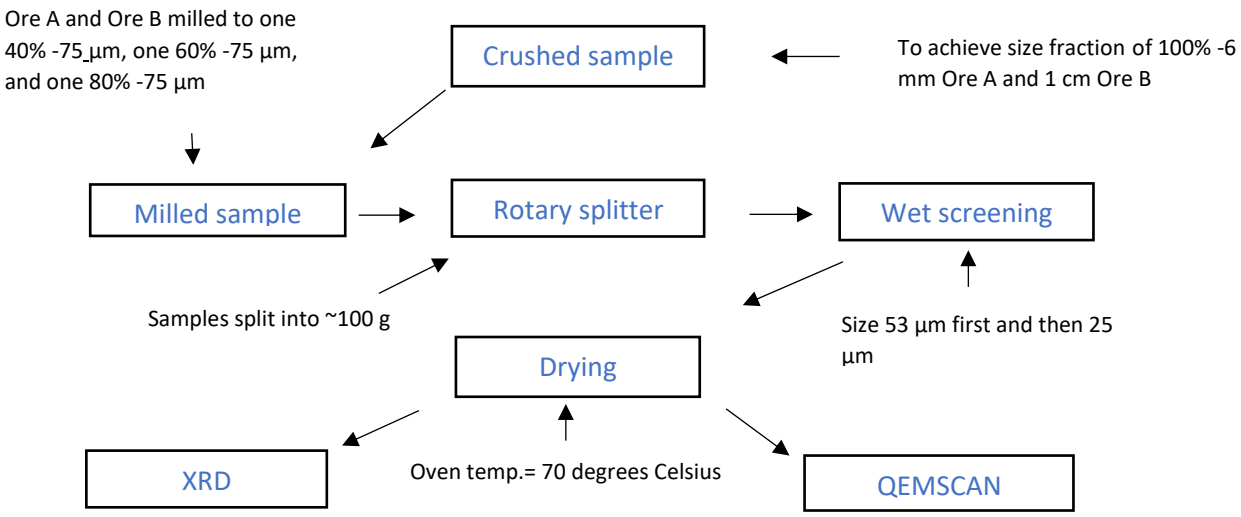

Figure 4.1: Bulk sample preparation for mineralogical analysis using XRD and QEMSCAN.

4.3.1. XRD Procedure

In order to achieve a uniform particle size distribution, samples were micronized in ethanol using a McCrone microniser. Powder XRD spectra were obtained with Co-Ka radiation using a Bruker D8 Advance powder diffractometer equipped with a LynxEye detector and fixed divergence and receiving slits. Bruker Topas 4.1 software was used to identify the phases, and the relative phase amounts (weight percent) were calculated using the Rietveld equation (Coelho, 2007).

4.3.2. QEMSCAN Procedure

All QEMSCAN analyses were done on an FEI 650F FEG QEMSCAN (See *Figure 4.2* below). QEMSCAN is the state of the art, top of the range automated mineral analyser. It is an analytical tool which provides rapid, reproducible and statistically reliable quantitative information on minerals and man-made materials for a variety of disciplines. This tool has been custom developed for the mining industry

Information obtained from QEMSCAN for this study:

- Bulk mineralogy of samples
- Element deportment
- Ore Characterisation
- Particle properties
- Mineral liberation
- Mineral association
- Theoretical grade recovery curve

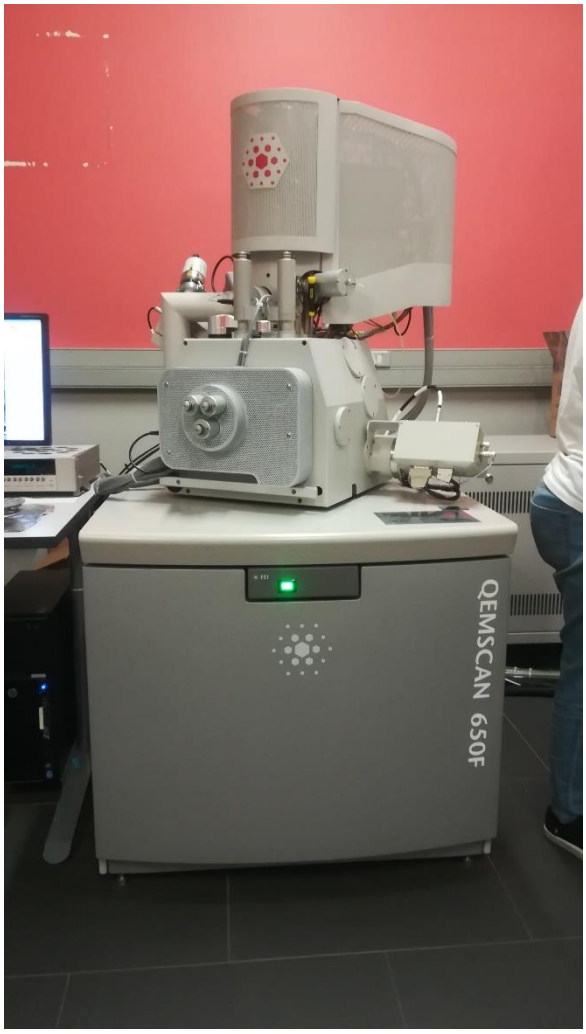

Figure 4.2: QEMSCAN 650F, the mineral analyser that was used in this study.

Sample preparation procedure for QEMSCAN

A Quantachrome micro riffler was used to divide each size fraction into three 1 g samples. 2 g of milled graphite (one size fraction smaller than the fraction being prepared for mineralogical analysis) was then added to eliminate contacting particles and increase electron conductivity during analysis. The graphite/ore combination was poured into moulds that had been labelled and greased and then resin was added. The samples were then mixed to spread the particles. To remove any air bubbles, the moulds were put under vacuum for 15 minutes using a Struers Cito-vac vacuum and then left overnight under pressure to cure.

The cured moulds were labelled by adding a printed label on the back (containing the Ore name, grind size, and number) and fixing it with additional resin. The blocks were removed from the moulds and polished to a mirror-like, scratch-free sheen with a Struers TeraPol-11 polisher before going through a series of grinding and polishing stages. After each grinding/polishing step, a rinse stage was added with water and dishwashing liquid to remove any residual dirt from the previous grinding step. The

blocks were then put in an ultrasonic bath with just clean water for 10 minutes before being cleaned with ethanol and dried for an hour at 30 °C.

4.4. Synthetic Plant Water

The scarcity of water in countries such as South Africa has pushed many mining operations to recycle their onsite water. In mineral processing operations, recycling water increases the number of dissolved ions in the plant water, which increases ionic strength and reduces plant performance. Increased concentrations of ions such as calcium, magnesium, nitrate, sulphate, and chloride in recycled water influence the reactions on the mineral surface, which in turn changes the hydrophobicity of minerals (Khraisheh et al., 2005; Wiese et al., 2007). As a result, synthetic plant water (SPW) containing only inorganic ions was developed to mimic the concentrators' traditional plant water analysis (Manono et al., 2012; Wiese et al., 2005). The University of Cape Town (UCT) Centre for Minerals Research (CMR) has established a standard synthetic plant water formula with a total dissolved solids (TDS) concentration of 1023 mg/L and an ionic strength (IS) of 0.0213 M, dubbed 1SPW. This water is used in research projects to reflect the typical water analysis of several South African PGM concentrators.

Synthetic plant water (1SPW) was prepared in bulk and used throughout the experiments. Six inorganic salts were added to distilled water to make synthetic plant waters (See *Table 4.1*). Merck provided all of the salts in powder form.

Table 4.1: The inorganic salts there were used to make the 1SPW that was used for the experiments in this study.

Inorganic salt	Formula	Salt concentrations used in 20 L (mg/L)
Magnesium sulphate	$MgSO_4.7H_2O$	615
Magnesium nitrate	$Mg(NO_3)_2.6H_2O$	107
Calcium nitrate	$Ca(NO_3)_2.4H_2O$	236
Calcium chloride	$CaCl_2$	147
Sodium chloride	NaCl	206
Sodium carbonate	Na_2CO_3	30

4.5. Lab-Scale Milling

A stainless-steel rod mill was used for comminution of both Ore A and Ore B (*Figure 4.3*). The mill had a 200 mm internal diameter and a 297 mm depth, and it was loaded with twenty rods of three different diameters (6 x 25 mm, 8 x 20 mm and 6 x 16 mm). 1 kg of ore was added to the mill together with 500 mL of the necessary plant water (*Table 4.1*) to generate a 66 wt. % slurry density and the slurry was milled at the necessary time to achieve the required grind. In this study three grind sizes were targeted for each ore, 40% -75 µm, 60% -75 µm and 80% -75 µm. The dimensions of the mill and the operational parameters of the two ores for every liberation profile are shown in

Table 4.2.

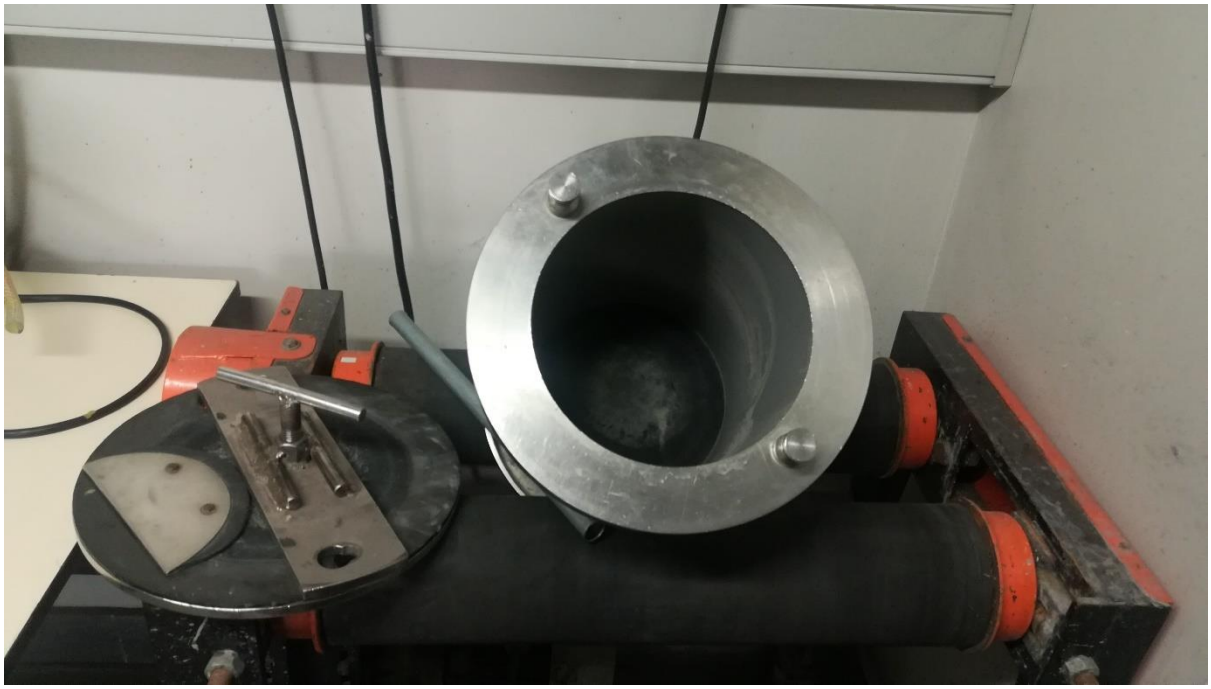

Figure 4.3: The stainless-steel grinding mill.

4.6. Milling Curves

For both Ore A and Ore B, milling curves were generated by grinding each of the ores at different time intervals in order to achieve the desired grind sizes, *Figure 4.4* and *Figure 4.5*. The grinding times are shown in

Table 4.2.

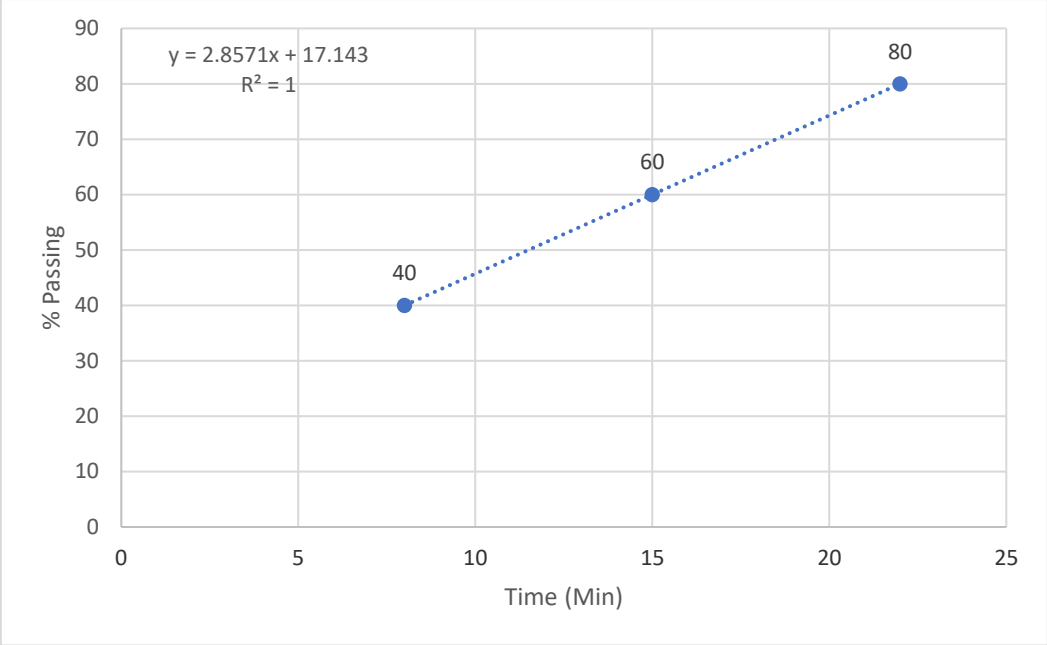

Figure 4.4: Milling curve for Impala UG2 for 40% -75 µm, 60% -75 µm, and 80% - 75 µm.

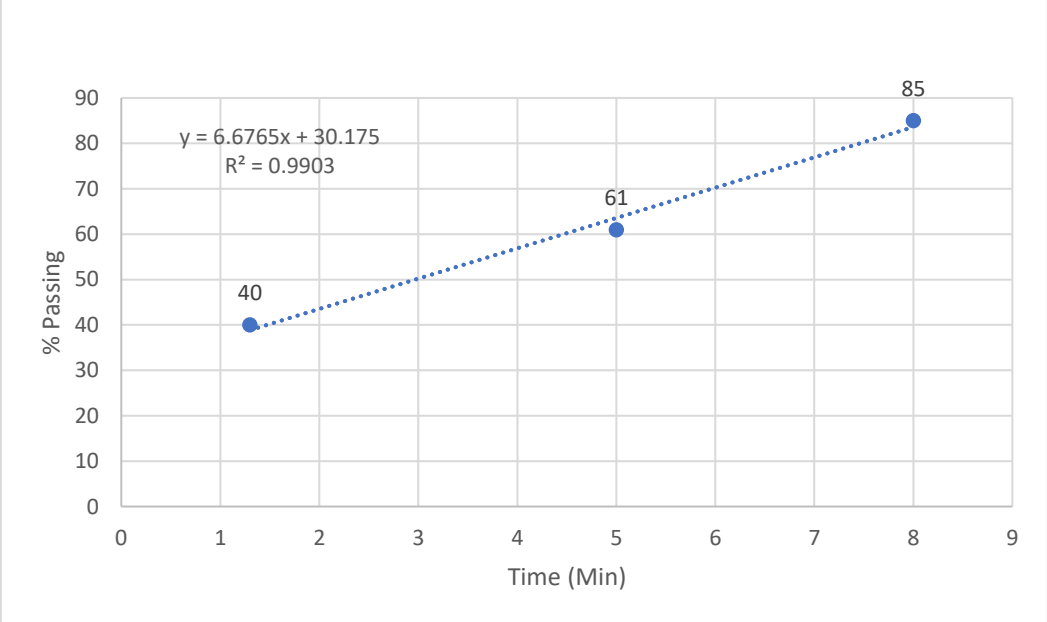

Figure 4.5: Milling curve for Kansanshi HG for 40% -75 µm, 60% -75 µm, and 80% -75 µm.

Table 4.2: Operational parameters that were used on Ore A, including the milling times for all three liberation sizes.

Parameters	*Ore A*	*Ore B*
Mill diameter (mm)	200	200
Mill depth (mm)	297	297
Number of rods (-)	20	20
Diameter of rods (mm)	6×25, 8×20 and 6×16	6×25, 8×20 and 6×16
Starting feed size	1 kg	1 kg
Mill speed (rpm)	256	256
Liberation size	Milling time T (minutes)	Milling time T (minutes)
i. 40% -75 µm,	i. 8	iv. 1.6
ii. 60% -75 µm	ii. 15	v. 5
iii. 80% -75 µm	iii. 22	vi. 8

4.7. Reagent Preparation and Storage

Details of reagents used for batch flotation are shown in *Table 4.3*.

4.7.1. Frother

DOW 200, a polypropylene glycol type frother, supplied by GoodFellow, was used for all flotation tests and dosed at 40 g/t. The frother was used as supplied, without dilution, and was stored at room temperature.

4.7.2. SIBX Preparation

Sodium isobutyl xanthate (SIBX), supplied by AECI Mining Chemicals, was made up to a 1% w/v solution; 1 g of SIBX was dissolved in a small volume of distilled water in a beaker and then added to a 100 mL volumetric flask, the beaker was rinsed with distilled water, and the flask was made up to the 100 mL mark with further distilled water. SIBX was prepared daily and discarded after use, as per the Material Safety Data Sheet (MSDS) to prevent decomposition. SIBX was dosed at 50 g/t.

4.7.3. pH Modifier

Sodium hydroxide (NaOH) supplied by Merck chemicals was used in this study as a pH modifier. NaOH was chosen specifically because it has high purity and does not introduce excess calcium ions into the solution. It was added before the EDTA and RN experiments to keep the pH in the necessary range.

Table 4.3: Reagents used for the tests and their Bulk solution concentrations.

Reagent	Chemical Formular	Purity	Concentration of bulk solution (%)	Dosage (g/t)
Frother	$CH_3(C_3H_6O)_3OH$	100	Neat	40 g/t.
SIBX	$(CH_3)_2CHCH_2OCS_2Na$	97	1	50 g/t

4.8. Experimental Method

4.8.1. Batch Flotation Tests

Following milling, the slurry was transferred to a 3 L Barker flotation cell. Water was added to achieve 35 wt.% solids, and the impeller speed set to 1200 rpm. A feed sample (60 mL) and an EDTA pre-float sample (25 mL) were taken from the stirred slurry using syringes. The slurry was first conditioned with SIBX and then DOW200 for 2 minutes and 1 minute respectively. Air was used as the flotation gas, and the air flow rate was maintained at 7 L/min for all tests. The froth was scraped into a collecting pan every 15 seconds to generate four concentrates (C1-C4) at 2, 6, 12 and 20 minutes of flotation. Adding plant water at set intervals maintained the froth height (of 2 cm) and water level constant. *Figure 4.6* shows the flotation cell that was used for the batch flotation tests.

Figure 4.6: 3 L flotation cell used for batch flotation tests.

When the full flotation cycle was complete, the air was switched off, two 60 mL samples were collected as Tails 1 and Tails 2 and one EDTA post float sample (25 mL) was collected from the stirred slurry with syringes. Solids and water recoveries were monitored throughout all tests. A summary illustration of this procedure is shown in *Figure 4.7*. The feed, Concentrate and Tailings samples were filtered, dried and sent for chemical analysis (X-Ray Fluorescence Spectrometers) for Cu and Ni ions. The quantitative Cu and Ni concentrations were measured with an energy dispersive Thermo-NITON XL3 950 GOLDD+XRF spectrometer (Thermo Scientific, USA) equipped with an Ag Anode X-Ray tube capable of 50 kV and 200 microA. The quantitative data were collected using Thermo Scientific's standard Niton Data Transfer (NDT) PC software system. Each flotation test was repeated two times to show the reproducibility of this work's experiment.

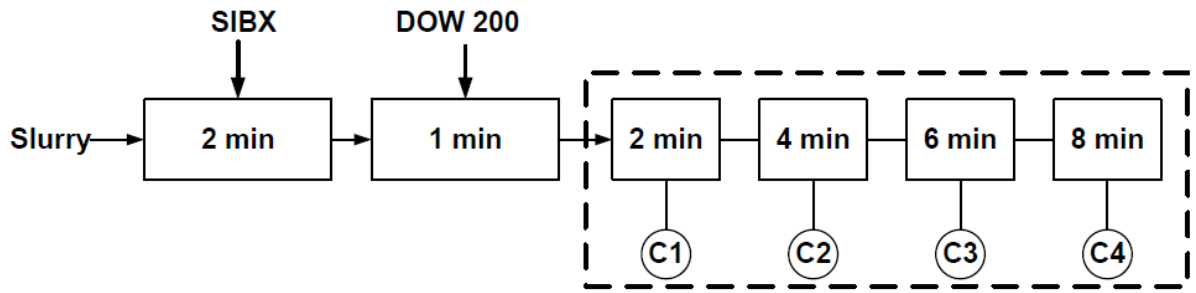

Figure 4.7: A summary of the experimental procedure used to float Ore A and Ore B (Manenzhe, 2018).

4.8.2. EDTA Extraction tests

EDTA Solution Preparation

To make up a 3% w/v solution of EDTA, 30 g of EDTA powder was added to 1 L of distilled water and a magnetic stirrer was used to stir the solution. NaOH pellets were then added to the solution to adjust the pH to approximately 7.5 using the HI8424 Portable pH/mV Meter. This solution was made in bulk (2-3 L at a time) and stored away from sunlight at ambient temperature, this improved productivity and efficiency.

Procedure

250 mL of 3% w/w EDTA solution was poured in a 400 mL beaker, along with 25 mL of EDTA pre or post float sample that was collected directly from the float cell and stirred for 30 minutes using a magnetic stirrer to ensure the solids remained suspended. Using the vacuum pump, the slurry was filtered to remove colloidal particles using a 0.22 m filter paper and the Millipore filtration funnel. The filtrate was then placed in a plastic container with a cover, and the solids, filtrates, a blank 3 percent

w/w EDTA solution, and a blank SPW sample that had no contact with ore were all sent for ICP-OES analysis. The analysis was performed using the Varian ES 730 ICP-OES Mars 6 Microwave Digester. EDTA measurements were repeated two times.

Since the EDTA samples were taken from a slurry sample, the solids must be submitted for assay so that an EDTA extractable percentage can be calculated. For an overview of the technique, please see the diagram below (*Figure 4.8*).

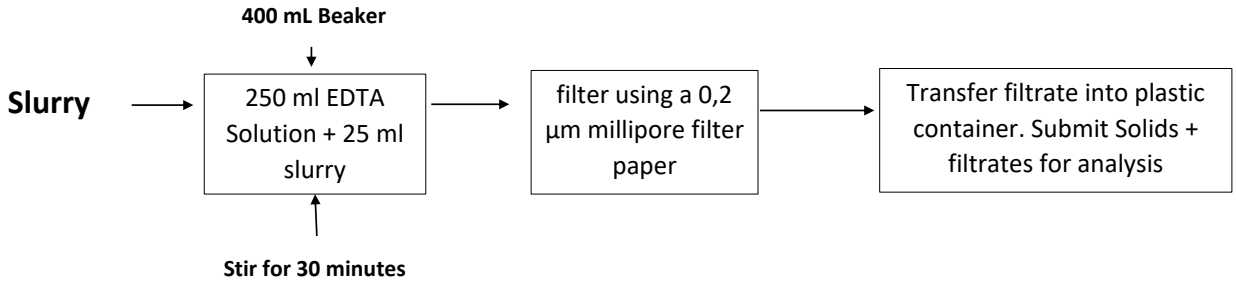

Figure 4.8: A summary of the experimental procedure used or EDTA Etraction tests for both Ore A and B

4.8.3. Reactivity Number (RN) tests

Reactivity Number (RN) is a method based on the measurement of the rate of dissolved oxygen decay. The RN factors were calculated using methodology developed by Afrox (Afrox, 2008), which was also used by (Becker, Villiers and Bradshaw, 2010). In the context of this study, the technique was used to measure the different reactivities of minerals found in the two different ores (Ore A and Ore B) by monitoring the differences in their rate of dissolved oxygen (DO) decay. *Figure 4.9* shows the RN apparatus, which consists of the following components: a 400 mL beaker, a multi-parameter probe, a magnetic stirrer and oxygen supply.

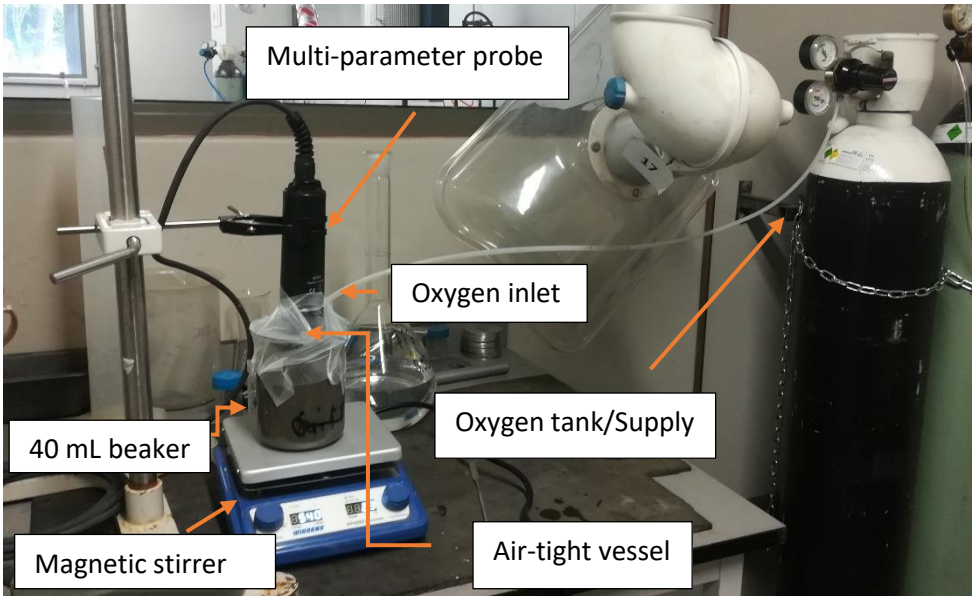

Figure 4.9: RN technique components, including the Multiprobe magnetic stirrer and medical oxygen.

Medical oxygen was utilized as the only source of oxygen in the RN technique tests. The medical oxygen tank was provided by AIR PRODUCTS and is 99 percent pure oxygen, making it more suited for DO testing.

Procedure

For each float, two sets of RN samples were taken: pre-float samples, which consisted of four 60 mL syringes before flotation, and post-float samples, which consisted of the same number of 60 mL syringes taken after flotation. In order to maintain consistency across the measurements, all samples were allowed 50 minutes between being taken from the float cell and starting the DO measurements The pre-float and post-float samples where first ultrasonicated for 5 minutes in plant water in order to de-aggregate smaller particles.

The samples where then transferred into 400 mL beakers together with 200 mL of water with calcium ions (3.33×10^{-3} M with 10^{-2} ionic strength). Prior to the RN tests, the samples were adjusted to the desired pH with NaOH (pH between approximately 8.5 and 9.5) in order to ensure that all the tests had the same pH range. The multiprobe was then inserted into the sample, along with the oxygen outlet, and the beaker's opening was sealed airtight with parafilm (Figure 4.9). The sample was stirred for one minute to develop a homogeneous pulp, after which initial pH, Eh, and DO readings were taken using the HI7698195 Multi-parameter probe. RN measurements were repeated two times.

Table 4.4: Summary of the reactivity number experiment technique

Activity	Conditions	Time (min)
Collect samples from float cell	four 60 mL syringes	-
Ultra-sonification	Ore samples from float cell, in plant water	5
Transfer into beaker	400 mL beaker	-
Addition of calcium water	200 mL 3.33 x 10^{-3} M calcium water (10^{-2} ionic strength)	-
DO measurement	Initial DO reading using multi-probe	1 min 30 sec
O_2 Introduction	O_2 Spiking at 3 L.min^{-1}	3
DO measurement	Sealed beaker	~ 15 for mill samples ~30 for tails samples
O_2 supply closed	-	-

The slurry was then spiked with oxygen for 3 minutes at a flow rate of 3 L.min^{-1} and monitored using a Process Kinetics Sierra Smart Trak flow meter. The aeration tap was closed after 3 minutes, and the DO content decay was monitored for 15 minutes. DO measurements together with the conductivity and pH were recorded every 10 seconds for 15 minutes to monitor the decay of oxygen in the sample. After that, the oxygen demand rate constant (Kla) was determined using the following formula:

$$DO = DO_o e^{-(kla \times t)}$$

where DO and DO_0 are the DO concentrations at time t and 0, respectively. The summary of the RN procedure that was followed is shown in Table 4.4.

5. Results

This chapter covers the findings of the experiments done to evaluate the capabilities of the chosen techniques in dealing with oxidation from different ore types with varying mineral compositions, liberation profiles, and grade. The flotation response was used as a diagnostic for particles from the mill, not for particles from the tailings. Therefore, Section 5.1 shows the mineralogical characterisation of Ore A and Ore B, and Section 5.2 will present the batch flotation findings. In Section 5.3, all the results from experiments involving EDTA extraction tests and RN tests will be reported.

5.1. Mineralogy

Mineralogy is important in this study because it highlights the value that is contained in the ore. In the context of this study, mineralogy highlights the differences in liberation that is a result of the different grind sizes that were chosen. The grind sizes that are targeted in these mineralogical tests are 40% -75 μm, 60% -75 μm, and 80% -75 μm. The choice of appropriate grind sizes is critical since how the minerals oxidize depends on how liberated they are. As a result, the grind sizes were chosen to mimic ores that have experienced mineral surface reactions such as oxidation.

5.1.1. Bulk Mineralogy

QEMSCAN was used to analyse the bulk mineralogy of the feed in order to help with the interpretation of the sulphide minerals' oxidation and how that influences flotation performance. Table 5.1 compares the bulk mineralogies of Ore A and Ore B, and 1 shows the base-metal sulphides (BMS) concentrations in the ores. The BMS concentrations in Ore A and Ore B are quite low in comparison to other minerals in the ores. Within both ores, the primary BMS are chalcopyrite, pyrite, pentlandite, and pyrrhotite, although the proportions of these minerals vary. Ore B has significantly higher base-metal sulphide grades than Ore A, with 3.9% chalcopyrite, 1.79% pyrite, 0.54% pyrrhotite and 0.22% of the other sulphides. Plagioclase, quartz, and mica made up the bulk of the gangue minerals in Ore B. Ore A, on the other hand, included trace quantities of chalcopyrite, pyrite, and pyrrhotite.

Table 5.1: QEMSCAN bulk mineralogy of Ore A and Ore B in wt. %

Mineral group	Mineral	Mineral content (%)	
		Ore A	Ore B
BMS	Pyrite	0.01	1.79
	Chalcopyrite	0.01	3.90
	Pyrrhotite	0.01	0.54
	Pentlandite	0.01	0.00
	Other sulphides	0.11	0.22
Silicates	Quartz	1.62	27.33
	K-Feldspar	0.34	1.40
	Mica	0.51	21.84
	Amphibole	2.17	0.07
	Plagioclase	17.08	35.15
Pyroxenes	Orthopyroxene	34.75	0.10
	Clinopyroxene	4.31	0.01
Alteration minerals	Chlorite	2.76	1.60
	Serpentine	0.76	0.00
	Talc	2.60	0.02
Fe-oxides	Chromite	30.71	0.20
	Other Fe-Ti oxides	1.98	3.05
Other	Calcite	0.19	2.61
	Other minerals	0.01	0.13
	Total	100.00	100.00

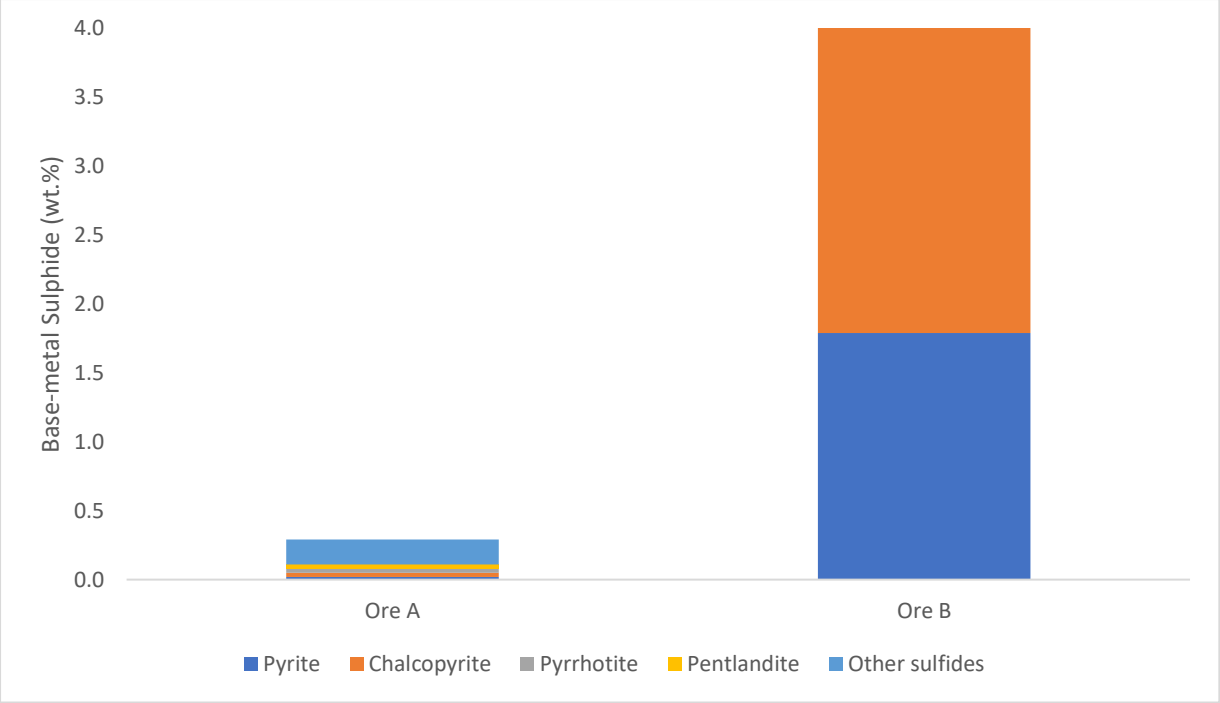

Figure 5.1: BMS proportions in ore feeds in wt.%.

5.1.2. BMS Liberation

QEMSCAN was used to evaluate the BMS minerals' liberation properties. This data will highlight the differences in liberation experienced by the three different grind sizes evaluated in this study. The minerals will oxidize in different ways depending on how liberated they are, and the extent of the mineral oxidation will subsequently be shown in the ore flotation recovery. Table 5.2 shows the changes in BMS liberation caused by different grind sizes from Ore A and Ore B.

The liberated BMS for Ore A increases slightly from 55.08% (from the grind size 40% -75 μm) to 59.57% (from the grind size 80% -75 μm) as shown in Table 5.2. Liberated BMS increases as the grind size becomes finer. The grind size 40% -75 μm has the highest locked BMS value (15.62%) compared to the other two grind sizes (14.37% and 12.92% for grind sizes 60% -75 μm and 80% -75 μm, respectively).

However, for Ore B, the liberated BMS has remained relatively constant throughout the three grind sizes. The grind size 80% -75 μm had the lowest locked BMS value (1.33%) compared to the other grind sizes (1.57% and 1.62% for grind sizes 60% -75 μm and 40% -75 μm respectively). Overall, Ore B has a higher Liberated BMS than Ore A.

QEMSCAN evaluated the overall percentage of liberated and unliberated BMS inside the feed to assess if the BMS contents within the feed may significantly dilute concentrate grade, and the findings are provided in Table 5.2. More than half of the total BMS mass is liberated within the feed for Ore A (55.09%, 57.07% and 59.75% for grind sizes 40% -75 μm, 60% -75 μm and 80% -75 μm respectively), whereas a lower percentage of BMS minerals is unliberated, as shown in Table 5.2.

As described in Chapter 2, the high amount of unliberated BMS in Ore A may have significant recovery repercussions during flotation, due to BMS interaction with gangue minerals. Majority of the BMS mass is liberated inside Ore B's feed, and just a smaller amount of the BMS remains unliberated (See Table 5.2). The high grades and high Cu recoveries indicate the degree of BMS liberation from Ore B.

Table 5.2: Liberated and unliberated BMS masses within the Ore A and Ore B feed.

	Ore A			**Ore B**		
Grind Size (-75 μm)	40%	60%	80%	40%	60%	80%
Liberated	55,09	57,07	59,75	84,45	83,12	84,10
Unliberated	44,91	42,93	40,25	15,55	16,88	15,90

5.1.3. Mineral Association

Figure 5.3 depicts the relationship of liberated BMS with other minerals in the feed for Ore A and Ore B. In Ore A, BMS is mostly associated with orthopyroxene, quartz, chromite, and other Fe-Ti oxides, accounting for 42.69% of the BMS throughout the three grind sizes. The interaction between BMS and other Fe-Ti oxides was also identified in the coarse particles.

The BMS in Ore B are mostly associated with quartz, mica, and other Fe-Ti oxides, accounting for 13.09 of the BMS association on average over the three grind sizes. Overall, the liberated BMS of Ore A are more closely associated with gangue than the BMS of Ore B. It is also important to note that in Ore A the BMS have a higher association percentage with Other Fe-Ti oxides than the BMS of Ore B. The "other Fe-Ti oxides" minerals include all of the oxidation minerals, related iron oxides, and other altered minerals such as titanium oxides. This is most likely where all oxidation products are grouped.

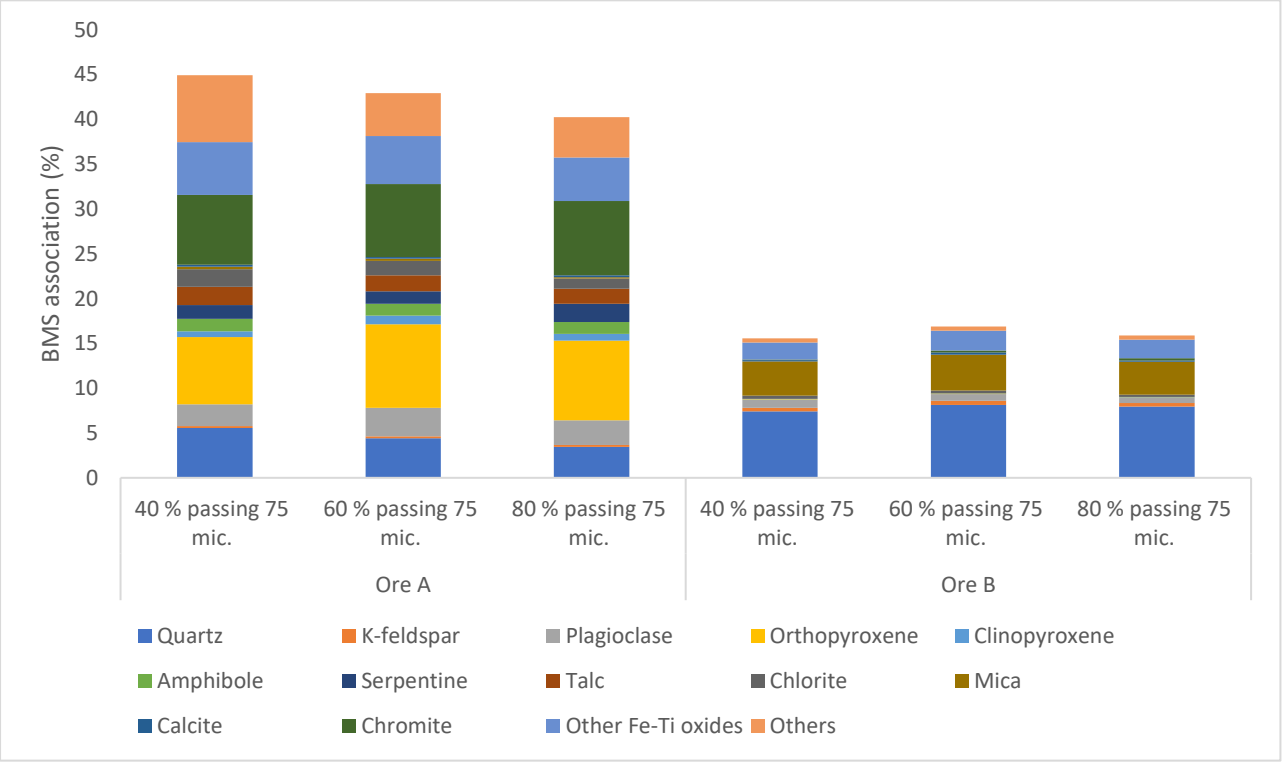

Figure 5.2: Association of liberated BMS in the Ore A and Ore B feed.

5.2. Batch Flotation

The flotation responses were evaluated using the following parameters: water recovery and total solids recovery, copper and nickel recovery and grade for Ore A, and copper recovery and grade for Ore B. The findings are split into two parts. Section 5.2.1 presents the results for Ore A, whereas Section 5.2.2 presents the results for Ore B. The accuracy of the tests was expressed using standard error analysis, which is depicted by error bars on the graphs. According to the UCT Standard Batch Flotation Procedure, the standard error in solids recovery should be not more than 5% of the total amount of solids recovered, and the standard error in water recovery should be no more than 10% of the total amount of water recovered. All batch float data given in this thesis had an estimated standard error that was found to be within acceptable parameters. Each Flotation test was duplicated, to ensure that results were reproducible

5.2.1. The influence of grind size on the flotation response of Ore A

5.2.1.1. Water and solids recovery

Figure 5.3 and Figure 5.5 illustrate the effect of grind size on the recovery of water and solids to the concentrate. Figure 5.5 depicts solids recovery as a function of water recovery whereas Figure 5.6 displays the influence of grind size on final water and solids recovery. As can be observed in Figure 5.3 and Figure 5.6, the rate of water recovery increased as the grind became finer. The grind size of 80% -75 μm yielded the highest final recovered water (440.32 g), followed by grind sizes of 60% -75 μm and 40% -75 μm, which yielded 383.31 g and 347.16 g, respectively. Figure 5.4 also demonstrates that as the grind got finer, more solids were recovered; the coarsest grind size (40% -75 μm) yielded the lowest solid recovery (36.82 g), while the finest grid size (80% -75 μm) obtained the highest recovered solids (59.58). Figure 5.5 illustrates that the rate of solid and water recovery increased as the grind became finer for ore A. The grind size 80% -75 μm has the highest water and solid recovery, followed by grind sizes 60% -75 μm and 40% -75 μm respectively.

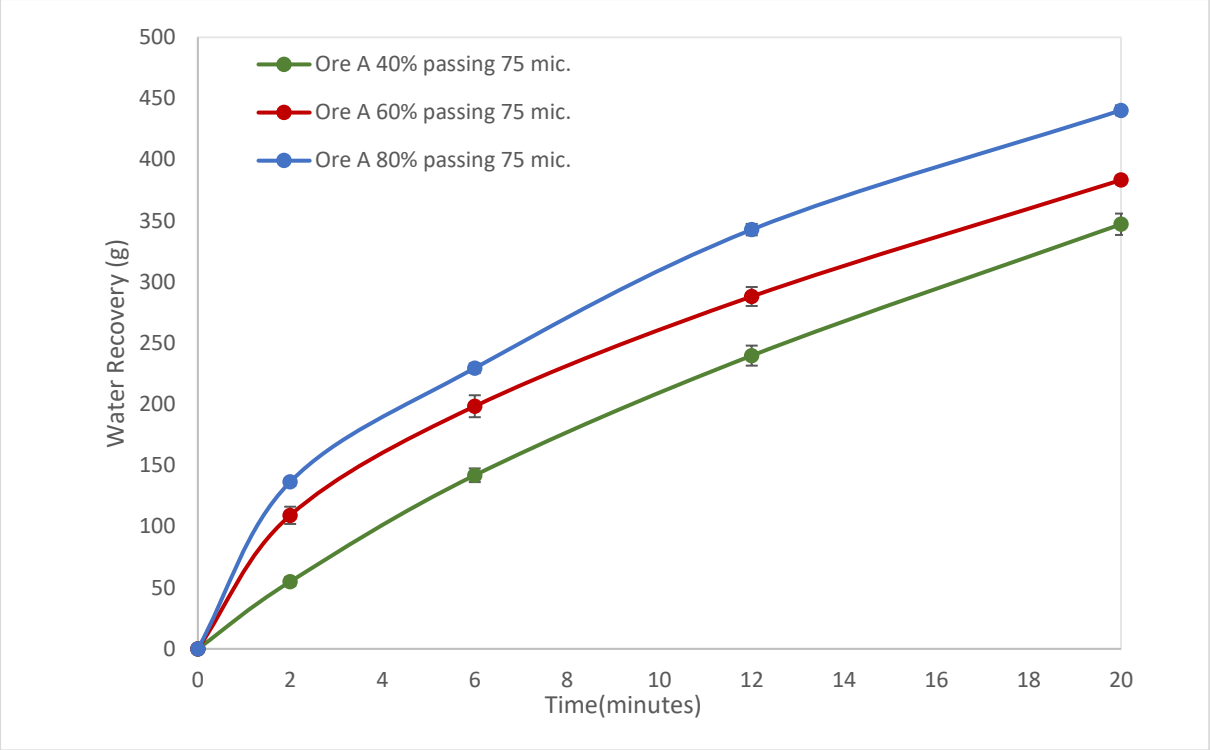

Figure 5.3: Water Recovery against time for Ore A floats (Error bars represent standard error between duplicate tests).

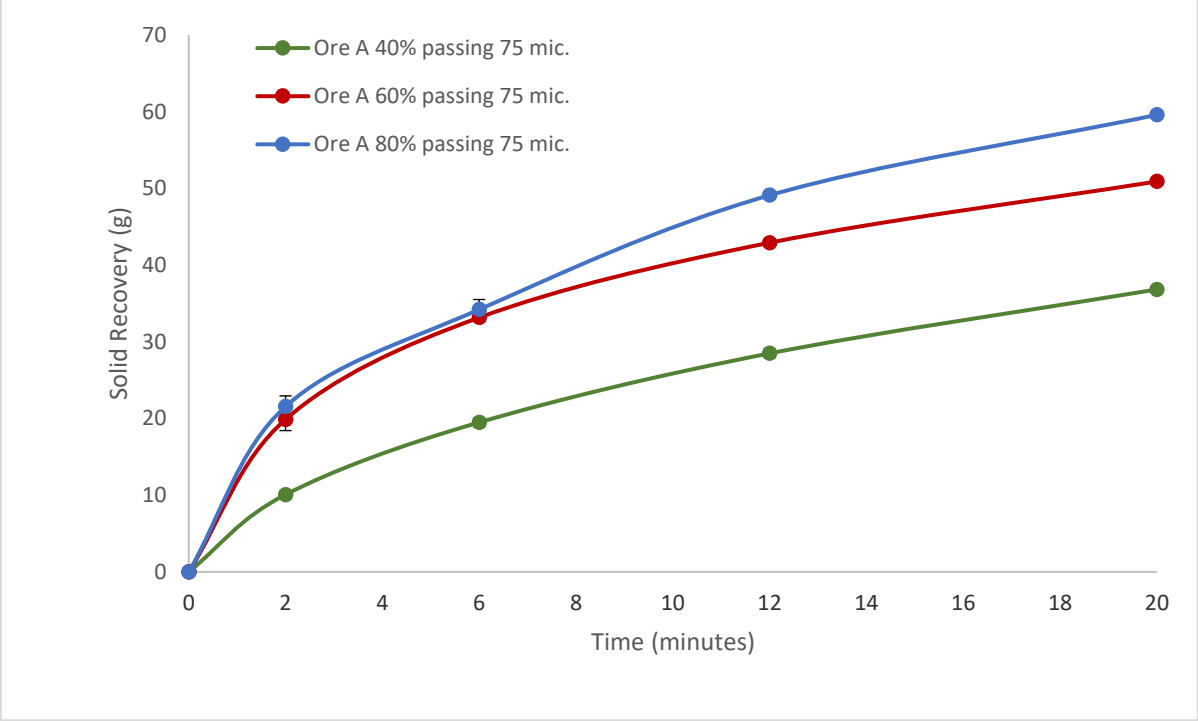

Figure 5.4 Solid recovery against time for Ore A floats (Error bars represent standard error).

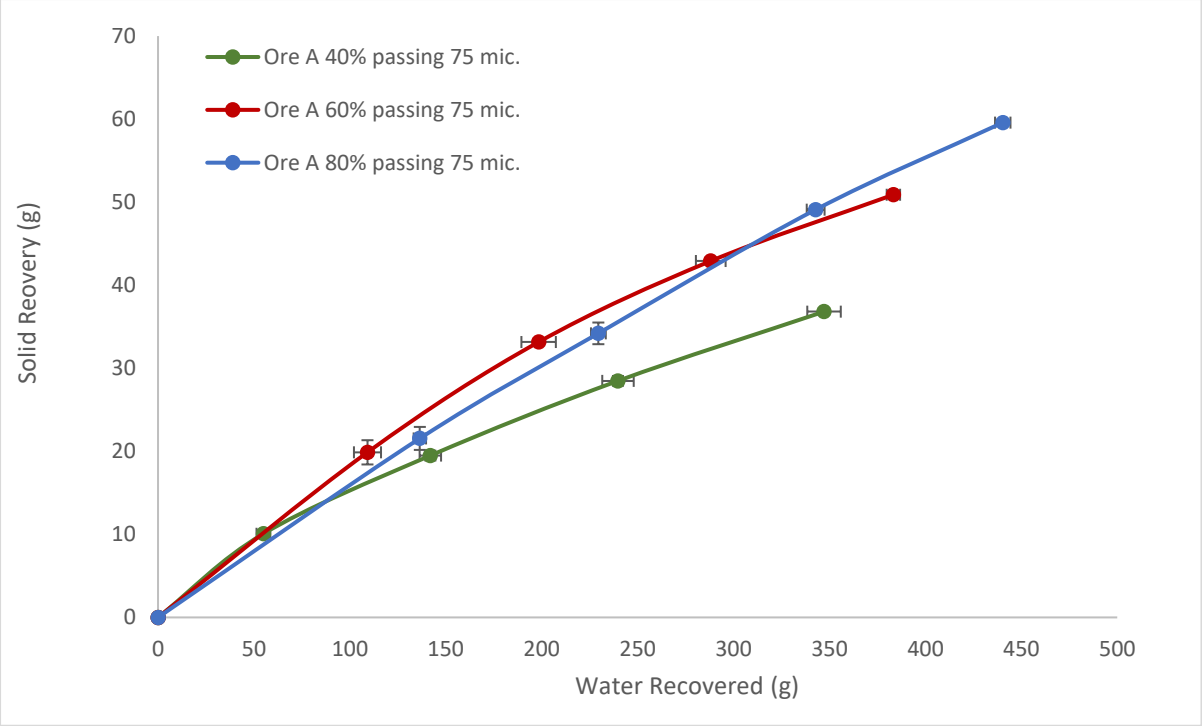

Figure 5.5: Recovered solids against water recovery for Ore A for grind sizes, 40% -75 µm, 60% -75 µm, and 80% -75 µm. (Error bars represent standard error).

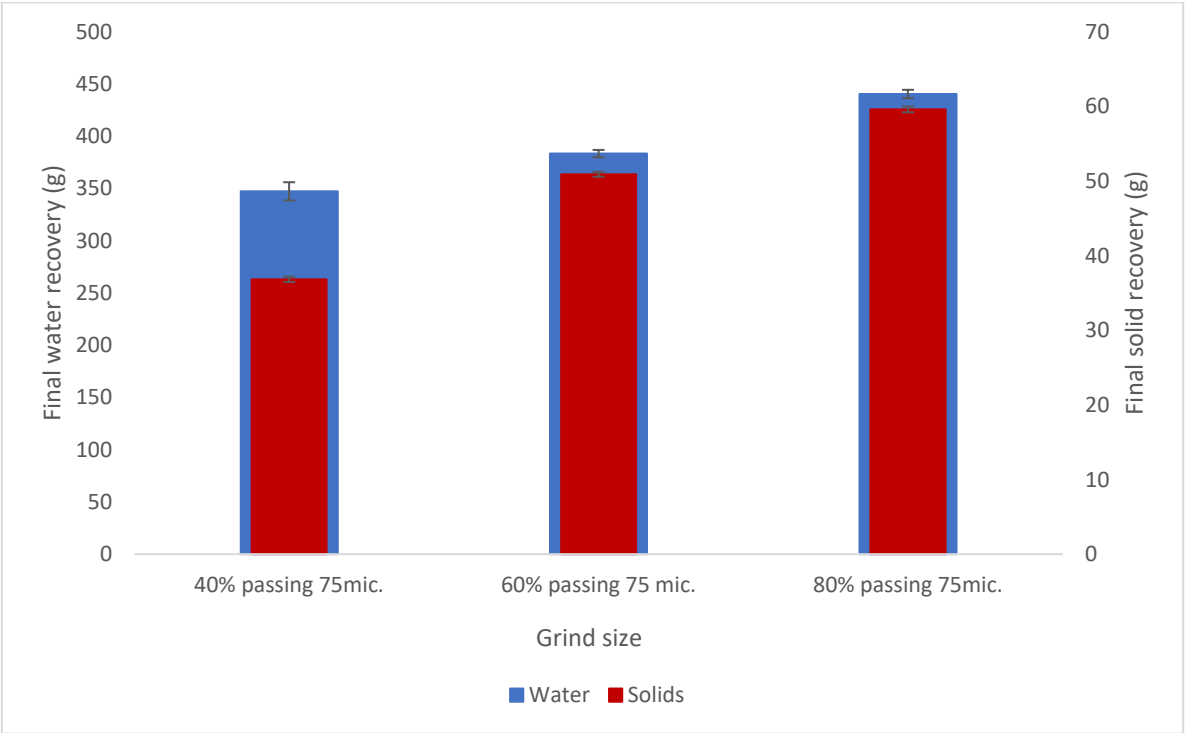

Figure 5.6: Final solids vs water recovered for Ore A for grind sizes, 40% -75 µm, 60% -75 µm, and 80% -75 µm. (Error bars represent standard error).

5.2.1.2. Cu Recovery and Grade

Figure 5.7, Figure 5.8 and Figure 5.9 show the Ore A Cu recovery and grade for all tested grind sizes. The highest Cu recovery was obtained when the ore was milled to achieve the particle size distribution of 60% -75 µm (59.53%). The grind size 40% -75 µm obtained the second highest Cu recovery (55.80%), and 80% -75 µm the lowest (52.04%). However, results also show that the highest Cu grade was obtained from the coarsest grind size of 40% -75 µm (0.15%), and grind sizes 60% -75 µm and 80% -75 µm have almost the same grade (0.12% and 0.11% respectively). In as much as the highest Cu recovery is obtained from the grind size 60% -75 µm, the amount of gangue recovered increases as the ore becomes more liberated, lowering the grade. Therefore, due to the high solids that were recovered for the grind sizes 60% -75 µm and 80% -75 µm (including gangue mineral recovery) Cu grade decreased slightly as the grind size became finer.

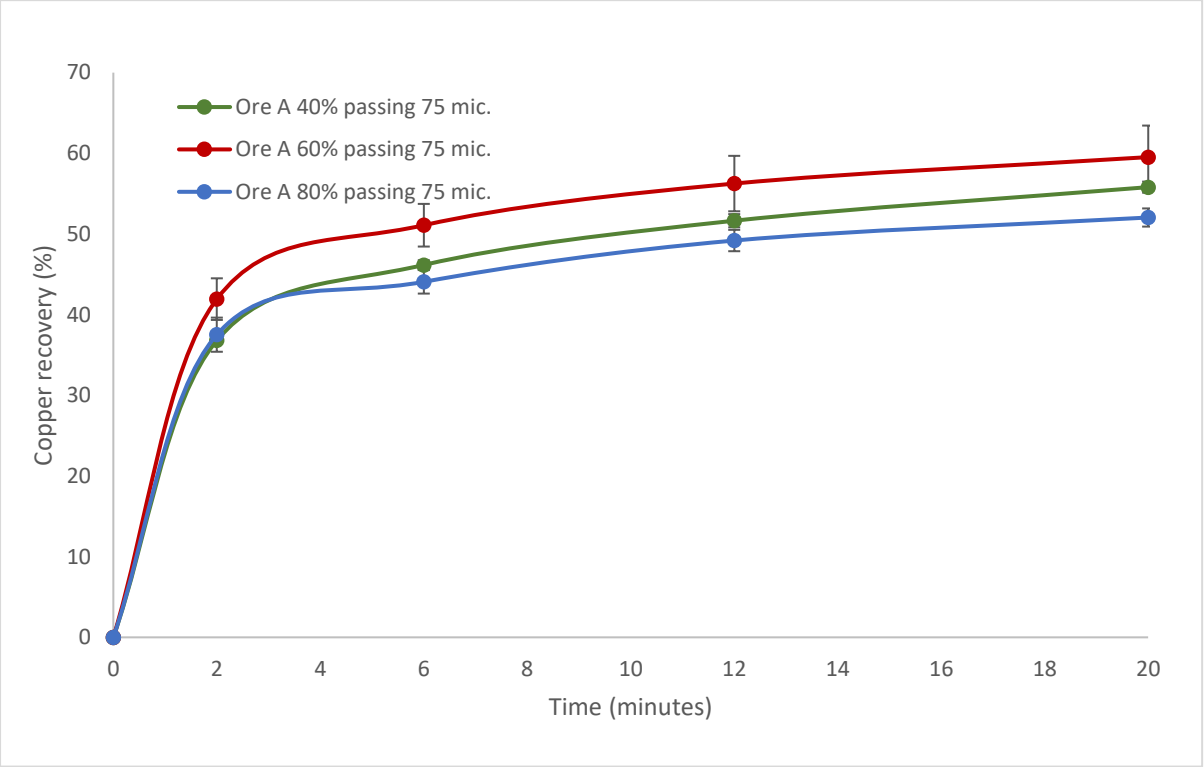

Figure 5.7: Copper recovery against time for Ore A for grind sizes, 40% -75 µm, 60% -75 µm, and 80% -75 µm. (Error bars represent standard error).

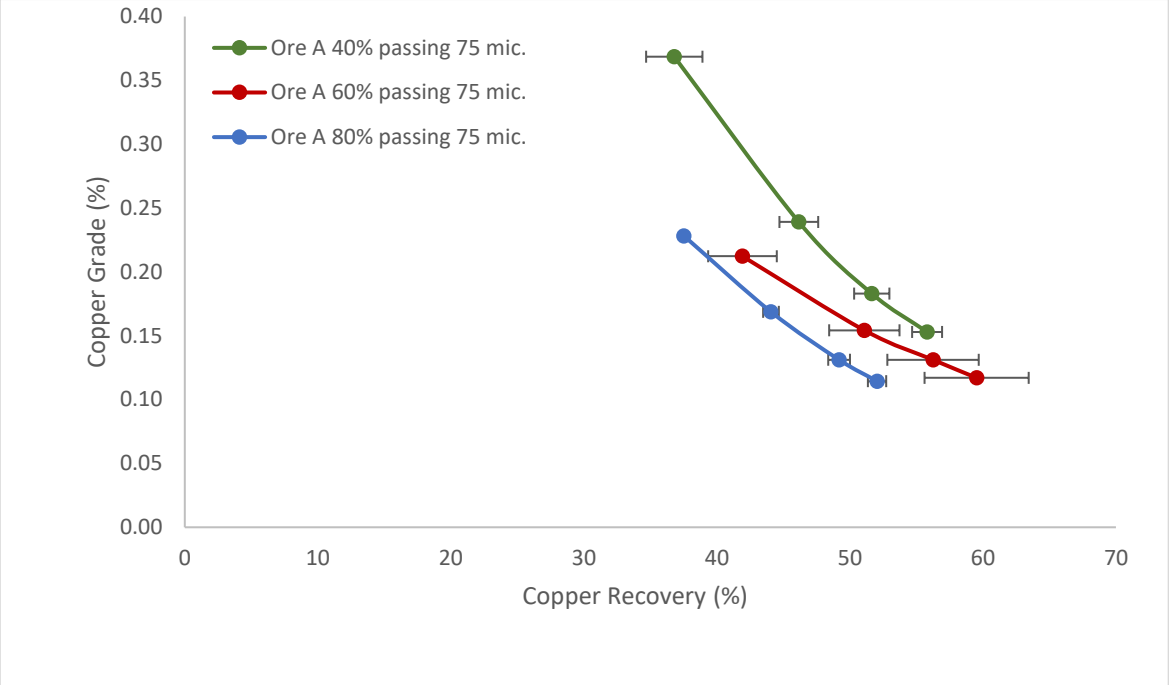

Figure 5.8: Copper grade against copper recovery for Ore A for grind sizes, 40% -75 µm, 60% - 75 µm, and 80% -75 µm. (Error bars represent standard error).

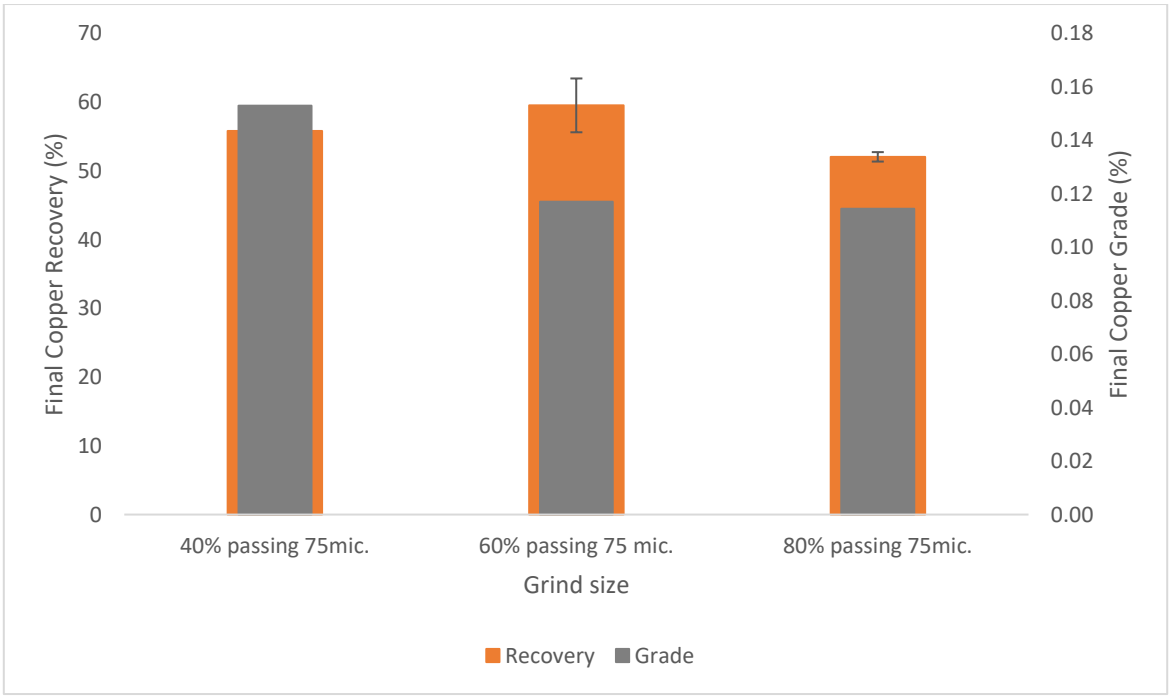

Figure 5.9: Final copper grade against recovery for the grind sizes 40% -75 µm, 60% -75 µm, and 80% -75 µm. (Error bars represent standard error).

5.2.1.3. Ni Recovery and Grade

Figure 5.10 – Figure 5.12 shows the flotation performance of Ni at three different grind sizes in terms of Ni recovery, Ni grade/recovery, and final grade and recovery values. The highest Ni recovery was obtained after milling the ore to achieve a particle size distribution of 60% -75 µm (15.59%). Ni

recovery decreased slightly as the ore was ground finer to achieve the particle size distribution of 80% -75 μm (12.51%). The lowest Ni recovery was achieved by the coarsest grind size, 40% -75 μm (10.86%). Figure 5.12 shows that the coarsest grind size (40% -75 μm) achieved the highest grade, while the other two grind sizes (60% -75 μm and 80% -75 μm) revealed their grades to be relatively stable (0.29% and 0.28% respectively). Ni grade increased as the grind size became coarser.

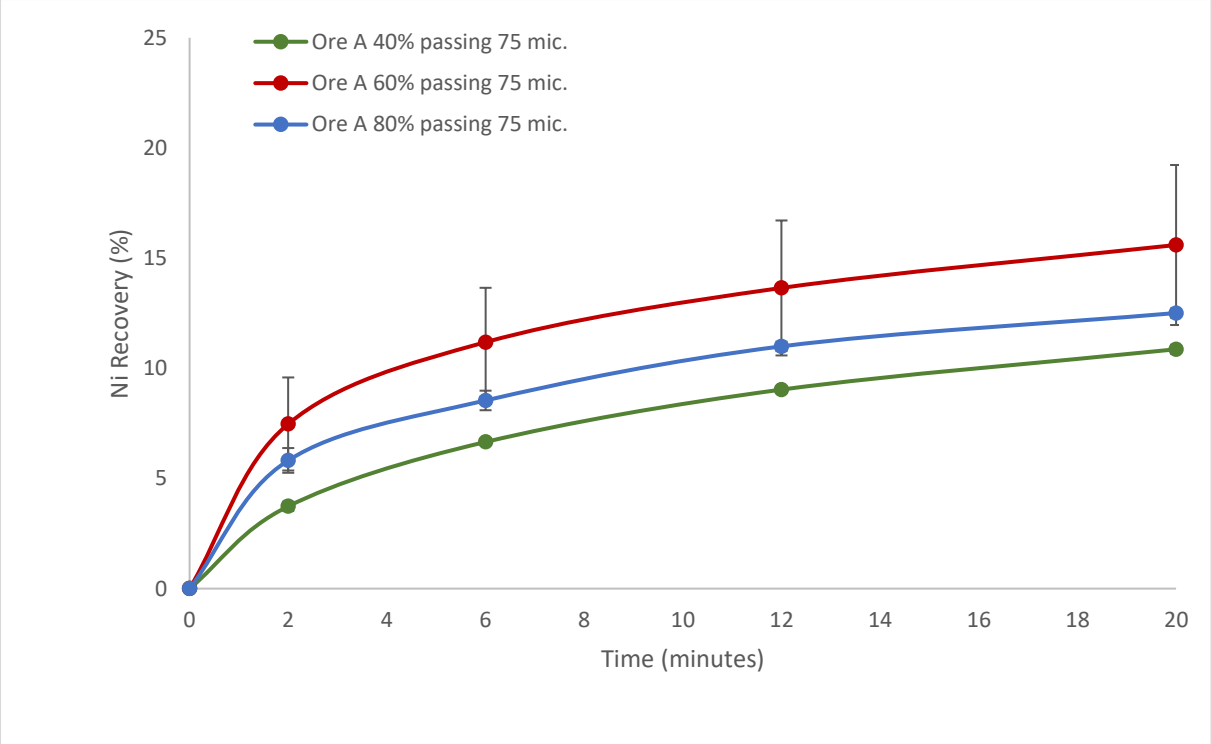

Figure 5.10: Nickel recovery against time for Ore A for grind sizes, 40% -75 μm, 60% -75 μm, and 80% -75 μm. (Error bars represent standard error).

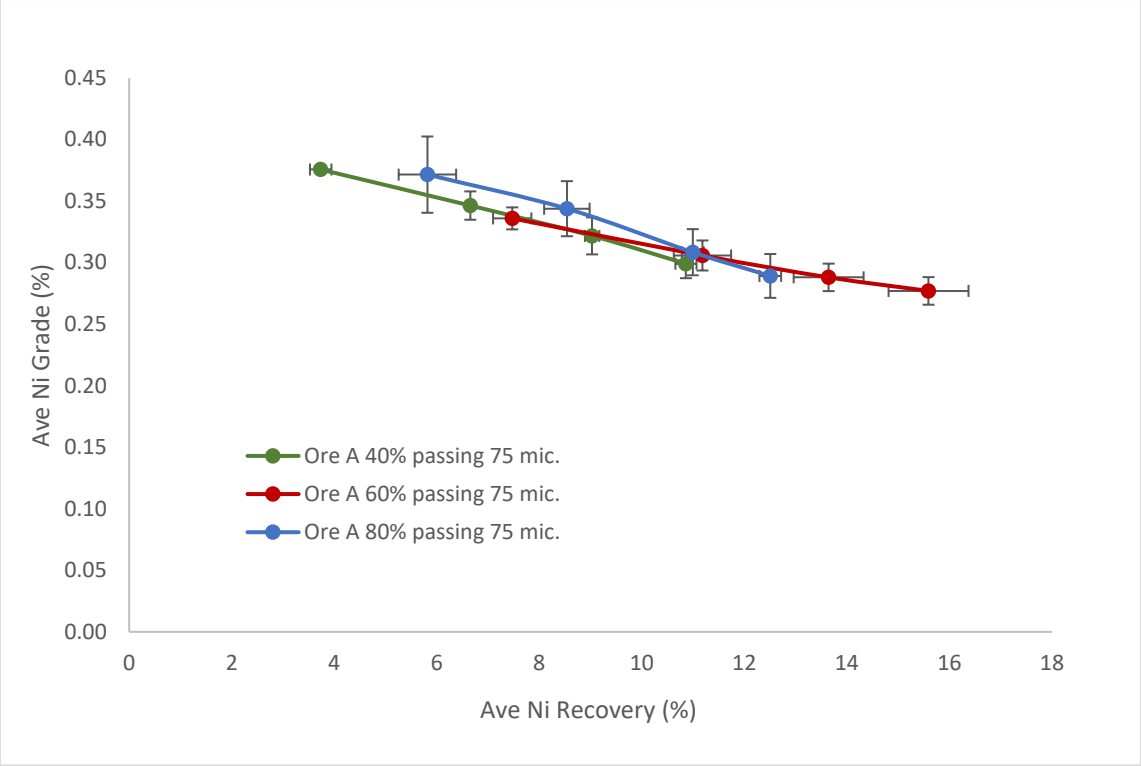

Figure 5.11: Nickel grade against copper recovery for Ore A for grind sizes, 40% -75 µm, 60% -75 µm, and 80% -75 µm. (Error bars represent standard error).

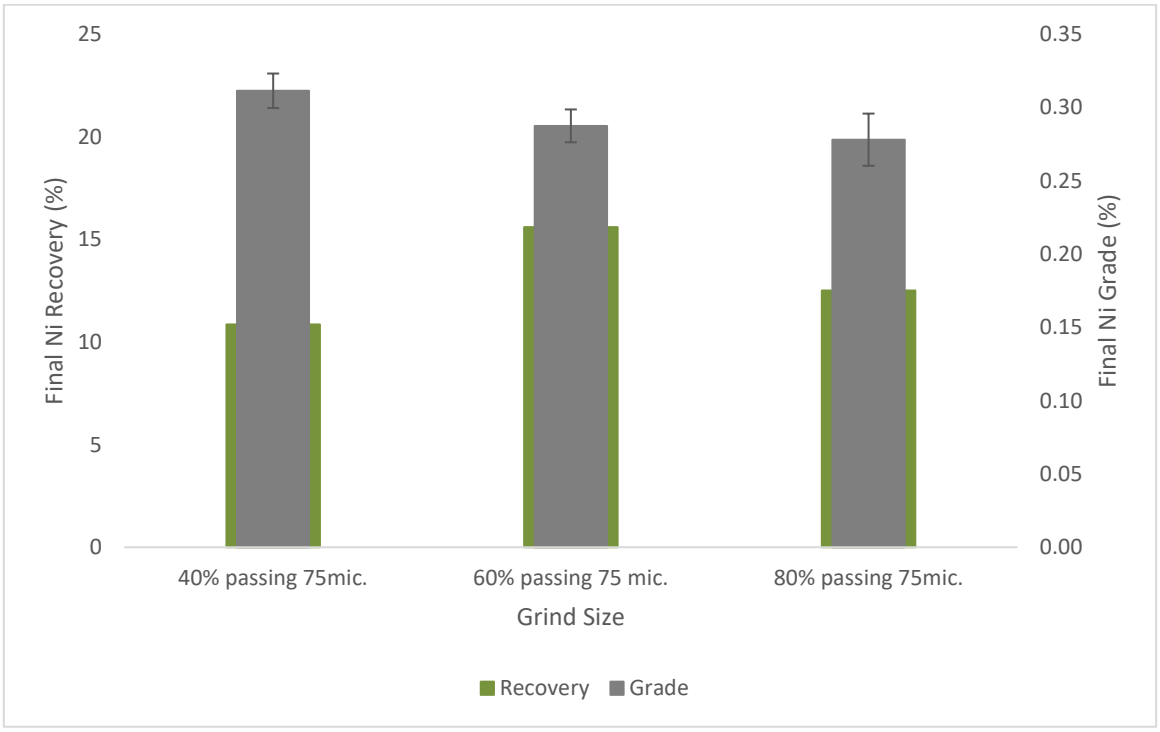

Figure 5.12: Final Nickel grade against recovery for the grind sizes 40% -75 µm, 60% -75 µm, and 80% -75 µm. (Error bars represent standard error).

5.2.2. The influence of grind size on the flotation response of Ore B

5.2.2.1. Water and solids recovery

Figure 5.13 shows the influence of grind size on the recovery of water to the concentrate for a dose of 50 g/t SIBX and 40 g/t Dow200, and Figure 5.15 shows the effect of grind size on the recovery of solids. Figure 5.16 shows solids recovery as a function of water recovery, whereas Figure 5.16 shows the effect of grind size on final water and solids recovery.

Figure 5.14 and Figure 5.15 show that increased water recoveries were accompanied by increases in solids recoveries, as seen in the Ore A solids/water trends. However, Ore B produced greater water and solid materials, compared to Ore A runs.

Figure 5.14 and Figure 5.17 indicate that as the grind grew finer, the rate of water recovery increased. The grind size of 80% -75 μm produced the highest final recovered water (578.44 g), followed by grind sizes of 60% -75 μm and 40% -75 μm, which produced 459.29 g and 341.23 g, respectively. Figure 5.15 also shows that as the grind size became finer, more solids were recovered; the coarsest grind size (40% -75 μm) produced the lowest solid recovery (89.30 g), while the finest grid size (80% -75 μm) produced the maximum recovered solids (150.69 g). The grind size 60% -75 μm fell somewhat in the middle for both solids and water recovery (459.29 g and 117.10 g for water and solids recovery, respectively). The grind size 60 % -75 μm came within the centre of the other two grind sizes for both solids and water recovery (459.29 g and 117.10 g for water and solids recovery, respectively)

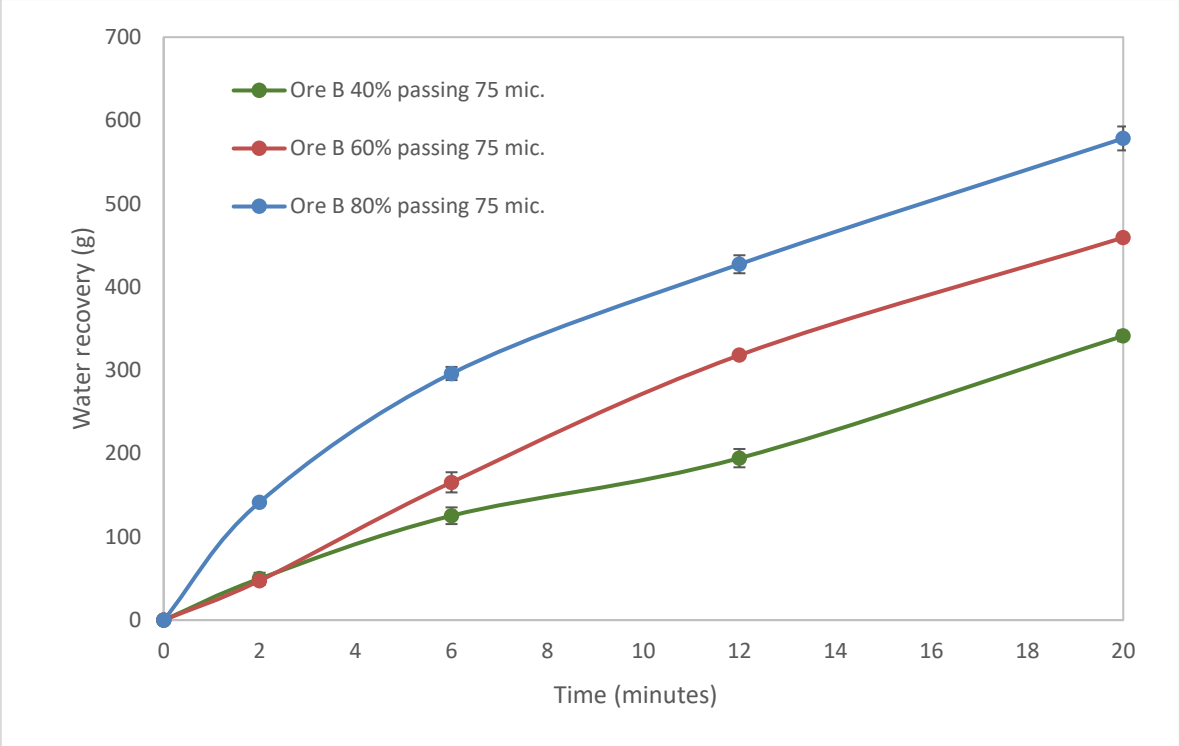

Figure 5.13: Water recovery against time for Ore B (Error bars represent standard error).

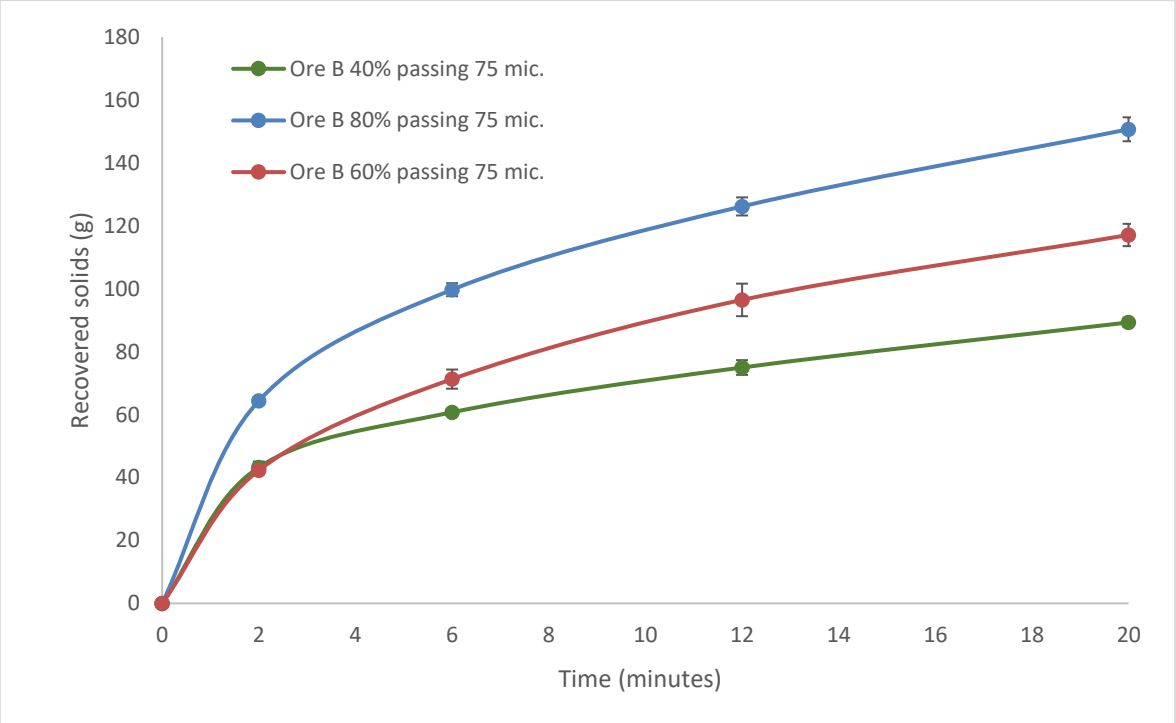

Figure 5.14: Solid recovery against time for Ore B (Error bars represent standard error).

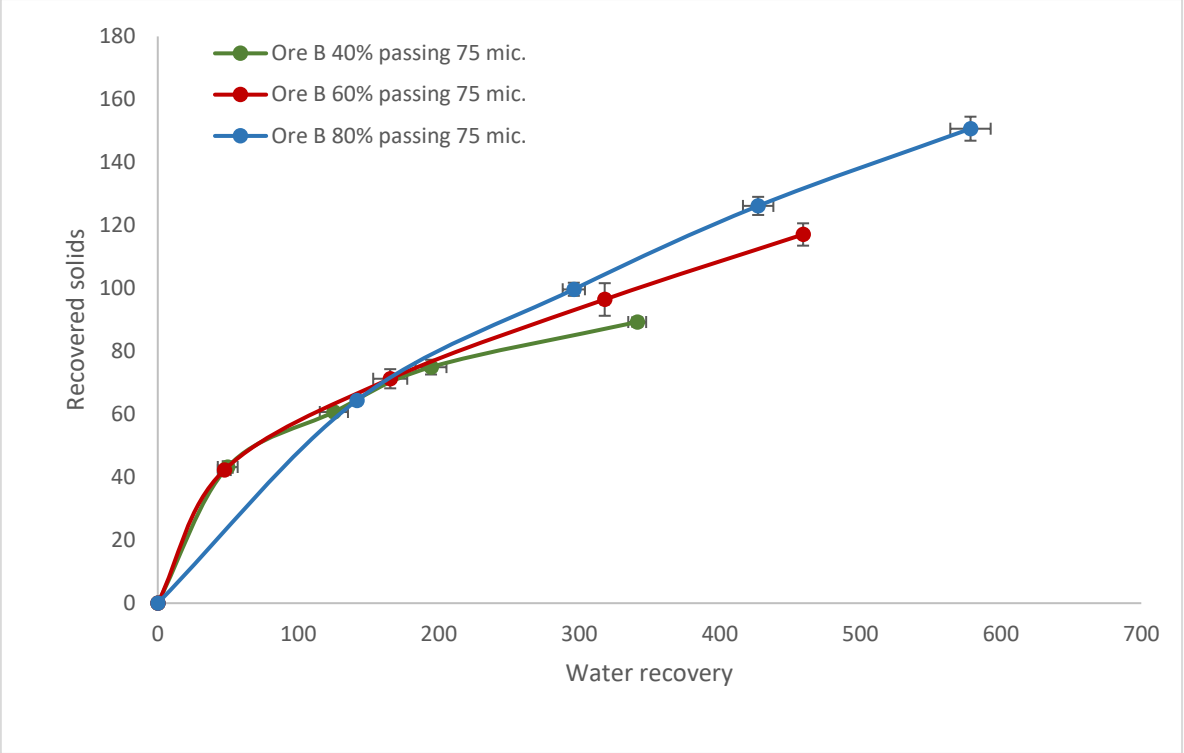

Figure 5.15: Recovered solids against water recovery for Ore B for grind sizes, 40% -75 µm, 60% -75 µm, and 80% -75 µm. (Error bars represent standard error).

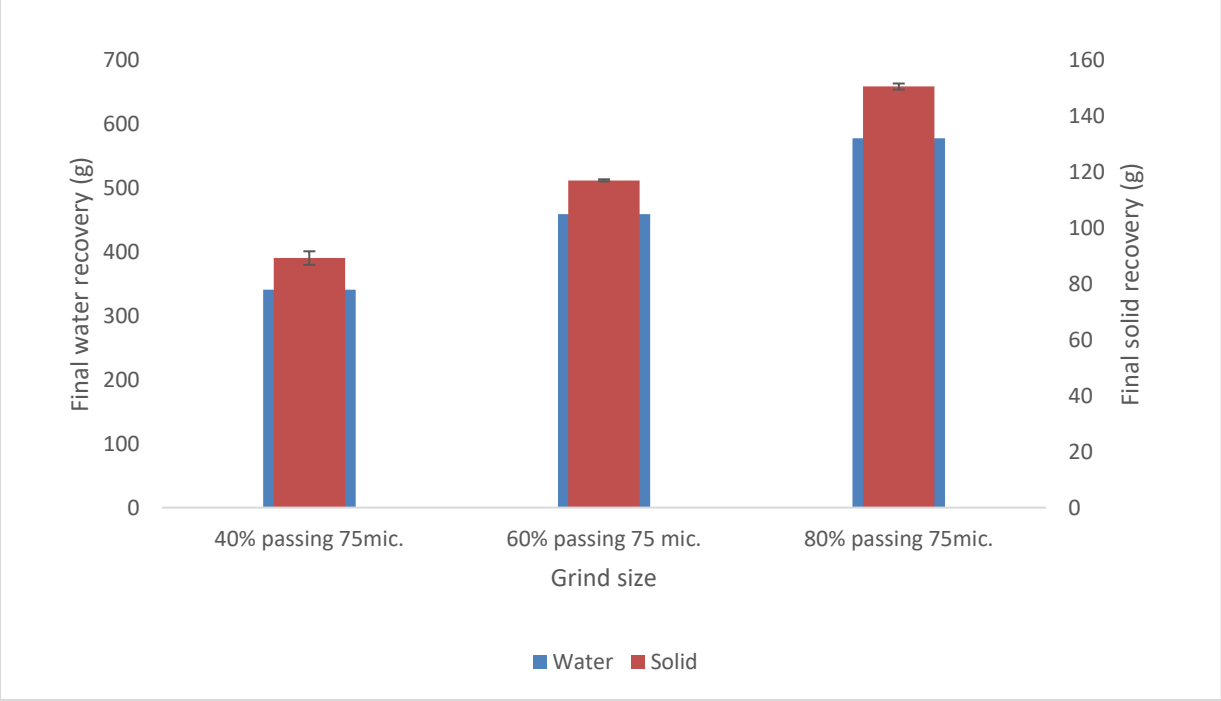

Figure 5.16: Total solids vs water recovered for Ore B for grind sizes, 40% -75 µm, 60% -75 µm, and 80% -75 µm. (Error bars represent standard error).

Figure 5.17 shows copper recovery to the concentrate, as a function of flotation time for Ore B in all tested grind sizes. Figure 5.18 depicts the copper grade vs. recovery curve, whereas Figure 5.19 depicts the final grade and recovery for Ore B. These figures show that copper recoveries and grades were

higher for Ore B than Ore A. Results also show that the highest Cu recovery was reached in the grind size 80% -75 µm (95.12%), whereas the highest final grade was produced in the grind size 40% -75 µm. (12.23%). Grind sizes 60% -75 µm and 40% -75 µm recovered 92.25% and 90.86% Cu recoveries respectively. It is evident that Cu recovery increased with a decrease in grind size (as the grind became finer) and grade was highest for the coarsest grind size. The Cu recovery for Ore B achieved from the grind size of 80% -75 µm, is directly proportional to the solid and water recovery from the same grind size. Cu recovery and grade increased as the ore became more liberated.

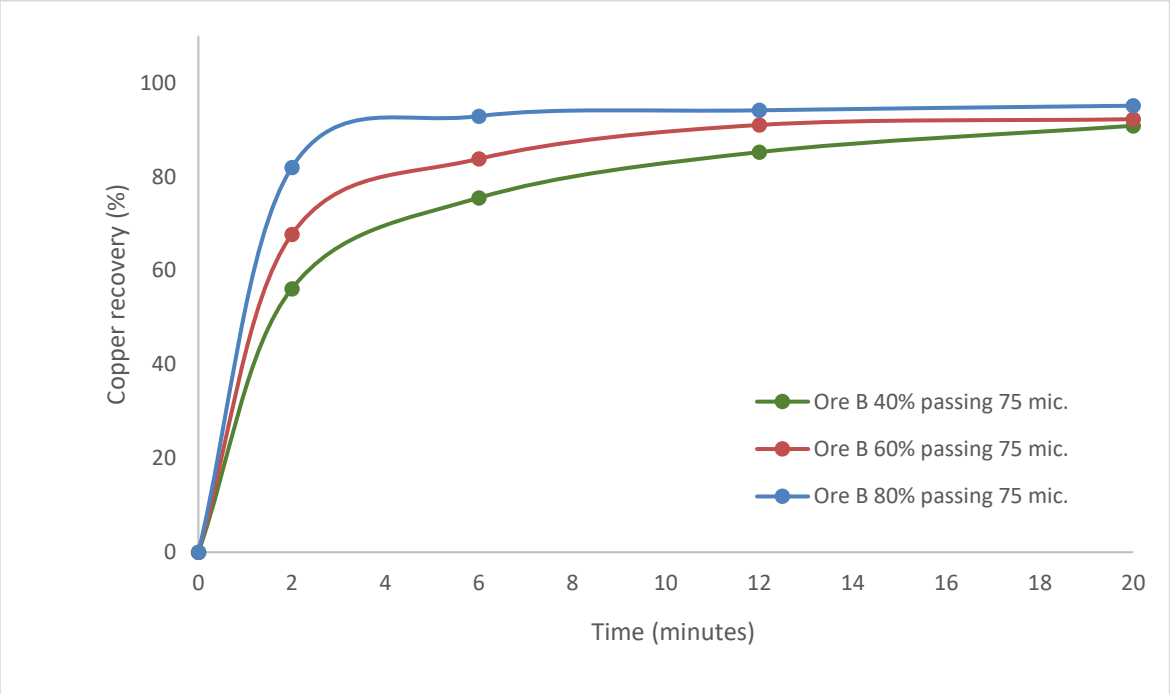

Figure 5.17: Copper recovery against time for the grind sizes 40% -75 µm, 60% -75 µm, and 80% -75 µm for Ore B. (Error bars represent standard error).

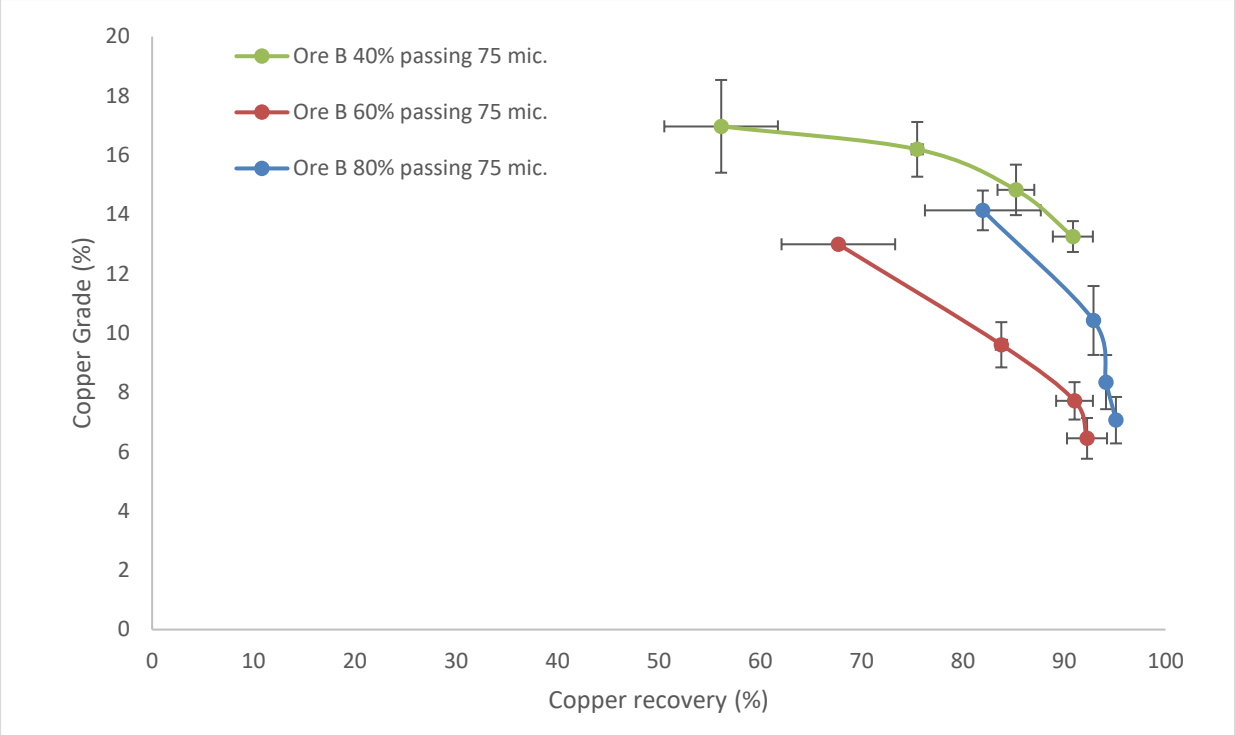

Figure 5.18: Copper grade against copper recovery for grind sizes 40% -75 µm, 60% -75 µm, and 80% -75 µm, for Ore B. (Error bars represent standard error).

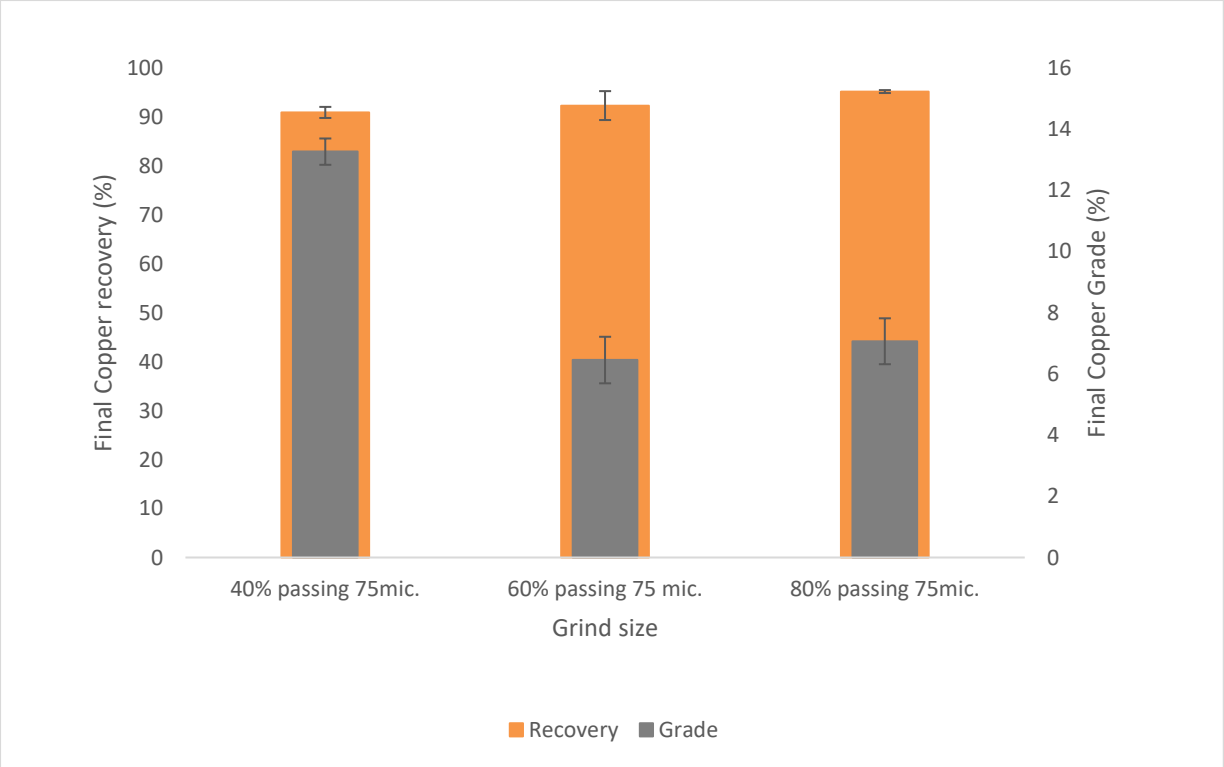

Figure 5.19: Final copper grade against recovery for the grind sizes 40% -75 µm, 60% -75 µm, and 80% -75 µm for Ore B (Error bars represent standard error).

5.3. Reactivity Number experiments for feed and tails samples

A series of reactivity tests were carried out to determine the Reactivity Number (RN) for Ore A and Ore B. The RN findings as well as the calculated Oxygen Consumption Factor (OCF) for each of the three grind sizes investigated are shown below.

5.3.1. Ore A reactivity tests for feed and tails samples

5.3.1.1. Feed samples

The natural dissolved oxygen (DO) content of the Ore A slurry prior to oxygen spiking was 6.89 ppm, 5.05 ppm, and 6.47 ppm for grind sizes 40% - 75 µm, 60% - 75 µm, and 80% - 75 µm respectively, as shown in Figure 5.21. The pH was not adjusted for all feed experiments, and the natural pH of Ore A was 9.15 on average across all three grind sizes. Figure 5.21 depicts an increase in DO content as the sample was spiked with oxygen for 3 minutes, followed by a steady decrease when the oxygen source was switched off.

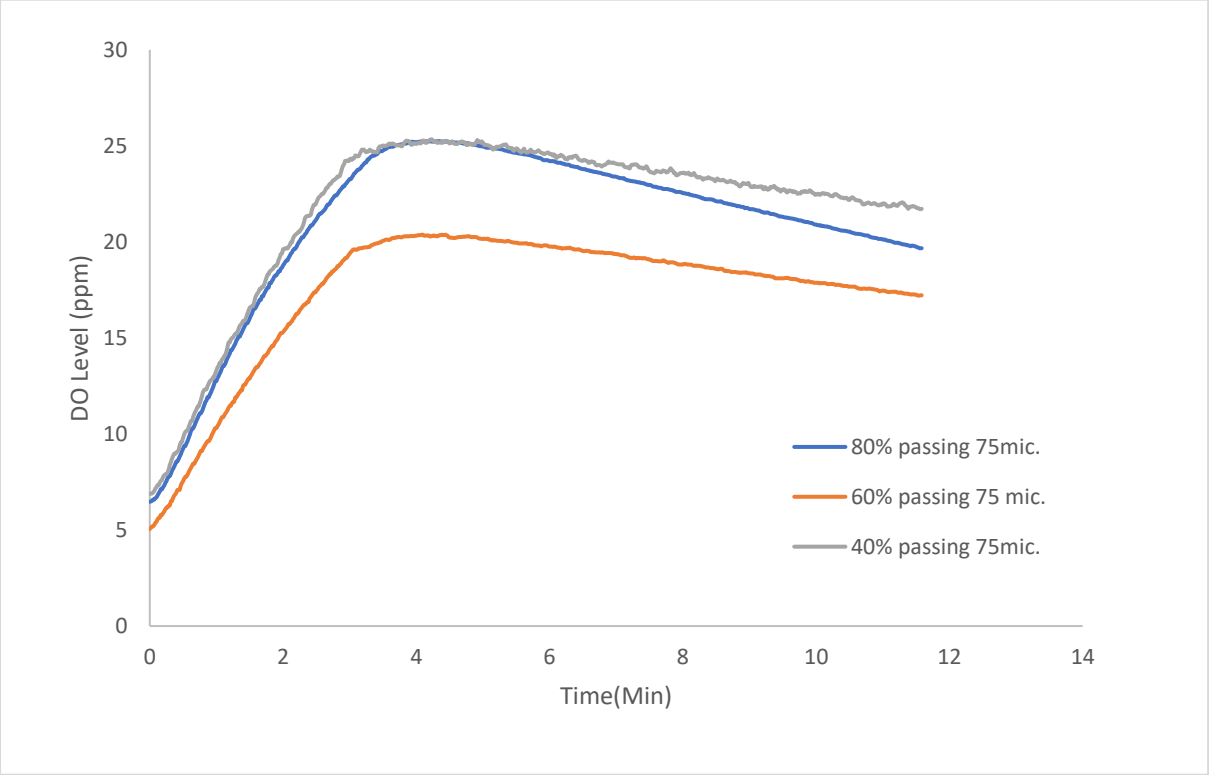

Figure 5.20: Change in DO content with time for Ore A slurry feed sample. The results for the three different grind sizes are shown.

The maximum DO content reached for the 40% - 75 µm experiment was 25.35 ppm, which was slightly higher than the maximum DO content obtained for the 80% -75 µm experiment (25.25 ppm), but lower than the maximum DO contents for 60% -75 µm experiment (20.38 ppm). However, of the three grind sizes, 40% -75 µm has the highest final reading, going from DO max of 25.35 ppm to 21.72 ppm DO final (see *Table 5.3*). The DO max content of the grind size 60% -75 µm was 20.38 ppm, which

decreased to 17.22 ppm final DO content. Of the three grind sizes, the grind size 80% -75 µm consumed the most oxygen (DO max 25.25 ppm – DO final 19.68 ppm = 5.57 ppm).

Table 5.3: Summary of the initial, maximum, and final DO contents obtained for the 'Ore A' feed sample reactivity tests for the various grind sizes.

	DO INITIAL (PPM)	DO MAX (PPM)	DO FINAL (PPM)
80% -75 µm	6.47	25.25	19.68
60% -75 µm	5.05	20.38	17.22
40% -75 µm	6.89	25.35	21.72

5.3.1.2. Tails samples

Following oxygen spiking, the DO content of the tails samples increased to 34.88 ppm for 40% -75 µm, 22.92 ppm and 19.98 ppm for 80% - 75 µm and 60% - 75 µm respectively. DO content then decreased for all the three grinds, indicating oxygen consumption. The final DO content of grind size 60% - 75 µm was 16.14 ppm, followed by grind sizes 80% - 75 µm and for 40% -75 µm with final DO contents of 19.73 ppm and 24.58 ppm respectively.

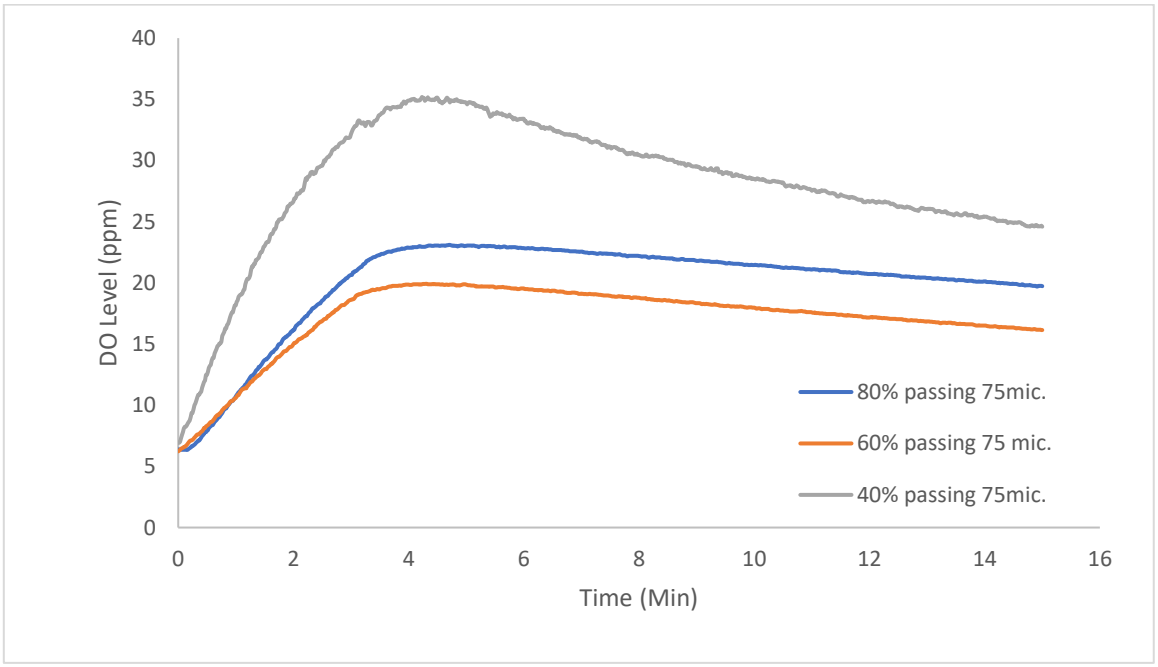

Figure 5.21: Change in DO content with time for Ore A tails samples. Results are shown for the three different grind sizes.

The DO content for Ore A tails samples showing the initial, maximum and the final DO content is shown in Figure 5.22 and Table 5.4. Prior to the oxygen spiking, the pH ranged between 8.85 ppm and 8.90 ppm with all 3 grind sizes. The natural DO content was 6.39 ppm, 6.23 ppm and 6.92 ppm for the grind sizes 80% -75 µm, 60% -75 µm, and 40% - 75 µm, respectively, as shown in Table 5.4.

Table 5.4: Summary of the initial, maximum, and final DO contents obtained for the 'Ore A' tails sample reactivity tests for the various grind sizes.

	DO INITIAL (PPM)	DO MAX (PPM)	DO FINAL (PPM)
80% -75 µm	6,39	25,10	19,73
60% -75 µm	6,23	19,88	16,14
40% -75 µm	6,92	35,10	24,58

5.3.1.3. Oxygen Consumption Factor

The OCF for Ore A (for the feed and tails samples) are illustrated in Figure 5.23. Figure 5.23 shows that the highest OCF of the feed sample was 3.6 for the grind size 80% -75 µm, while the lowest OCF was 2.2 for the grind size 40% -75 µm. Despite having the lowest initial DO content, the grind size 60% -75 µm had a higher OCF than the grind size 40% -75 µm (2.4). The OCF decreased with increasing particle size, with the grind size with the smallest particle size having the highest OCF.

The change in OCF for the tails samples followed a pattern that was the opposite of what was seen in the feed sample experiments. For instance, the OCF for the grind size 80% -75 µm was the lowest of the tails samples and it increased from 1.6 to 2.0 at 60% -75 µm. A further increase in OCF was observed as particle size increased to 3.8 at 40% -75 µm. The OCF for the tails samples increased as the particle size of Ore A became bigger. The OCF for Ore A grind size 80% - 75 µm decreased by 2.0 (from 3.6 to 1.6) from the feed to the tails experiments, while the grind size 60% -75 µm decreased by 0.4 (from 2.4 feed to 2.0 tails). However, the OCF for the grind size 40% -75 µm increased by 1.6 (from 2.2 to 3.8), following an opposite trend to the other grinds.

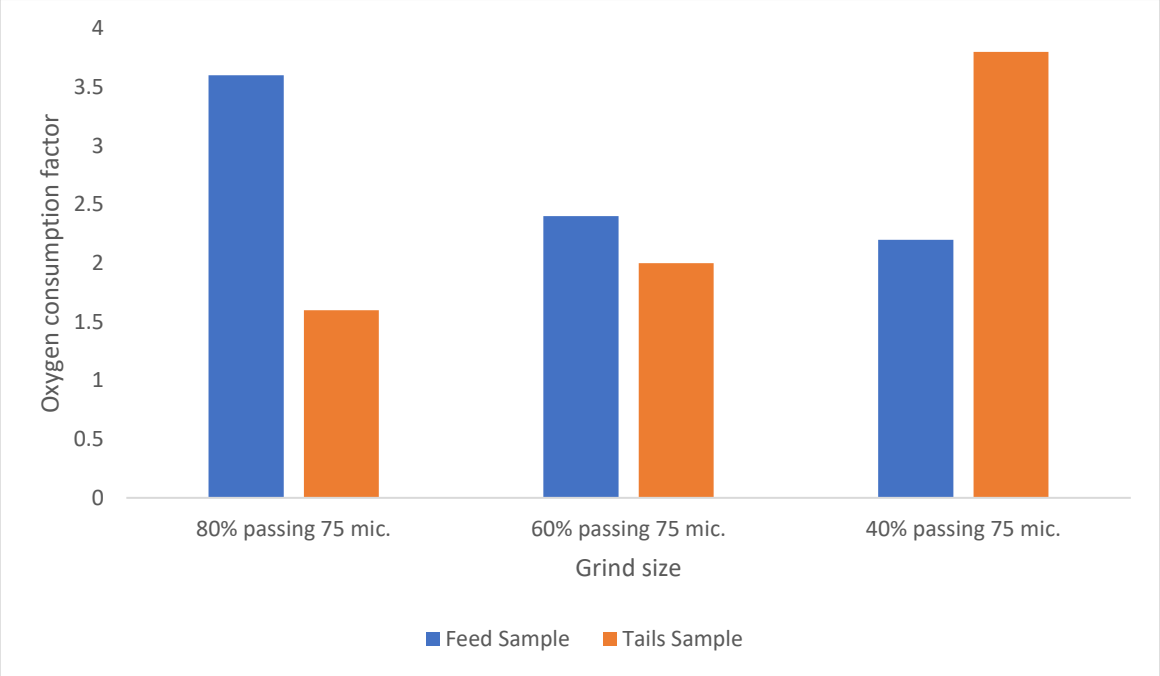

Figure 5.22: The calculated OCF for Ore A (feed and tails samples).

5.3.2. Ore B reactivity tests for feed and tails samples

5.3.2.1. *Feed samples*

Figure 5.23 shows the DO content for Ore B feed samples. The pH of Ore B feed samples was 8.3; 8.5; and 8.8 for grind sizes 80% -75 µm, 60% -75 µm, and 40% -75 µm respectively. Prior to oxygen spiking, the natural DO content for Ore B feed samples was 8.91 ppm, 8.64 ppm, and 3.12 ppm for grind sizes 40% -75 µm, 60% -75 µm, and 80% - 75 µm respectively. Following oxygen spiking, the feed slurry's DO content increased gradually, reaching a maximum of 24.56 ppm for the grind size 40% -75 µm, and 23.32 ppm for the grind size 60% -75 µm. The grind size 80% -75 µm had a slightly lower maximum DO content of 17.80 ppm.

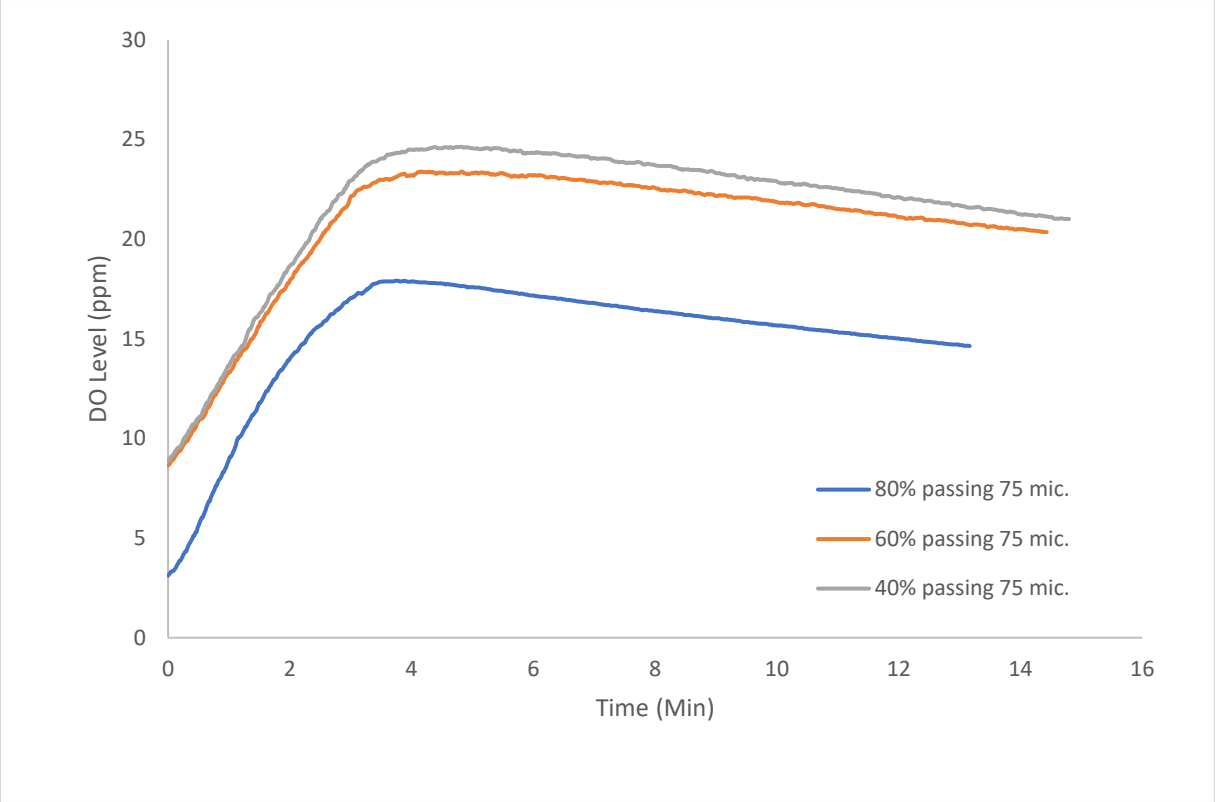

Figure 5.23: Change in DO content with time for the Ore B feed samples. Results are shown for the three different grind sizes.

Prior to the oxygen spiking, the pH ranged between 8.85 ppm and 8.90 ppm with all 3 grind sizes. The natural DO content (DO Initial) was 3.12 ppm, 8.64 ppm and 8.91 ppm for the grind sizes 80% -75 µm, 60% -75 µm, and 40% - 75 µm, respectively, as shown in Table 5.5 The final DO readings were 14.64 ppm, 20.71 ppm and 21.58 ppm of grind sizes 40% -75 µm, 60% -75 µm, and 80% - 75 µm respectively. Overall, the grind size obtained to achieve the finest grind size had the lowest initial DO Initial, max, and final readings, whereas the coarsest grind size had the highest DO Initial, max, and final readings.

Table 5.5: Summary of the initial, maximum and final DO contents obtained for the Ore B feed reactivity tests for the various grind sizes.

	DO INITIAL (PPM)	DO MAX (PPM)	DO FINAL (PPM)
80% -75 µm	3.12	17.90	14.64
60% -75 µm	8.64	23.30	20.71
40% -75 µm	8.91	24.64	21.58

5.3.2.2. *Tails samples*

Figure 5.25 and *Table 5.6* show that the natural DO float sample content was quite different, with 60% -75 µm, and 80% -75 µm having DO content that is in the same range (4.07 ppm and 3.73 ppm

respectively) and 40% - 75 µm having the highest natural DO content of 10.02 ppm. The grind sizes 60% -75 µm and 80% - 75 µm had the lowest DO content prior to oxygen spiking compared to the experiments from Ore A as well as Ore B feed sample.

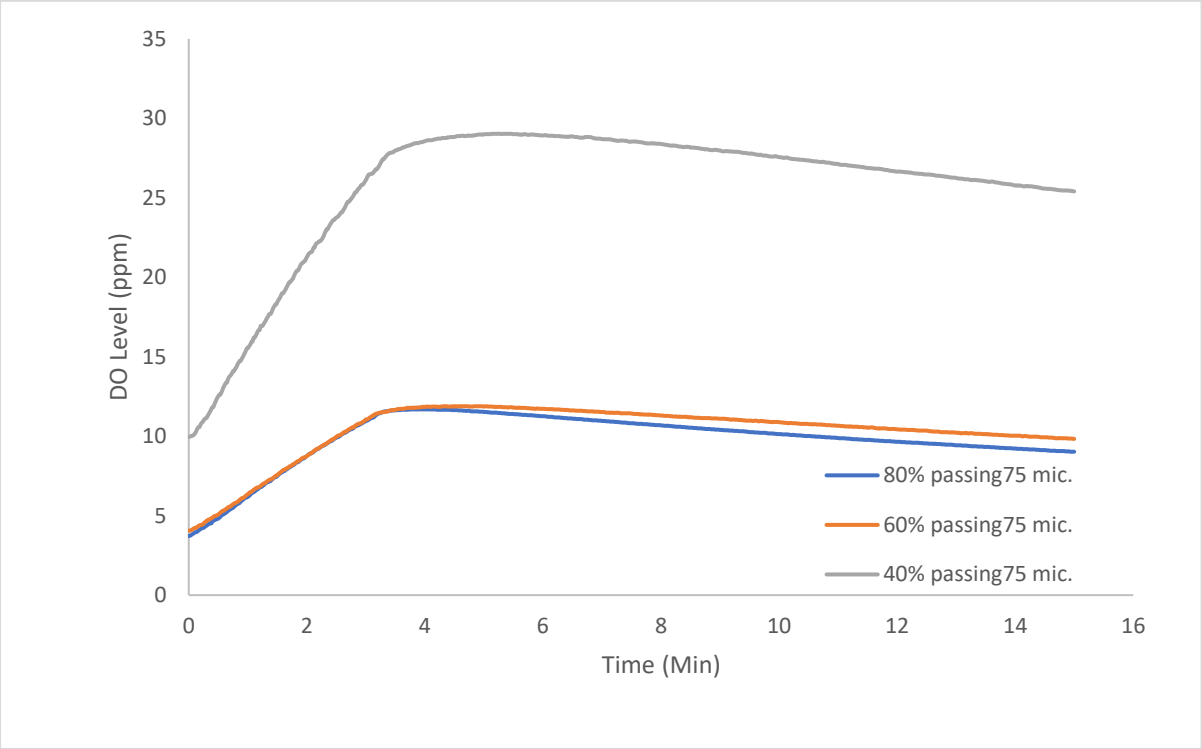

Figure 5.24: Change in DO content with time for Ore B float samples. Results are shown for the three different grind sizes.

Following the spiking of Ore B tails samples with oxygen, the maximum DO contents were 11.69 ppm and 11.89 ppm for grind sizes 80% -75 µm, and 60% -75 µm respectively, while the maximum DO content reached for the 40% -75 µm was the highest (29.01 ppm). The final DO content of grind size 80% - 75 µm was 9.02 ppm, followed by grind sizes 60% - 75 µm and for 40% -75 µm with final DO contents of 9.83 ppm and 25.40 ppm respectively.

Table 5.6: Summary of the initial, maximum and final DO contents obtained for the Ore B tails reactivity tests for the various grind sizes.

	DO INITIAL (PPM)	DO MAX (PPM)	DO FINAL (PPM)
80% -75 µm	3.73	11.69	9.02
60% -75 µm	4.07	11.89	9.83
40% -75 µm	9.96	29.01	25.40

5.3.2.3. *Oxygen Consumption Factor*

The rate of DO consumption for Ore B, as quantified by the calculated OCF is shown in Figure 5.25. The feed and tails sample OCFs for the grind size 40% -75 µm were 1.5 and 1.3 respectively, while the OCFs for the grind sizes 80% -75 µm and 60% -75 µm were 1.4 and 1.8 for the grind size 60% -75 µm, and 2.3 and 2.6 for the grind size 80% -75 µm. For the feed samples, the grind size 80% -75 µm had the quickest decline of dissolved oxygen with time (OCF = 2.3), followed by the grind size 40% -75 µm which had a somewhat slower decay (OCF =1.5), and the grind size 60% -75 µm had the slowest decay (OCF = 1.4).

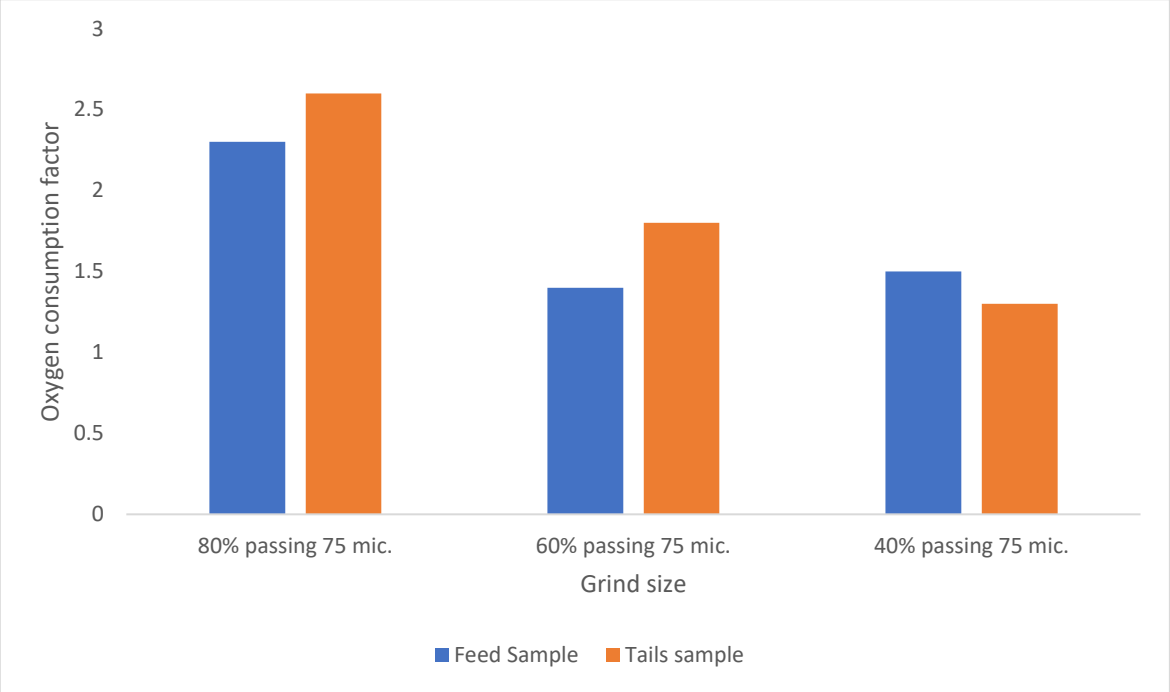

Figure 5.25: The calculated Oxygen Consumption factors for Ore B (feed and tails samples).

When the OCF values for Ore B feed and tails experiments were examined, the feed sample tests with the highest natural DO content had the lowest OCF values. Although the OCF for the tails (OCF = 2.6 and 1.8 for grind sizes 80% - 75 µm and 60% -75 µm respectively) samples were higher than the feed samples (OCF = 2.3, 1.4 for 80% -75 µm and 60% -75 µm respectively) they followed the same trend

of decreasing with increasing particle size. This trend was however only followed by grind sizes 60% -75 µm and 80% -75 µm. The feed sample OCF for the grind size 40% -75 µm was 0.1 greater than the OCF for the grind size 60% -75 µm.

5.4. EDTA

5.4.1. Ore A EDTA extraction tests for feed and tails samples

Filtrates, a blank EDTA sample, and a blank plant water sample were all submitted for testing for EDTA extraction experiments, and the findings are presented in this section.

5.4.1.1. *Feed samples*

Surface oxidation and/or the presence of EDTA extractable secondary Cu ions were variable, with the highest value of 0.15 mg/L obtained from the grind size 80% -75 µm, followed by 0.13 mg/L obtained from the grind size 60% -75 µm. From the grind size 40% -75 µm, the lowest value of isolated Cu secondary oxidation products was 0.09 mg/L. The amount of EDTA extractable Cu and Ni increased as the particle size became smaller (See Figure 5.27).

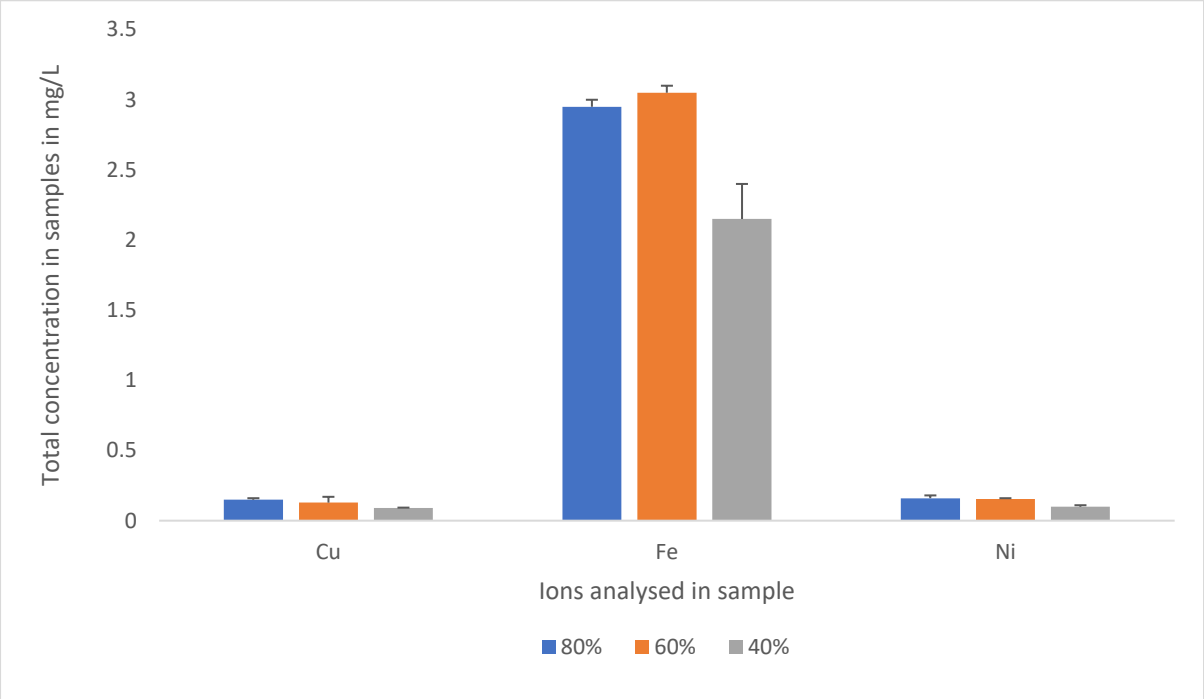

Figure 5.26: EDTA extraction experiment results obtained for Ore A feed samples (Error bars represent standard error).

Feed samples of Ore A have much greater EDTA extractable Fe than the other metals. The highest amount of EDTA extractable Fe is 3.05 mg/L for the grind size 60% - 75 µm, followed by 2.95 mg/L for the grind size 80% -75 µm and then the lowest amount of EDTA extractable Fe is 2.15 mg/L for the grind sizes 40% -75 µm. The EDTA extractable Fe values did not follow the same trend as the EDTA extractable Cu values.

The EDTA extractable Ni values followed the same trend as the EDTA extractable Cu values in that the values increased as the particle size became finer. The EDTA extractable Ni values were also more or

less equal to the EDTA extractable Cu values, which could mean that Cu and Ni have similar compositions and can be related to mineralogy.

For Ore A tails samples, the EDTA extractable Cu values also increased as the particle size became smaller (Figure 5.27). The EDTA extractable Cu values for the grind size 80% -75 µm was the highest (0.19 mg/L), followed by 60% -75 µm (0.07 mg/L) and 40% -75 µm (0.07 mg/L) respectively. The EDTA extractable Fe values followed a similar trend to Ore A feed samples in that the highest EDTA extractable Fe value was from the grind size 60% -75 µm (3.25 mg/L), followed by grind size 80% -75 µm (2.40 mg/L) and 40% -75 µm (2.31 mg/L) respectively. The EDTA extractable Ni value for the grind size 60% -75 µm was 0.12 mg/L, while the EDTA extractable Ni value for the other two grind sizes was the same (0.10 mg/L for both 80% -75 µm and 40% -75 µm).

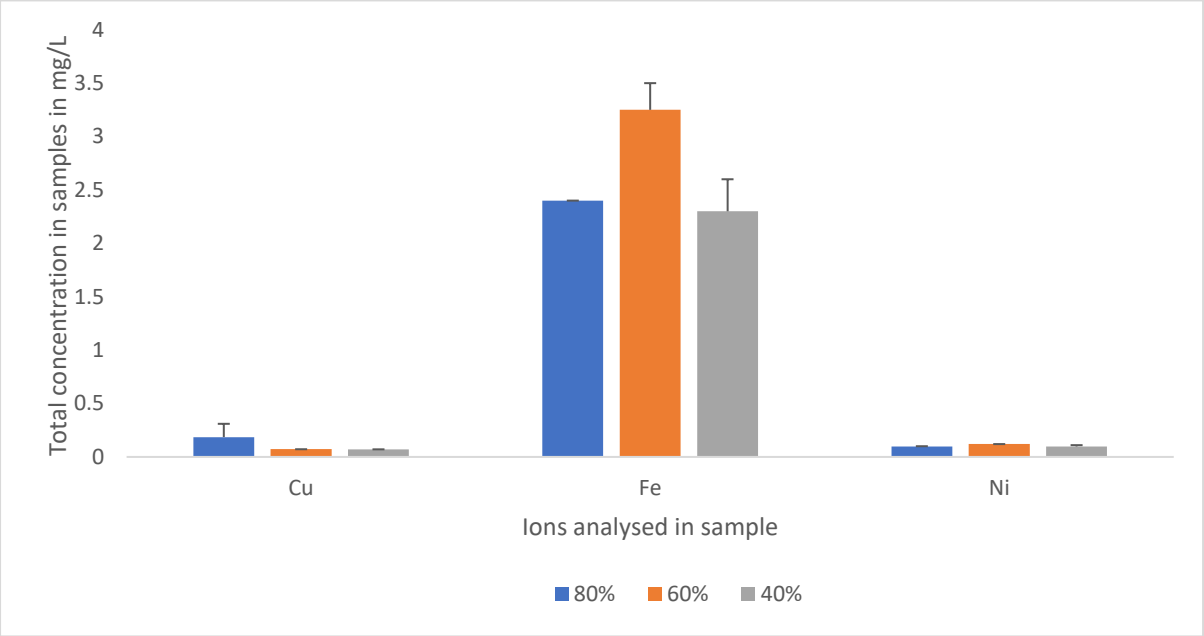

Figure 5.27: EDTA extraction experiment results obtained for Ore A tails samples. (Error bars represent standard error).

The trends seen in Ore A feed and tails samples for EDTA extractable Cu and EDTA extractable Ni levels are consistent with the results obtained by batch floats and minerology. Figure 5.27 and Figure 5.28 demonstrate that the grind size 60% -75 µm achieved the lowest EDTA extractable Cu and Ni levels, and batch flotation data show that the grind size 60% -75 µm achieved the highest Cu and Ni recoveries. Figure 5.27 and Figure 5.28 also reveal that the grind size with the lowest Cu and Ni recoveries, 80% -75 µm, yielded the highest EDTA extractable Cu and Ni values.

5.4.2. Ore B EDTA extraction tests for feed and tails samples

5.4.2.1. *feed samples*

Figure 5.29 shows the cumulative final EDTA extractable values for Ore B's feed samples for the tested conditions. It is clear that the EDTA values for Ore B are higher than the EDTA values from Ore A. This is mainly because Ore B is a high-grade ore. It can also be seen that EDTA values for Cu and Fe increase as the particle size becomes smaller.

The highest EDTA extractable Cu value was 8.1 mg/L from the grind size 80% - 75 µm, followed by 6.81 mg/L from 60% -75 µm. The lowest value of EDTA extractable Cu secondary oxidation products was 5.10 mg/L from the grind size 40% -75 µm.

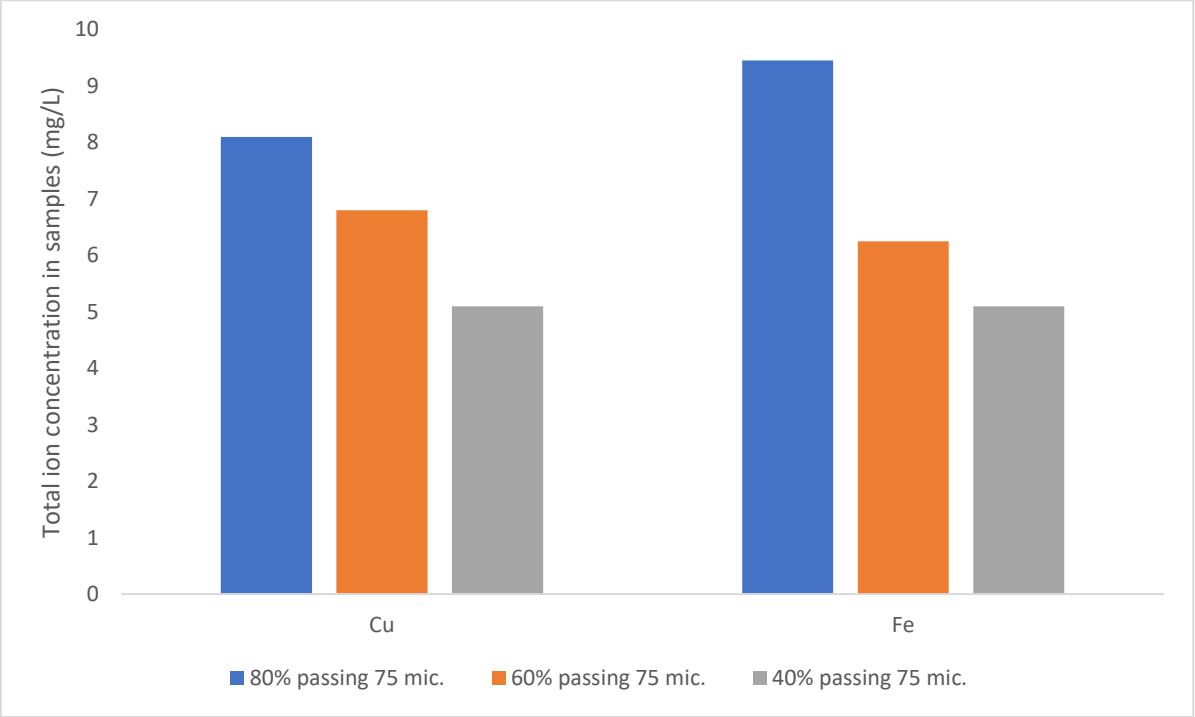

Figure 5.28: EDTA extraction experiment results obtained for Ore B feed samples. (Error bars represent standard error).

5.4.2.2. *Tails samples*

The cumulative final EDTA values for Ore B tails samples were generally lower than the feed sample values. The highest Cu EDTA value was 3.15 mg/L from the grind size 80% -75 µm, followed by the 2.60

mg/L from 60% -75 µm. The lowest value of EDTA extractable Cu secondary oxidation products was 2 mg/L from the grind size 40% -75 µm (Figure 5.29).

Fe EDTA values of 6.35 mg/L were obtained from a grind size of 80% -75 µm, followed by 4.65 mg/L from a grind size of 60% -75 µm. From the grind size 40% -75 µm, the lowest value of EDTA extractable Fe secondary oxidation products was 3.20 mg/L. (Figure 5.29).

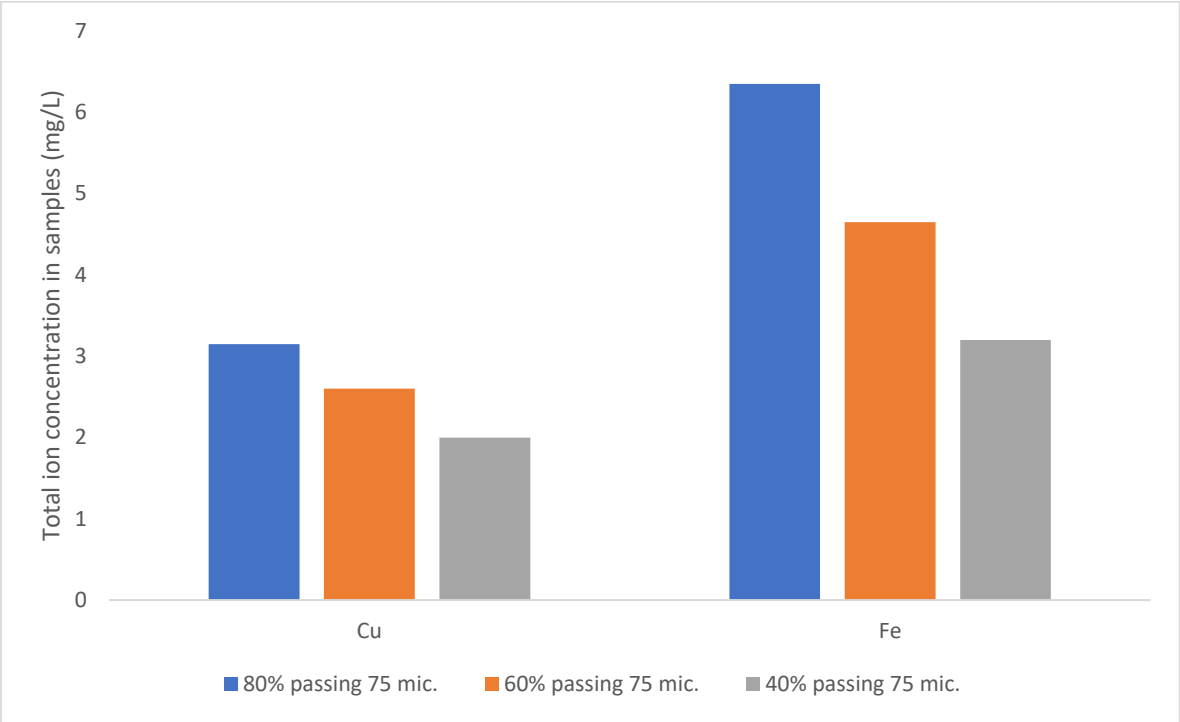

Figure 5.29: EDTA extraction experiment results obtained for Ore B tails samples. (Error bars represent standard error).

6. Discussion

The purpose of this study was to look at the capabilities of the chosen techniques in dealing with different ore types that have different mineral compositions, liberation profiles, and grades. This was accomplished by first validating the chosen techniques' ability to determine the rate/level of oxidation for Impala UG2 (Ore A) and High-grade Cu Ore (Ore B). The grind sizes addressed in this study were 40% -75 μm, 60% -75 μm and 80% -75 μm, which were chosen to represent ores that experienced different milling conditions, different liberation and presumably different mineral surface reactions. The overall purpose was to examine how these different ores with varying liberation profiles floated. To aid in the interpretation of sulphide mineral reactivity, XRD and QEMSCAN were employed to examine the minerology of the two ores. The findings are addressed in the sections that follow: (a) Validation of the EDTA technique for determining the oxidation level and/or rate of the chosen ores. (b) The relationship between oxidation of the minerals contained in the ore and, (c) Correlation of the level and/or rate of oxidation with the original mineralogy and/or liberation of the ore samples. This section will also include tailings data as it provides information on the amount of value that may potentially remain in the tails after flotation, as revealed by EDTA and RN data.

6.1. Validation of the EDTA and RN technique for determining the oxidation level and/or rate of the chosen ores

Two main questions are addressed in this section, including "*How will the EDTA and RN values change based on the ore types? What are the changes in surface chemistry that arise from increased mineral liberation and how does it alter the EDTA and RN numbers*?" In order to understand the nature of the BMS surface in the different studies, the data from the RN and EDTA experiments in Chapter 5 are first examined and discussed.

6.1.1. The change in EDTA and RN numbers based on the ore type

According to the RN data, Ore A was more reactive than Ore B, overall. This was demonstrated by Ore A's OCFs (3.6; 2.4; and 2.2 for grind sizes 80% - 75 μm, 60% -75 μm, and 40% -75 μm respectively) being greater than Ore B's (2.3; 1.4; and 1.5 for grind sizes 80% - 75 μm, 60% -75 μm, and 40% -75 μm respectively). Ore B was projected to have a higher oxidation rate than Ore A, owing to its mineralogy and the presence of a larger percentage of Fe, which presumably enhances the reactivity of Ore B, especially as ferric ion is a stronger oxidising agent than oxygen (Kang and Hwang, 2000). However, this was not the case, and one reason might be that the pyrite associated with chalcopyrite in Ore B contains 2.61 wt.% calcite, and calcite is a neutral mineral. This may contribute to low consumption. According to Owusu et al. (2013), dolomite has the potential to directly absorb the acid produced

during the pyrite oxidation process, reducing mineral surface oxidation and the OCF. Dolomite and calcite are both carbonate minerals and have similar mineralogies. Therefore, they both have the potential to absorb the acid produced during the pyrite oxidation process (Calcite reacts with HCL stronger) (Owusu et al., 2013).

Further, The QEMSCAN results showed that Ore B includes relatively minute levels of trace metals including As. As is an electron acceptor, therefore its substitutional insertion into pyrite crystals has a major impact on both the electrical characteristics and the electrochemical reactivity. Pyrite minerals develop a p-type semiconducting feature due to the presence of As, which reduces their conductivity and reactivity (Abraitis et al., 2004; Huston et al., 1995).

Ore B, however, obtained higher EDTA levels than Ore A. This can be attributed to the fact that Ore B is a higher-grade Cu ore with more Cu and Fe ions to leach. Since EDTA only forms complexes with free ions in solution, it is unlikely that it will recognize any of those that have complexed with other species (Pribil, 1972). It is therefore possible that on top of Ore A having lower BMS proportions, it is showing lower EDTA values because some of the solution's ions precipitated before exposure to the EDTA. Some fluctuations in Eh over time would imply ion precipitation, which would have altered EDTA levels. The pulp pH remained constant for Ore A and Ore B, with only minor changes in Eh values, creating a more oxidizing environment as the oxygen levels increased. Huang and Grano (2006) observed that grinding medium with 30% Cr provided a more oxidizing environment, this might have been one of the contributing factors in this study as well. A study by Owusu et al. (2013) explained that successive cycles demonstrated regular increase-decrease tendencies in Eh levels. These were accompanied by a monotonic fall in pH, which was repeated across all of the cycles. These pH - Eh fluctuations with increased aeration cycle/time were stated to be compatible with the pyrite oxidation response with air (O_2 consumption).

Even though the sulphide minerals in the ores showed very slight variations in their surface chemistry, the EDTA and RN values differed between the different ores, and this was mainly influenced by the mineralogical composition of the ores.

6.1.2. The change in EDTA and RN numbers based on the liberation

Figure 6.1 depicts a comparison of the EDTA and RN values across the three grind sizes. The figure shows how the RN and EDTA values increased with finer grinding for both ores A and B, that follow a similar trend. For Ore A EDTA and RN results, the grind size 40% -75 µm was the least reactive of the grind sizes evaluated in this study (obtaining the lowest calculated OCF) and the EDTA extraction technique discovered the least number of ferric species (oxidation products) on its mineral surface (Figure 6.1).

The grind size 80% - 75 µm had the highest EDTA extractable Cu and Fe values, indicating that there was a lot more ferric species on its surface than the other two grind sizes. Further, 80% - 75 µm obtained the highest OCF, indicating that it was in fact the most reactive of the three grind sizes. The grind size 60% - 75 µm was also relatively reactive (OCF = 2.4) although the reaction rates were not as rapid as for the grind size 80% - 75 µm (OCF= 3.6) (See Figure 5.23). The EDTA extractable Cu and Fe value for 60% - 75 µm was somewhere in between the least reactive 40% - 75 µm and very reactive 80% - 75 µm (Figure 6.1). Similarly, it's calculated OCF was greater than 40% - 75 µm and less reactive than the grind size 80% - 75 µm (Figure 6.1).

The findings for Ore B showed a similar pattern, with the grind size 80% - 75 µm obtaining the highest EDTA extractable Cu and Fe values as well as the highest OCF compared to the other two grind sizes. The findings of the Ore B EDTA extractable Cu and Fe analysis revealed that when the grind became finer, an increasing amount of ferric hydroxide species formed on mineral surfaces. Although little difference was observed between the OCF of grind sizes 60% - 75 µm and 40% - 75 µm, the latter had the OCF that was slightly higher (Figure 6.1).

The slurry of the grind size of 80% - 75 µm for Ore B had the lowest dissolved oxygen level before it was sparged with oxygen, which is particularly interesting to note (Figure 5.24). The results from Figure 5.24 also showed that the pulp initial oxygen content was generally higher for grind sizes 60% - 75 µm and 40% - 75 µm, (8.64 ppm and 8.91 ppm respectively) but with lower OCF. This demonstrates how reactive the sample was, since the minerals at 80% - 75 µm had already used up all of the available oxygen in the solution before the oxygen was sparged into the solution.

Interestingly, as revealed by Peng and Grano (2010b), iron hydroxide species produced from grinding media showed a greater affinity to fine (−10 µm) galena and chalcopyrite particles than intermediate size fractions (–53 + 10 µm). The reason for this phenomenon is that the surfaces of fine galena and chalcopyrite particles are more susceptible to oxidation than the particles in intermediate size fractions. The grinding media used in this study was 30% Cr, which is not intended to yield iron hydroxide species; yet the RN and EDTA values increased as the grind went finer, indicating that the oxidation level increased as the grind became finer. The increase in surface area generated by finer grinding suggests that more surfaces were exposed for mineral reactions to occur, which might explain the increase in reactivity.

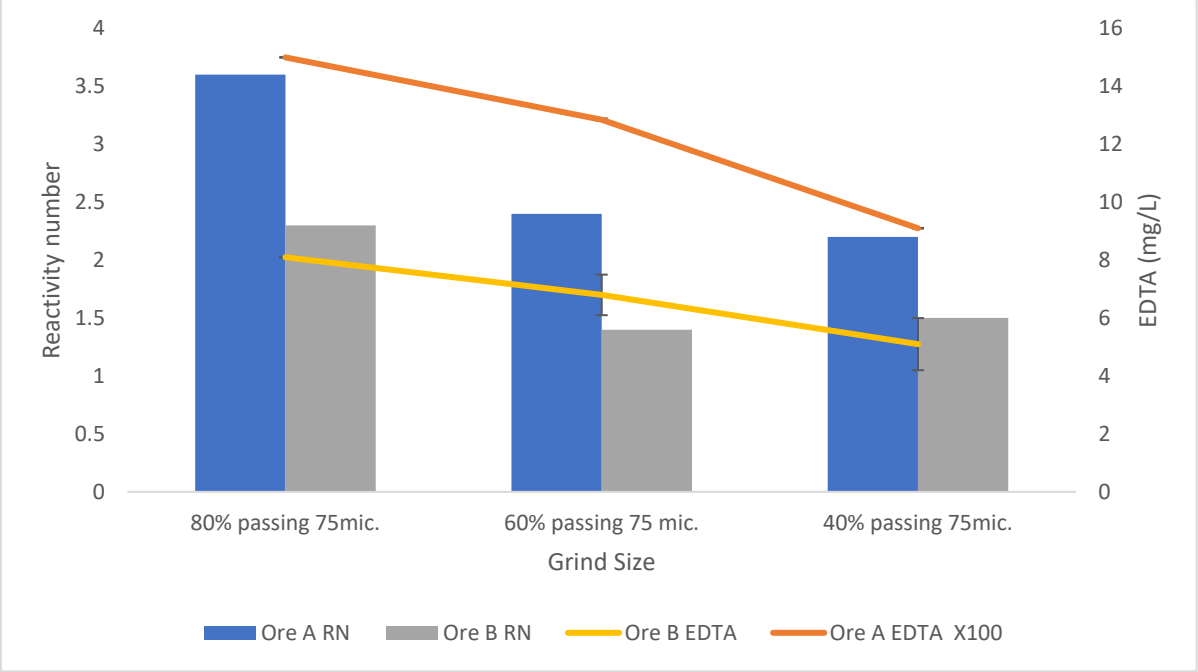

Figure 6.1: Variation in EDTA and OCF levels among the three grind sizes

6.2. The relationship between oxidation of BMS minerals contained in the ore and Flotation Performance

The amount of iron hydroxide species in complex sulphide ores and single sulphide mineral systems is inversely related to flotation recovery, and the distribution of iron hydroxide species on mineral surfaces changes with the ratio of mineral surface area (Peng and Grano 2010c; Moimane et al. 2020). The aim of this section is to answer and discuss the question: *How will the changes in liberation relate to the flotation performance of Ore A and Ore B.*

The liberation comparison between Ore A and Ore B revealed substantial differences. For instance, the liberated BMS for Ore A rose from 55.08% to 59.57%, as the grind size became finer. In the case of Ore B, the average degree of BMS liberation between the three grind sizes was around 84%. Figure 6.2 and Figure 6.3 illustrates the relationship between the liberated BMS and water recovery for all the grind sizes tested for Ore A and Ore B. The flotation tests for Ore A showed that increased liberation resulted in higher water recoveries for the grind size 80% -75 µm (440.32 g), and water recoveries then declined as the grind size grew coarser, from 383.31 g and 347.16 g for grind sizes 60% -75 µm and 40% -75 µm respectively. This is because increased mineral liberation resulted in increased fines, which then gave higher water recoveries because finer particles stabilize the froth (Rahman et al., 2012). Trahar (1981) postulated that finer particles will entrain more, and such circumstances will ultimately result in increased water recovery in the concentrate, resulting in a high

amount of entrainment of fine gangue. Therefore, entrainment accounts for a large portion of the solid and water recovery from this grind size for Ore A.

Further, the results revealed that the finer the grind, the more liberated gangue was recovered, resulting in the finest grind size not yielding the highest Cu and Ni grade and recoveries (Figure 5,18 and Figure 5.20). The poor flotation behaviour of this grind size (80% -75 µm) is mostly owing to a low particle/bubble collision efficiency during the flotation process as a result of an unfavourable particle/bubble size ratio (Leistner et al., 2017). Overall, there was a distinct trend of decreasing particle size, increasing liberation, with increasing water recovery.

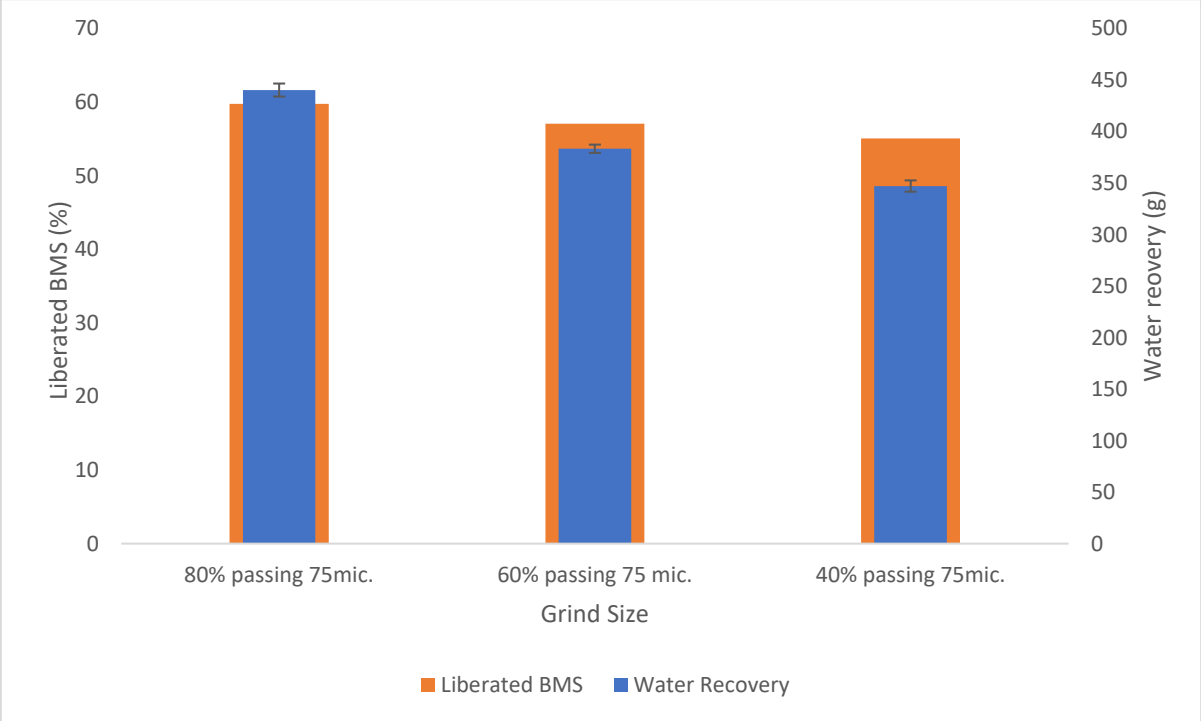

Figure 6.2: The relationship between the liberated BMS and water recovery for all the grind sizes tested for Ore A

For Ore B, increased fine grinding also led to larger water recoveries for the grind size 80% -75 µm (578.42 g). Water recoveries then decreased as the grind size grew coarser, from 459.29 g to 341.23 g for grind sizes 60% -75 µm and 40% -75 µm respectively. Ore B showed no liberation trend, indicating that the BMS are unaffected by grinding; however, because particle size affects froth stability, it may be concluded that the gangue is more liberated. This trend is similar to the one described above for Ore A and is consistent with a study by Kirjavainen (1996), who explained that fine particle recovery through entrainment is directly proportional to feed water recovery to the concentrate. Trahar (1981) further states that entrainment is an important contributing mechanism to the recovery of fine particles which, when coupled with a low rate of genuine flotation, can account for much of the observed behaviour of such fine grinds. An increase in the number of hydrophobic

species in the froth phase destabilizes the froth, resulting in higher water drainage rates and drier froths (Wang et al., 2020; Harris., 1982; Wang et al., 2016; Ata., 2004; Konopacka and Drzymala., 2010).

Ore B also had better Cu recoveries than Ore A because it is a high-grade Cu ore. This is because the primary minerals in Ore A are orthopyroxene and plagioclase, with smaller quantities of BMS, quartz, amphibole, chlorite, various Fe-Ti oxides, and talc (Table 5). The high concentration of alteration minerals contained in Ore A might have had a negative impact on flotation performance (Ndlovu et al., 2014). Orthopyroxene and serpentine are prone to mix heterogeneously in solutions because of their opposing charges, which might produce rheological issues during froth flotation (Burdukova et al., 2008: 2176; Behnsen & Faulkner, 2012: 54; Ndlovu et al., 2014: 195). Although the BMS concentrations in Ore A are quite low in contrast to other minerals in the ore, they are where the value is, given that the cost of extraction is economically worthwhile. (Figure 5.1).

The highest Cu recovery for ore B was obtained by the grind size 80% -75 µm, followed by grind sizes 60% -75 µm and 40% -75 µm respectively. According to Kalichini (2015), 93.6% of the copper in the Ore B sample was contained as chalcopyrite, 2.7% as secondary copper sulphides (bornite, covellite, and chalcocite), and 1.7% as chrysocolla. Mica, plagioclase-feldspar, and quartz made up the majority of the gangue minerals. As the grind became finer, more chalcopyrite was being liberated, which then increased Cu recoveries. The typical bulk mineralogy of Ore B is also summarized in Table 5.1.

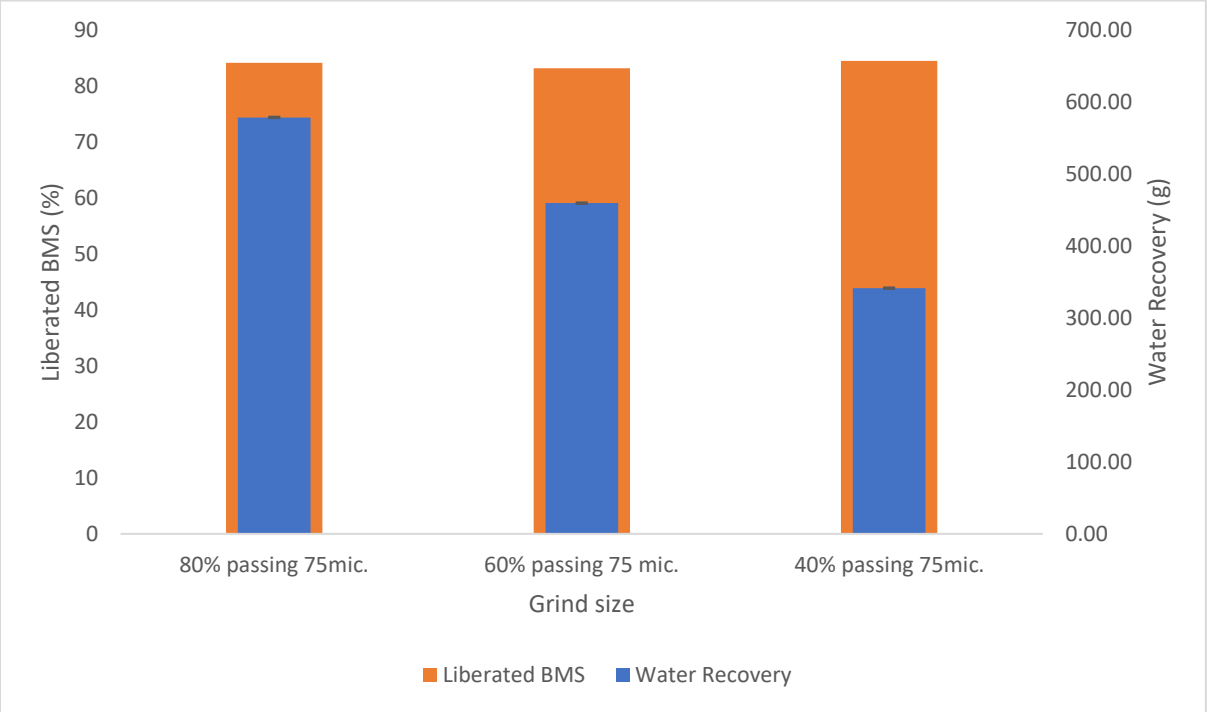

Figure 6.3: The relationship between the liberated BMS and water recovery for all the grind sizes tested for Ore B

6.3. Correlation of the level and/or rate of oxidation with the original mineralogy and/or liberation of the ore samples.

The aim of this section is to provide an answer to the last question: *"Will EDTA and RN results, as well as the flotation process, provide an indicator of the level of oxidation, and how will that relate to mineralogy?"* To do this, the findings of the batch flotation experiments in Chapter 5 are examined and discussed in order to fully understand the interactions between BMS liberation, EDTA and RN results, and flotation performance. Only once these data have been analysed can attempts to link the rate/level of oxidation to a grind size be made.

6.3.1. Ore A trends (Low-grade ore)

The association between the three grind sizes investigated in this study, with liberated BMS, Cu recovery and grade, as well as their EDTA number and OCF for Ore A is depicted in Figure 6.4. For comparison purposes, the variables mentioned are all plotted on one graph. In order to do so, variable have been magnified; grade (x100) and EDTA (x10).

According to Figure 6.4 the grind size 60% -75 μm yielded the highest Cu recovery, the coarsest grind size 40% -75 μm yielded the second highest Cu recovery, and the grind 80% -75 μm yielded the lowest Cu recovery. The Figure also shows that as the grind became finer and Ore A became more liberated, Cu recoveries increased until they reached a maximum (at 60% -75 μm) and then began to fall. The ore began to over-liberate somewhere between grind sizes 60% -75 μm and 80% -75 μm, and over-liberation often leads to slime coatings and overstabilization of the froth, which limits Cu recovery (Feng and Aldrich, 1999). These findings are consistent with the findings of Jameson (2012), who reported that the recovery of mineral particles by flotation is a function of particle size. According to Jameson (2012), as the size of floatable particles increases, so does the recovery, until it hits a maximum before monotonically declining. However, while recovery is a relevant notion, especially from an operational standpoint, the rate constant as a function of particle size and liberation class is more useful for evaluating the behaviour of a system with particle size and liberation class distributions. This study sought to expand on their idea by determining a measure of oxidation using the two techniques; these techniques assist in anticipating the behaviour of the ore in terms of oxidation and recovery when the ore is floated.

A lower Cu recovery was obtained with the coarsest grind (40% -75 μm) because the BMS were not liberated sufficiently, as demonstrated by the lowest liberated BMS value in Figure 6.4. Bloom and Heindel (2002) proposed that the loss in recovery in the coarse particle size range is not always caused by liberation (composite formation) or collector concentration. This decrease is sometimes due to hydrodynamic processes, namely the rise in detachment forces with increasing particle size and the

loss of coarse particle suspension. The decline in recovery is that as particles became larger, it became more difficult to obtain complete off bottom suspension in the float cell, without increasing the energy input and hence leading to detachment (Van der Westhuizen and Deglon, 2007).

The highest grade was obtained by the grind size 40% -75 μm, followed by grind sizes 60% -75 μm and 80% -75 μm respectively. Furthermore, Figure 6.4 shows that liberated BMS is inversely related to grade; the finer the grind size, the more liberated the ore is and the lower the grade, as mentioned previously (Refer to section 6.2). The results show that even though more minerals were recovered as the ore became more liberated, more and more gangue was also getting liberated and recovered, lowering the grade. The grade obtained by the grind sizes is therefore a factor of particle size. The finer the grind size, the greater the surface area available to attach to the bubbles during flotation and the more gangue recovered. Similar findings were made by Feng and Aldrich (1999); fine particles often have slow recovery rates due to reduced particle-bubble collisions and are prone to entrainment.

Liberated BMS for Ore A is directly proportional to the EDTA value and the OCF. The grind size with the most liberated BMS (80% -75 μm) also has the greatest OCF and EDTA value. The lowest Cu recovery and grade were obtained with the same grind size. During its preparation, the grind size 80% -75 μm had clearly suffered significantly more oxidation than the other grind sizes and this is indicated by the high OCF and the EDTA value. The grind size 40% -75 μm obtained the lowest OCF and EDTA value and its flotation recovery was the second highest and the highest grade. This suggests that the degree of oxidation that was experienced by this grind size was mild, which promoted the production of hydrophobic species and favourable Cu and Ni recoveries. Overall, the Ore A results showed that where the grind sizes had high reactivity (high OCF) and high EDTA value, poor flotation recovery was observed and where the OCF and EDTA values were lower, favourable recoveries were obtained. EDTA and RN numbers therefore aided in giving an indication of the extent of oxidation that the ore had undergone, which ultimately translated to flotation recoveries.

These findings support Kelebek's (1993) notion that moderate oxidation of the mineral surface increases the number of surface sites available for xanthate adsorption, favouring recoveries. However, extensive oxidation alters the balance to the point where the hydrophilic ferric hydroxide layer covering the surface of Ore A BMS would have prevented adequate xanthate adsorption. Therefore, differences in the floatability of the different grind sizes are understood to be impacted by Ore A's propensity to oxidation.

The flotation of sulphide minerals requires some moderate oxidation, as explained in Chapter 2 Section 2.2. The decrease in recovery in the investigation can be attributed to extensive mineral

oxidation, with a large percentage of hydrophilic species produced on mineral surfaces (Kant et al., 1994; He et al., 2006; Kelebek, 1993).

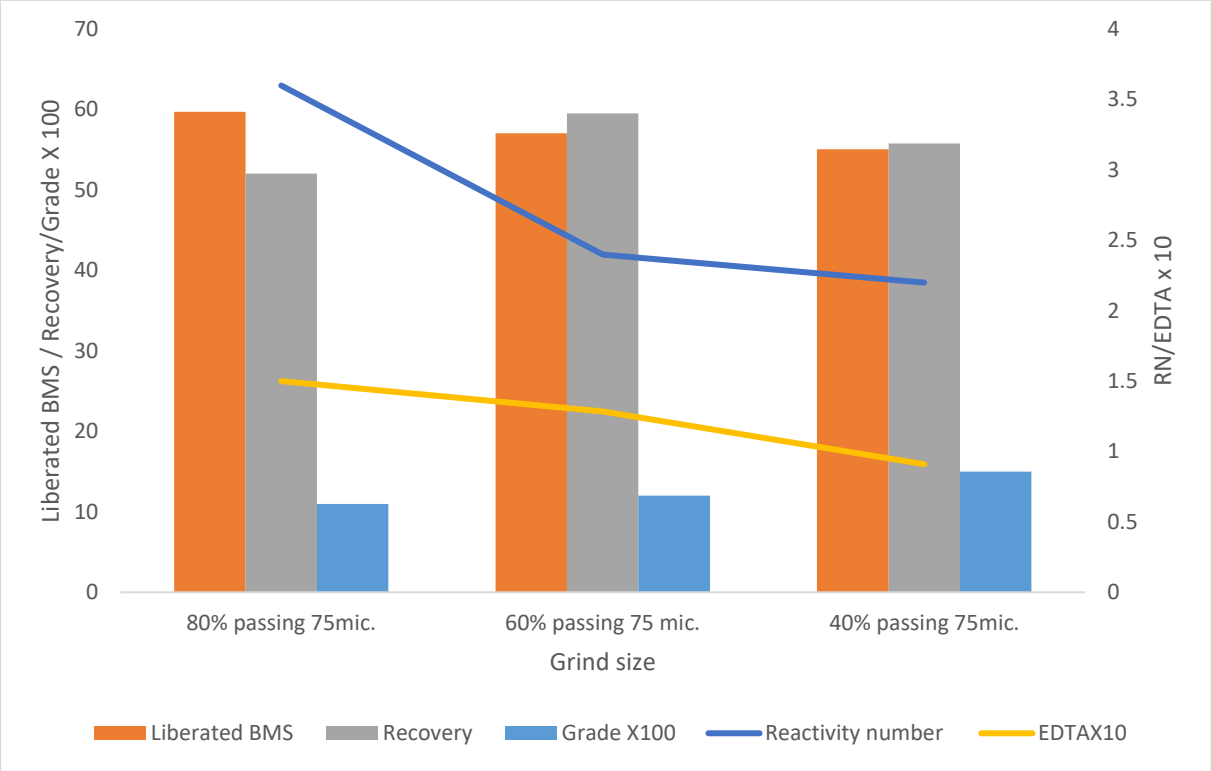

Figure 6.4: The relationship between the three grind sizes studied in this work and liberated BMS, Cu recovery and grade, as well as their EDTA number and OCF for Ore A

6.3.2. Ore B trends (High-grade ore)

Figure 6.5 shows the correlation between the liberated BMS, Cu recovery and grade, EDTA number, and OCF for Ore B for the three grind sizes tested in this study. Note that Ore B has higher liberated BMS values and Cu recoveries than Ore A because Ore B is a high-grade Cu ore. Additionally, it is important to highlight that the BMS for Ore A have a greater association percentage with "other Fe-Ti oxides" minerals than the BMS for Ore B. These "other Fe-Ti oxides" minerals include all oxidation minerals, related iron oxides, and other changed minerals like titanium oxides. All oxidation products are most likely represented here (Figure 5.3).

The liberated BMS for Ore B is generally consistent throughout the three grind sizes, however, the highest recovery is achieved by the grind size 80% -75 µm (95.11%), followed by grind sizes 60% -75 µm and 40% -75 µm respectively (92.25% and 90.86%). The recovery of this ore increases as the grind size becomes finer. This is because it is a high-grade ore, and more chalcopyrite was liberated from the ore as the grind grew finer. Although the liberation characteristics (Liberated BMS) of the

chalcopyrite in Ore B did not show significant variation, the conditions from the grind size 80% -75 μm were favoured.

The BMS quantities in the tailings of Ore B were very low, owing to the very high recoveries which were obtained (Figure 5.18), and this may be attributed to the Ore being largely liberated (84% average across all three grind sizes). The rate constant for a largely liberated ore is controlled by hydrodynamics and fully liberated particles follow the classical recovery-particle size behaviour (Welsby et al., 2010a). The highest grade was obtained from the grind size 80% -75 μm (12.33%), followed by a grade 7.13% and 6.27% from grind sizes 40% -75 μm and 60% -75 μm respectively. The grade showed to be inversely proportional to the expected maximum recovery, with the intermediate grind size yielding the lowest grade, possibly due to partially liberated compound particles in which the value is sufficiently hydrophobic to be recovered along with the associated gangue, as opposed to the lower grind of 40% -75 μm where particles could be locked in gangue and thus the gangue is not recovered, and at 80% -75 μm where the value is liberated and floats without gangue.

The milling time of Ore B is proportional to the OCF and EDTA levels as shown in Figure 6.5. It can be seen that rate of oxidation increases with increasing milling time. The flotation of chalcopyrite and other sulphide minerals has been extensively studied and shown to be dependent on a number of factors including pulp potential (Heyes & Trahar, 1979; Guo & Yen, 2003; Greet et al., 2005) and pH as long as the optimum reagent dosage is used (Göktepe, 2002). Researchers have linked the increase in recovery to xanthate adsorption on the mineral, whereas a reduction in recovery has been linked to an increase in mineral oxidation and a larger percentage of hydrophilic species produced on the mineral surface, such as ferric hydroxide and sulphate (He et al., 2006). However, in this case Figure 6.5 demonstrates that, while the EDTA value for ore B increased as the grind size became finer, so did the recovery. It is possible that the particles that were ground to achieve particle size 80% -75 μm were at their most hydrophobic state, owing to the increased liberation of the BMS and the high-grade nature of the ore, particularly chalcopyrite. Section 6.1.1 demonstrated that Ore B was not as quick to react than Ore A by minerology investigation. This implies that the degree of oxidation undergone by Ore B was just moderate enough to result in the formation of hydrophobic species. The calculated OCF and EDTA values and the minerology correlate, indicating that Ore B was the least reactive of the two ores studied.

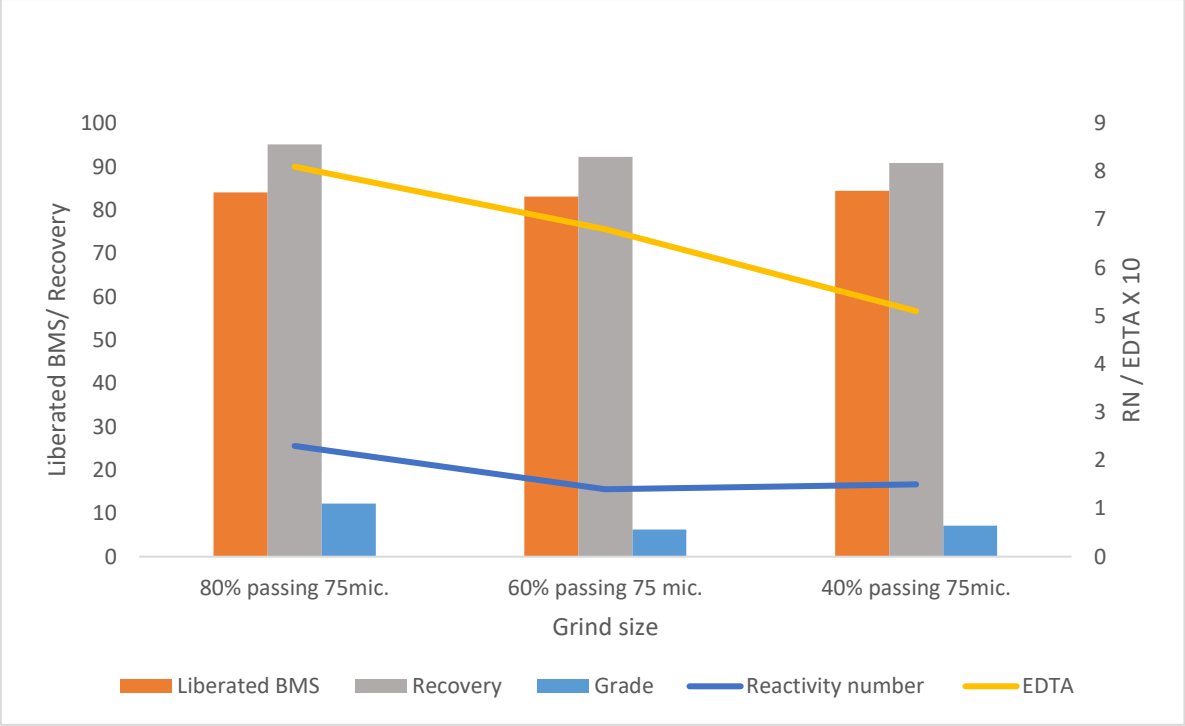

Figure 6.5: The relationship between the three grind sizes studied in this work and liberated BMS, Cu recovery and grade, as well as their EDTA number and OCF for Ore B

6.3.3. Tailings EDTA and RN data

This tailings data will attempt to show what was left behind after flotation and the EDTA value as well as the RN value will indicate if there might still be value left behind.

Table 6.1 shows that there is still some value that is left in the tails, and Figure 6.6 and Figure 6.7 gives an indicator on whether that value can be extracted from the tails or not, because of oxidation. For instance, Ore A tailing EDTA and RN results showed that the grind size 40% -75 µm obtained the highest OCF (3.8), followed by grind sizes 60% -75 µm and 80% -75 µm with OCFs of 2 and 1.6 respectively, while the EDTA results showed the grind size 80% -75 µm to have the highest EDTA value. The low OCF recorded for Ore A as the grind became finer is interpreted as a result of the fact that it was already coated by ferric hydroxide species and passivated at the time of measurement due to its highly reactive nature, as demonstrated by the EDTA value. As a result, the likelihood of this translating into flotation recoveries is high.

Table 6.1: Summary table of the combined BMS bulk minerology from QEMSCAN for Ore A and Ore B.

(wt. % in fraction)	Ore A feed	Ore A tails	Ore B feed	Ore B tails
Bulk minerology (BMS)	0,29	0,15	6,46	1,71

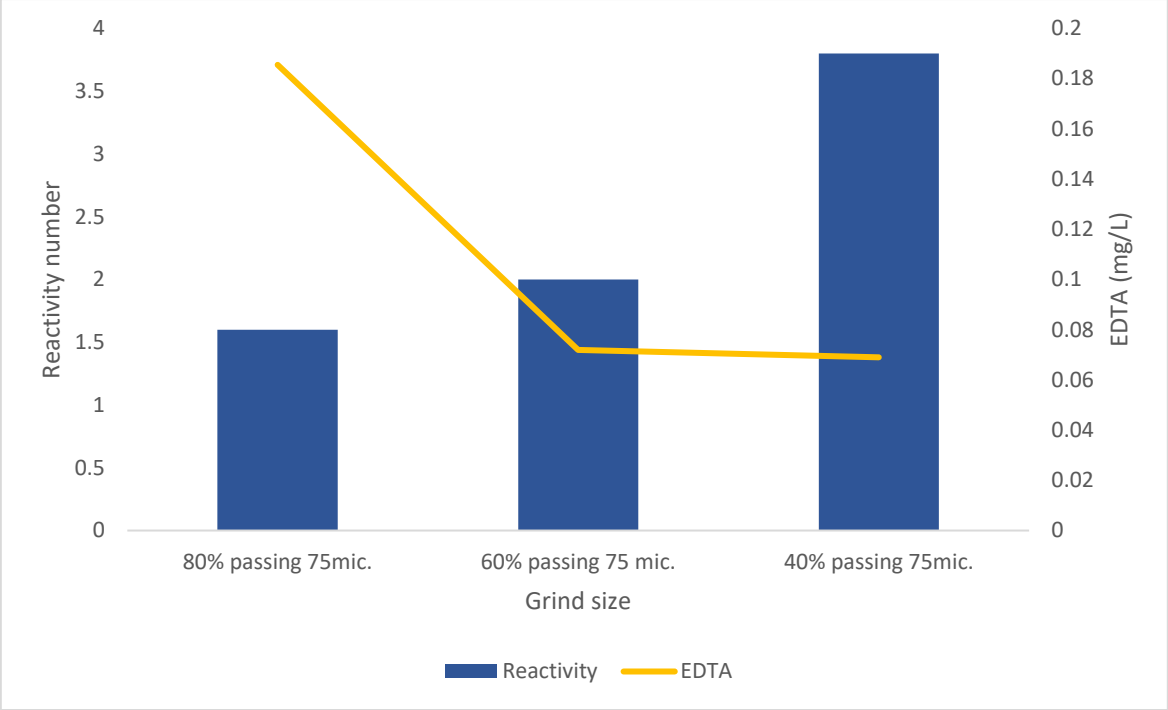

Figure 6.6: Ore A tailing EDTA value and RN results (OCF)

Figure 6.7 shows that the Ore B EDTA and OCF values followed the same trend as the feed samples reported earlier (6.3.2). Both the EDTA value and OCF increased as the grind size became finer. Further, bulk minerology (Table 5.1) revealed that there was still a significant quantity of value in the tailings. Despite the fact that the two techniques reveal the tailings to be more oxidized than the feed, the measurements suggest that there is value in the tails and this result might be translated positively in flotation recoveries.

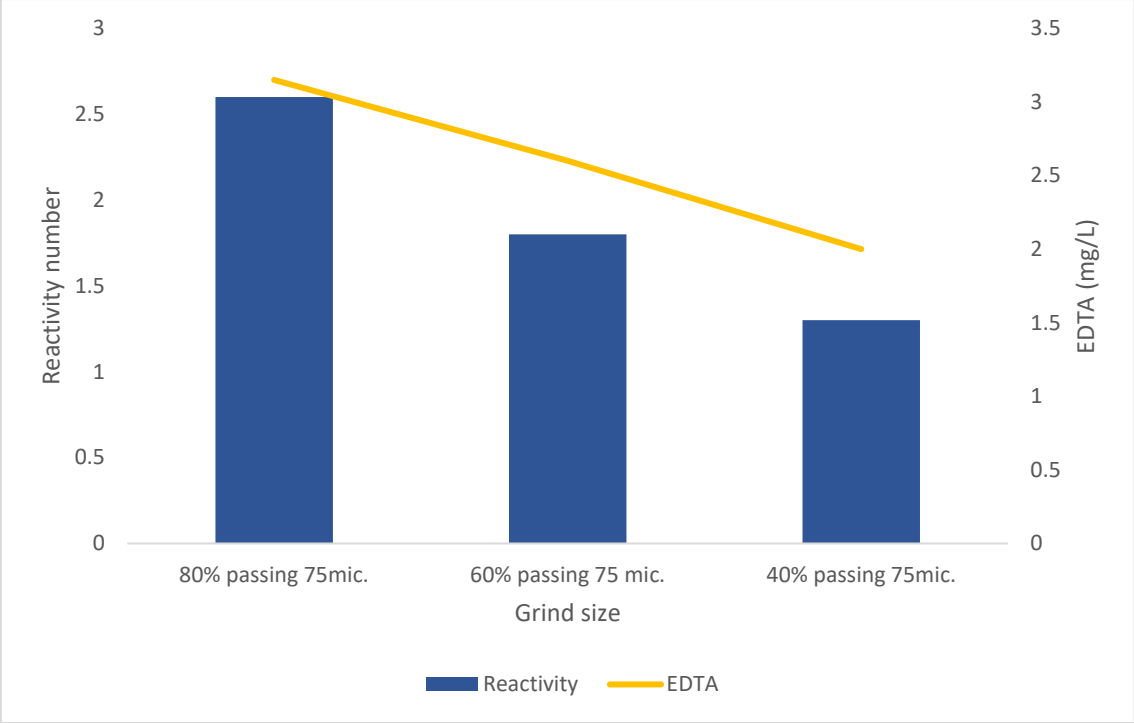

Figure 6.7: Ore B tailing EDTA value and RN results (OCF)

6.4. High-level industrial relevance

Grinding not only reduces particle size, allowing precious minerals to be liberated, but it also causes differential surface characteristics on the surfaces of valuable and gangue minerals (Zhao and Peng, 2012). One of the processes that causes mineral alteration is oxidation, which is closely linked to the liberation of precious minerals. There is a gap in industry for techniques that are not only less expensive and maintain overall economic variable capabilities, but also ones that will help us understand the level of oxidation indicated by the quantity of oxidation products present on the mineral surface. This study has shown that these simple, cost-effective techniques would be able to indicate surface oxidation which imply the likelihood of flotation performance based on how much the surfaces have oxidized. As a result, they will act as a guideline to assist flotation plants in managing oxidized ores better in order to potentially prevent losses in recoveries as well as to investigate alternative solutions that may be adapted to the flotation of ores with differing degrees of oxidation.

7. Conclusion

The objective of this study was to validate whether simple, low-cost techniques can be used to give an indication of surface oxidation for varied ore types. This was done by first validating the use of the EDTA and RN techniques to determine the level and/or rate of oxidation of the selected ores. The study then considered the correlation of the level and/or rate of oxidation with the original mineralogy and/or liberation of the ore samples. Three key questions were formulated in Chapter 3 to investigate the named objectives and the validity of the postulated hypothesis was tested by answering these questions:

1. ***How did the EDTA and RN numbers change based on the ore types?***

The EDTA and RN values differed between the different ores. This was mainly influenced by the differences in the chemical and mineralogical composition of the ores. Although there were minor variations in the degree of surface chemistry that the sulphide minerals present in the ore experienced, some minerals had a higher degree of surface oxidation than others. For instance, Ore A was more reactive than Ore B, overall and this was demonstrated by Ore A's OCF being greater than Ore B's. The pyrite associated with chalcopyrite in Ore B contained 2.61 wt.% calcite, and calcite is a neutral mineral. Calcite has the potential to directly absorb the acid produced during the pyrite oxidation process, reducing mineral surface oxidation and the OCF.

2. ***How does mineral liberation affect the EDTA and RN numbers?***

The RN and EDTA values increased with finer grinding for both ores A and B, following a similar trend. The grind size 80% - 75 µm obtained the highest EDTA extractable Cu and Fe values as well as the highest OCF compared to the other two grind sizes. The findings of the Ore A and Ore B EDTA extractable Cu and Fe analysis revealed that when the grind became finer, an increasing amount of ferric hydroxide species formed on mineral surfaces.

The RN and EDTA values increased as the grind became finer, indicating that the oxidation level increased as the grind became finer. The reason for this phenomenon is that the surfaces of fine particles are more susceptible to oxidation than the particles in intermediate size fractions. The increase in surface area generated by finer grinding suggests that more surfaces were exposed for mineral reactions to occur, which might explain the increase in reactivity.

3. ***Will EDTA and RN results, and the flotation process, give an indicator of the level of oxidation and how will that relate to the mineralogy?***

For Ore A, the grind size 60% -75 μm yielded the highest Cu recovery, the coarsest grind size 40% -75 μm yielded the second highest Cu recovery, and the grind 80% -75 μm yielded the lowest Cu recovery. Overall, the Ore A results showed that where the grind sizes had high reactivity (high OCF) and high EDTA value, poor flotation recovery was observed and where the OCF and EDTA values were lower, favourable recoveries were obtained. EDTA and RN numbers therefore aided in giving an indication of the extent of oxidation that the ore had undergone, which ultimately translated to flotation recoveries.

Moderate oxidation of the mineral surface increased the number of surface sites available for xanthate adsorption, favouring recoveries. However, extensive oxidation altered the balance to the point where the hydrophilic ferric hydroxide layer covering the surface of Ore A BMS would have prevented adequate xanthate adsorption. Therefore, differences in the floatability of the different grind sizes are understood to be impacted by Ore A's propensity to oxidation.

However, for Ore B, the EDTA value and OCF increased as the grind size became finer, so did the recovery. It is possible that the particles that were ground to achieve particle size 80% -75 μm were at their most hydrophobic state, owing to the increased liberation of the BMS and the high-grade nature of the ore, particularly chalcopyrite. This implies that the degree of oxidation undergone by Ore B was just moderate enough to result in the formation of hydrophobic species. The calculated OCF and EDTA values and the minerology correlate, indicating that Ore B was the least reactive of the two ores studied.

References

Abraitis, P.K., Pattrick, R.A., Vaughan, DJ. 2004. Variations in the compositional, textural and electrical properties of natural pyrite: a review, *Int. J. Miner. Process.* 74 (1–4) 41–59.

Abrosimova, N., Gaskova, O., Loshkareva, A., Edelev, A. and Bortnikova, S. 2015. Assessment of the acid mine drainage potential of waste rocks at the Ak-Sug porphyry Cu–Mo deposit. *Journal of Geochemical Exploration*, 157, pp.1-14.

Afenya, P.M., 1991. Treatment of carbonaceous refractory gold ores. *Miner. Eng.* 4 (7e11), 1043e1055.

Aktas, Z., Cilliers, J. J. & Banford, A. W., 2008. Dynamic froth stability: Particle size, airflow rate and conditioning time effects. *International Journal of Mineral Processing,* Volume 87, pp. 65-71.

Andres, U., Timoshkin, I., Jirestig, J., Stallknecht, H. 2001. Liberation of valuable inclusions in ores and slags by electrical pulses. *Powder Technol*. 114 (1–3), 40–50.

Anglo Platinum. 2009. *Annual Sustainability Report, Years 2002 to 2009.* Johannesburg: Anglo Platinum Ltd.

Ata, S., Ahmed, N., & Jameson, G. J. 2004. The Effect of Hydrophobicity on the Drainage of Gangue Minerals in Flotation Froths. *Minerals Engineering*, 897-901.

Becker, M., Villiers, J. and Bradshaw, D., 2010. The flotation of magnetic and non-magnetic pyrrhotite from selected nickel ore deposits. *Minerals Engineering*, 23(11-13), pp.1045-1052.

Behnsen, J. & Faulkner, D.R. 2012. The effect of mineralogy and effective normal stress on frictional strength of sheet silicates. *Journal of Structural Geology.* 42:49–61. DOI: 10.1016/j.jsg.2012.06.015.

Bicak, O., 2019. A Technique to Determine Ore Variability in a Sulphide Ore. *Minerals Engineering*.

Bloom, F., Heindel, T.J., 2002. On the structure of collision and detachment frequencies in flotation models. *Chemical Engineering Science 57, 2467–2473.*

Bosch, D. W., 1987. Retreatment of Residues and Waste Rock. In G. G. Stanley, *The Extractive Metallurgy of Gold in South Africa* (pp. 707-743). Johannesburg: South African Institute of Mining and Metallurgy.

Brundle, CR., Evans, CA Jr., Wilson, S eds. Encyclopedia of Materials Characterization. Stoneham, MA: Butterworth-Heinemann and Manning, 1992.

Buckley, A.H., et al. 1985. Investigation of the surface oxidation of sulphide minerals by linear potential sweep voltammetry and X-ray photoelectron spectroscopy. Flotation of sulphide minerals, ed KSE. Forssberg, Elsevier, Amsterdam, 41.

Burdukova, E., Becker, M., Ndlovu, B., Mokgethi, B. & Deglon, D. 2008. Relationship between slurry rheology and its mineralogical content. In *XXIV International Mineral Processing Congress*. 2169–2178.

Caruccio FT, Hossner LR, Geidel G. Pyritic materials: acid drainage, soil acidity, and liming. In: Hossner, editor. Reclamation of Surface-Mined Lands. Boca Raton, Florida: CRC Press, 1989:129–148.

Cawthorn, R., 2005. Pressure fluctuations and the formation of the PGE-rich Merensky and chromitite reefs, Bushveld Complex. *Mineralium Deposita, 40(2), pp.231-235.*

Chander, S., 1988. Electrochemistry of sulfide mineral flotation. *Miner. Metal. Process.,* 5: 104- 114.

Corin, K., Kalichini, M., O'Connor, C. and Simukanga, S., 2017. The recovery of oxide copper minerals from a complex copper ore by sulphidisation. *Minerals Engineering*, 102, pp.15-17.

Crozier. R.D. 1984. Plant reagents. Part 1: Changing pattern in the supply of flotation reagents, *Mining Mag (Sept.),* 202.

Dagdelen, K. 1992. "Cutoff grade optimization". In *Proceedings of the 23rd International Symposium on Application of Computers and Operations Research in Minerals Industries* 157–165

DeBavey, 1904. US Patent 864597.

Feng, D. and Aldrich, C., 1999. Effect of particle size on flotation performance of complex sulphide ores. *Minerals Engineering*, 12(7), pp.721-731.

Fernández, R.R., Sohn, H.Y., LeVier, K.M., 2000. Process for treating refractory gold ores by roasting under oxidizing conditions. *Miner. Metall. Proc.* 17 (1), 1e6

Fontana, M.G., Greene, N.D., 1978. Materials Science and Engineering Series. McGraw-Hill, USA.

Fornasiero,D., Li, F., Ralston, J., Smart, R. 1994. Oxidation of Galena Surfaces: I. X-Ray Photoelectron Spectroscopic and Dissolution Kinetics Studies. *Journal of Colloid and Interface Science, Volume 164, Issue 2.* Pages 333-344, ISSN 0021-9797, https://doi.org/10.1006/jcis.1994.1175.

Forsmo, S. P. E., 2005. Oxidation of magnetite concentrate powders during storage and drying. *International Journal of Mineral Processing, 75(1-2), 135–144.* doi:10.1016/j.minpro.2004.08.010

Fse.org.za. 2020. *THE IMPACT OF MINING ON THE SOUTH AFRICAN ECONOMY AND LIVING STANDARDS*. [online] Available at: <http://fse.org.za/index.php/item/593-the-impact-of-mining-on-the-south-african-economy-and-living-standards> [Accessed 21 June 2020].

Fuerstenau, D., Diao, J. and Williams, M., 1991. Characterization of the wettability of solid particles by film flotation 1. Experimental investigation. *Colloids and Surfaces*, 60, pp.127-144.

Fullston, D., Fornasiero, D. and Ralston, J., 1999. Oxidation of Synthetic and Natural Samples of Enargite and Tennantite: 2. X-ray Photoelectron Spectroscopic Study. *Langmuir*, 15(13), pp.4530-4536.

Garvie, A.M, Linklater, C.M, Lestari, R & McCaffery, K., 2008. Using In Situ Measurements and Modelling to Effectively Manage Large Copper Sulfide Bearing Ore Stockpiles. in AB Fourie (ed.), *Proceedings of the First International Seminar on the Management of Rock Dumps, Stockpiles and Heap Leach Pads*, Australian Centre for Geomechanics, Perth, pp. 167-177.

Gaudin, A.M., Groh, J.O., Henderson, H.B. 1931. Effect of particle size in flotation American Institute of Mining Engineers Technical Publication, 414, pp. 3-23

Gil Bueno A, Val Caballero C, Macías F, Monterroso C. Influence of waste selection in the dump reclamation at Puentes Mine. In: Rainbow, editor. Reclamation, treatment and utilization of coal mining wastes. *Rotterdam: Bolkema*, 1990:203–208.

Göktepe, F. 2002. Effect of pH on Pulp Potential and Sulphide Mineral Flotation. *Turkish Journal of Engineering and Environmental Sciences*, *26*, 309–318.

Grano, S., 2009. The critical importance of the grinding environment on fine particle recovery in flotation. *Minerals Engineering*, 22(4), pp.386-394.

Greet, C. J., Kinal, J., & Steinier, P. 2005. Grinding Media — Its Effect on Pulp Chemistry and Flotation Behaviour — Fact or Fiction? In *Centenary of flotation symposium* (pp. 967–972). Brisbane.

Gruner, Holger and Lorig, Clarence H. 2006. "mineral processing". *Encyclopedia Britannica*, 17 Nov. 2006, https://www.britannica.com/technology/mineral-processing. Accessed 19 September 2022... (1911 Encyclopedia Britannica, 2006)

Guo, H., & Yen, W.-T. 2003. Pulp potential and floatability of chalcopyrite. *Minerals Engineering*, *16*(3), 247–256. doi:10.1016/S0892-6875(03)00015-3

Guy, P.J.; Trahar, W.J. 1984. The effects of oxidation and mineral interaction on sulphide flotation. In: Forssberg, K.S.E. Editor, editor/s. Flotation of Sulphide Minerals, Lulea, Swed.. Amsterdam, *Neth. and New York, NY: Elsevier; 1985. 91-110.* http://hdl.handle.net/102.100.100/277595?index=1

Hadizadeh, M., Farzanegan, A. and Noaparast, M., 2017. Supervisory Fuzzy Expert Controller for Sag Mill Grinding Circuits: Sungun Copper Concentrator. *Mineral Processing and Extractive Metallurgy Review*, 38(3), pp.168-179.

Harris, P. J. 1982. Frothing Phenomena and Froths. In R. P. King, *The Principles of Flotation* (pp. 237-250). *Johannesburg: The South African Institute of Mining and Metallurgy.*

Heyes, G., Trahar, W., 1977. The natural flotability of chalcopyrite. *Int. J. Miner. Process*. 4, 317–344.

Heyes, G. W., & Trahar, W. J. 1979. Oxidation-reduction effects in the flotation of chalcocite and cuprite. *International Journal of Mineral Processing*, *6*, 229–252.

Huang, G., Grano, S., 2006. Galvanic interaction between grinding media and arsenopyrite and its effect on flotation. *International Journal of Mineral Processing*, 78(3), pp.182-197.

Hunt, J., Berry, R., Bradshaw, D., 2011. *Characterising chalcopyrite liberation and flotation potential: Examples from an IOCG deposit. Minerals Engineering, 24(12), 1271–1276.* doi: 10.1016/j.mineng.2011.04.016

Huston, D.L., Sei, S.H., Suter, G.F., Cooke, R.A. 1995. Both, Trace elements in sulphide minerals from Eastern Australia volcanic-hosted massive sulphide deposit: Part1. Proton microprobe analysis of pyrite chalcopyrite and sphalerite, and Part II. Selenium levels in pyrite: comparison with (ð34S values and implications for the source of sulfur in volcanogenic hydrothermal systems, *Econ. Geol. 90 1167–1196.*

Jameson, G.J. 2012. The effect of surface liberation and particle size on flotation rate constants. *Minerals Engineering, 36-38(), 132–137.* doi:10.1016/j.mineng.2012.03.011

Jankovic, A., Valery, W., Maloney, K. & Markovic, Z., 2006. Improving Overall Concentrator Performance with Stirred Milling. Metsominerals.Nl. (October):1–6

Johnson, D. and Hallberg, K., 2005. Acid mine drainage remediation options: a review. *Science of The Total Environment*, 338(1-2), pp.3-14.

Kalichini, M. S. 2015. *A Study of the Flotation Charactersitics of a Complex Copper Ore, MSc Thesis.* Cape Town: University of Cape Town.

Kang, Y. and Hwang, K., 2000. Effects of reaction conditions on the oxidation efficiency in the Fenton process. *Water Research*, 34(10), pp.2786-2790.

Kant, C., Rao, S. and Finch, J., 1994. Distribution of surface metal ions among the products of chalcopyrite flotation. *Minerals Engineering*, 7(7), pp.905-916.

Kasmaee, S., Tinti, F. and Bruno, R., 2018. CHARACTERIZATION OF METAL GRADES IN A STOCKPILE OF AN IRON MINE (CASE STUDY- CHOGHART IRON MINE, IRAN). *Rudarsko-geološko-naftni zbornik*, 33(2), pp.51-59.

Kelebek. S., 1993. The Effect of Oxidation on the Flotation Behaviour of Nickel-Copper Ores. XVlll *International Mineral Processing Congress. Pp. 999-1006.*

King, B., 2001. Optimal Mine Scheduling Policies. Dissertation, *Royal School of Mines, Imperial College, London University, UK.*

Kirjavainen, V., 1996. Review and analysis of factors controlling the mechanical flotation of gangue minerals. *International Journal of Mineral Processing*, 46(1-2), pp.21-34.

Kocabag, D., Smith, M.R., 1985. The effect of grinding media and galvanic interaction on the flotation of sulfide mineral. Proc. Conf., Complex Sulfides-Proc. of Ores, Conc. and Byproducts, San Diego, CA, U.S.A., pp. 13– 20

Kríbek, B., Kneésl, I., Pasava, J., Malý, K., Caruthers, H., Sykorová, I., & Jehlicka, J. (2005). Hydrothermal alteration of the graphitized organic matter at the Kansanshi Cu (Au-,U-) deposit, Zambia. Mineral Deposit Research: Meeting the Global Challenge*, 277–280.* doi:10.1007/3-540-27946-6_72.

Lamia, B., and B. Mouhamed., 2017. Reprocessing and environmental desulphurization of sulphide mining waste from sphalerite flotation: Case of Chaabet El Hamra mine. World Journal of Engineering 14:42–46. doi:10.1108/WJE-11-2016-0128.

Lascelles, D., Finch G.A. 2002. Quantifying accidental activation. *Part I. Cu ion production Minerals Engineering, 15, pp.* 567-571

Learmont, M. and Iwasaki, I., 1984. Effect of Grinding Media on Galena Flotation. *Mining, Metallurgy & Exploration*, 1(2), pp.136-143.

Lèbre E., Glen D., Corder G.D., Golev A., 2017. Sustainable practices in the management of mining waste: A focus on the mineral resource, *Minerals Engineering,* 107, 34–42

Leistner, T., Peuker, U. and Rudolph, M., 2017. How gangue particle size can affect the recovery of ultrafine and fine particles during froth flotation. *Minerals Engineering*, 109, pp.1-9.

Li, Z., F. Rao, M. A. Corona-Arroyo, A. Bedolla-Jacuinde, and S. Song., 2019. Comminution effect on surface roughness and flotation behavior of malachite particles. Minerals Engineering 132:1–7. doi:10.1016/ j.mineng.2018.11.056.

Miyoshi, K., Chung, Y.W. 1993.Surface Diagnostics in Tribology: Fundamental Principles and Applications. River Edge, NJ: World Scientific Publishing Co.,

Mills, A.L. Acid mine waste drainage: microbial impact on the recovery of soil and water ecosystems. In: Tate, Klein DA, editors. Soil reclamation processes. New York: Marcel Dekker, 1985:35–80.

Moimane, T., Plackowski, C., & Peng, Y. 2020. *The critical degree of mineral surface oxidation in copper sulphide flotation. Minerals Engineering, 145, 106075.* doi:10.1016/j.mineng.2019.106075

Monterroso, C., & Macías, F.1998. *Drainage waters affected by pyrite oxidation in a coal mine in Galicia (NW Spain): Composition and mineral stability. Science of The Total Environment,* 216(1-2), 121–132. doi:10.1016/s0048-9697(98)00149

Ndlovu, B., Forbes, E., Farrokhpay, S., Becker, M., Bradshaw, D. & Deglon, D. 2014. A preliminary rheological classification of phyllosilicate group minerals. *Minerals Engineering*. 55:383–389. DOI: 10.1016/j.mineng.2013.06.004.

Nel, E., Theron, J., Martin, C., Raabe, H. 2004. *PGM Ore Processing at Impala's UG2 Concentrator in Rustenburg, South Africa.* SGS.

Newell, A.J.H., Bradshaw, D.J., Harris, P.J., 2006a. The effect of heavy oxidation upon flotation and potential remedies for Merensky type sulfides. *Min. Eng*. 9, 675–686

Ngulube, C., 2016. Review, evolution, and optimization of the treatment of Kansanshi mixed copper ore. *Journal of the Southern African Institute of Mining and Metallurgy*, 116(6), pp.561-567.

Nordstrom, D.K. 2011. Sulfide Mineral Oxidation. https://www.researchgate.net/publication/299747155 DOI: 10.1007/978-1-4020-9212-1_198

Nordstrom, D. and Alpers, C., 1999. Negative pH, efflorescent mineralogy, and consequences for environmental restoration at the Iron Mountain Superfund site, California. *Proceedings of the National Academy of Sciences*, 96(7), pp.3455-3462.

Owusu, C., Addai-Mensah, J., Fornasiero, D. and Zanin, M. 2013. Estimating the electrochemical reactivity of pyrite ores-their impact on pulp chemistry and chalcopyrite flotation behaviour. *Advanced Powder Technology*, 24(4), pp.801-809.

Parker, T., Shi, F., Evans, C. and Powell, M., 2015. The effects of electrical comminution on the mineral liberation and surface chemistry of a porphyry copper ore. *Minerals Engineering*, 82, pp.101-106.

Peng, Y., Grano, S., 2010a. Effect of grinding media on the activation of pyrite flotation. *Minerals Engineering*, 23(8), pp.600-605.

Peng, Y., Grano, S., 2010b. Inferring the distribution of iron oxidation species on mineral surfaces during grinding of base metal sulphides. *Electrochimica Acta*, 55(19), pp.5470-5477.

Peng, Y., Grano, S., 2010c. Effect of iron contamination from grinding media on the flotation of sulphide minerals of different particle size. *International Journal of Mineral Processing*, 97(1-4), pp.1-6.

Pribil, R., 1972. *Analytical applications of EDTA and related compounds*. 1st ed. New York: Oxford Pergamon Press Inc, pp.4-8.

Quinn T.F.J., 1991. Physical Analysis for Tribology. Cambridge, U.K.: Cambridge University Press.

Rahman, R., Ata, S. and Jameson, G., 2012. The effect of flotation variables on the recovery of different particle size fractions in the froth and the pulp. *International Journal of Mineral Processing*, 106-109, pp.70-77.

Rao, S.R., Moon, K.S., Leja, J., 1976. Effect of grinding media on the surface reactions and flotation of heavy metal sulphides. In: Fuerstenau, M.C. (Ed.), Flotation, A.M. Gaudin Memorial Volume. *SME-AIME, New York,* pp. 509– 527.

Richardson, S., & Vaughan, D. J. 1989. Surface alteration of pentlandite and spectroscopic evidence for secondary violarite formation. *Mineralogical Magazine,* 53(370), 213–222. doi:10.1180/minmag.1989.053.370.08

Rumball, J. A., & Richmond, G. D. 1996. Measurement of Oxidation in a Base Metal Flotation Circuit by Selective Leaching with EDTA . *Int. J. Miner. Process*, 1-20.

Senior, G. D., & Trahar, W. J., 1991. The influence of metal hydroxides and collector on the flotation of chalcopyrite. *International Journal of Mineral Processing, 33(1-4), 321–341*. doi:10.1016/0301-7516(91)90061-m

Shamsuddin, M., Ngoc, N. V. and Prasad, P. M. 1990. Sulphation roasting of an off-grade copper concentrate, *Met. Mater. Process*. **1**, pp 275–292.

Shengo, L. M., Gaydardzhiev, S., & Kalenga, N. M., 2016. Malachite and Heterogenite Behavior During the Locked-Cycle Recycling of Process Water in Flotation of Copper-Cobalt Oxide Ores. *International Journal of Mineral Processing*, 152-162.

Smart, R. S. 1991. Surface Layers in Base Metal Sulphide Flotation. *Minerals Engineering*, 891-909.

Smart, R.S.C., Skinner, W.M., Gerson, A.R., Mielezarcsky, J., Chryssoulis, S., Pratt, A.R., Lastra, R., Hope, G.A., Wang, X.F.A.K., Miller, J.D., 2007., Surface Characterization and New Tools for Research. Flotation: A Century of Innovation, SME, Littleton, CO, pp. 283–338.

Steger,H.F. 1982. Oxidation of sulfide minerals: VII. Effect of temperature and relative humidity on the oxidation of pyrrhotite, *Chemical Geology*, Volume 35, Issues 3–4. Pages 281-295, ISSN 0009-2541

Sutherland. K.L., Wark, I.W. 1955. Principles of flotation, *Australian IMM*.

Taggart, A.F., Taylor, T.C., Knoll, A.F., 1930. Chemical reactions in flotation. *AIME Tech. Publ*. 312, 3-33.

Teger, H., 1977. Oxidation of sulphide minerals—III determination of sulphate and thiosulphate in oxidised sulphide minerals*. Talanta, 24(11), 675–679.* doi:10.1016/0039-9140(77)80064-7

Tolley W., Kotlyar, D., R. 1996. Van Wagoner Fundamental electrochemical studies of sulfide mineral flotation. *Minerals Engineering*, 9, pp. 603-637

Trahar, W.J., 1981. A rational interpretation of the role of particle size in flotation*. 8(4), 289–327.* doi:10.1016/0301-7516(81)90019-3

Van der Westhuizen, A.P., Deglon, D.A., 2007. Evaluation of solids suspension in a pilot-scale mechanical flotation cell: the critical impeller speed. *Minerals Engineering* 20 (3), 233–240

Wang, C., Sun, C. and Liu, Q., 2020. Entrainment of Gangue Minerals in Froth Flotation: Mechanisms, Models, Controlling Factors, and Abatement Techniques—a Review. *Mining, Metallurgy & Exploration*, 38(2), pp.673-692.

Wang, L., Peng, Y. and Runge, K., 2016. Entrainment in froth flotation: The degree of entrainment and its contributing factors. *Powder Technology*, 288, pp.202-211.

Wang, H., A. Pring, Y. Xie, Y. Ngothai and B. O'Neill: *Thermochim. Acta*., 2005, vol. 427, pp. 13–25.

Welsby, S.D.D., Vianna, S.M.S.M., Franzidis, J.-P., 2010a. Assigning physical significance to floatability components. International Journal of Mineral Processing 97, 59–67

Wills, B. A., 2006. Froth Flotation. In: T. Napier-Munn, ed. *Will's Mineral Processing Technology.* 7th ed. Oxford: Elsevier Ltd, pp. 267-352.

Winchell, A.N; Mineral Oxidation. *American Mineralogist* 1946;; 31 (5-6): 288–293. doi:

Winland, RL., Traina, SJ., JM Bigham Chemical composition of ochreous precipitates from Ohio coal mine drainage J Environ Qual, 20 (1991), pp. 452-460

Woods, R., 1987. Flotation of sulfide minerals. In: P. Somasundaran and B.M. Moudgil (Editors), Reagents in Mineral Technology. *Marcel Dekker, New York*, NY, pp. 39-78.

Young, D., n.d. High-Temperature Oxidation and Corrosion of Metals.

Zaklina Konopacka; Jan Drzymala. 2010. Types of particles recovery—water recovery entrainment plots useful in flotation research. *16(4-5), 313–320.* doi:10.1007/s10450-010-9246-x

Zhao, S. and Peng, Y., 2012. The oxidation of copper sulfide minerals during grinding and their interactions with clay particles. *Powder Technology*, 230, pp.112-117.

Zhang, Y H., Kawatra. 2020. Effects of Grinding Media on Grinding Products and Flotation Performance of Sulfide Ores, *Mineral Processing and Extractive Metallurgy Review*, DOI: 10.1080/08827508.2019.1692831

Zhu, H., Chen, J., Deng, J., Yu, R. and Xing, X., 2012. Oxidation Behavior and Mechanism of Pentlandite at 973 K (700 °C) in Air. *Metallurgical and Materials Transactions B*, 43(3), pp.494-502.

Appendix A: EDTA and RN data

EDTA vs Cu Recovery for UG2 Impala (Top) and Kansanshi (Bottom)

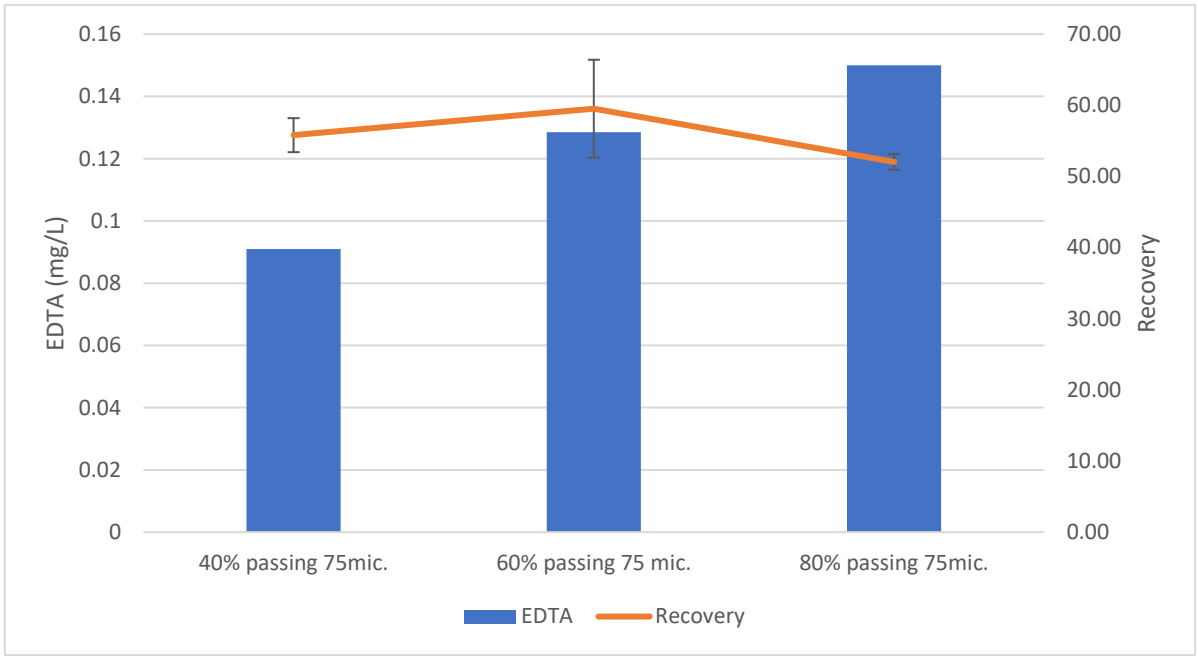

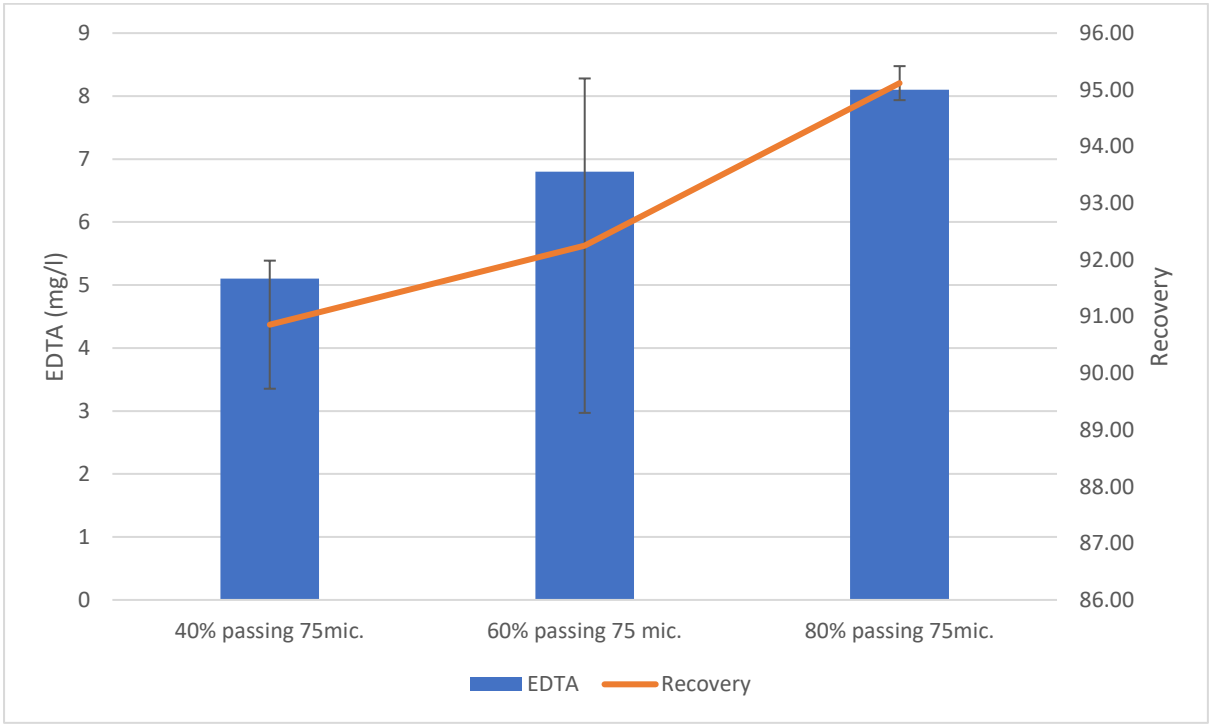

RN vs Cu Recovery for UG2 Impala (Top) and Kansanshi (Bottom)

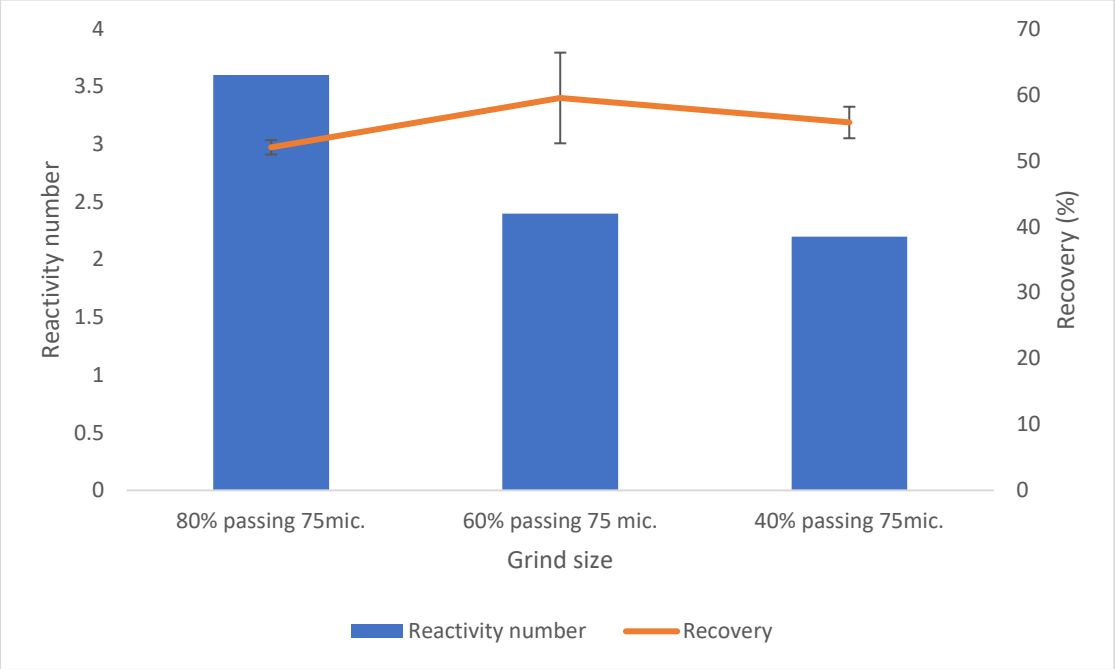

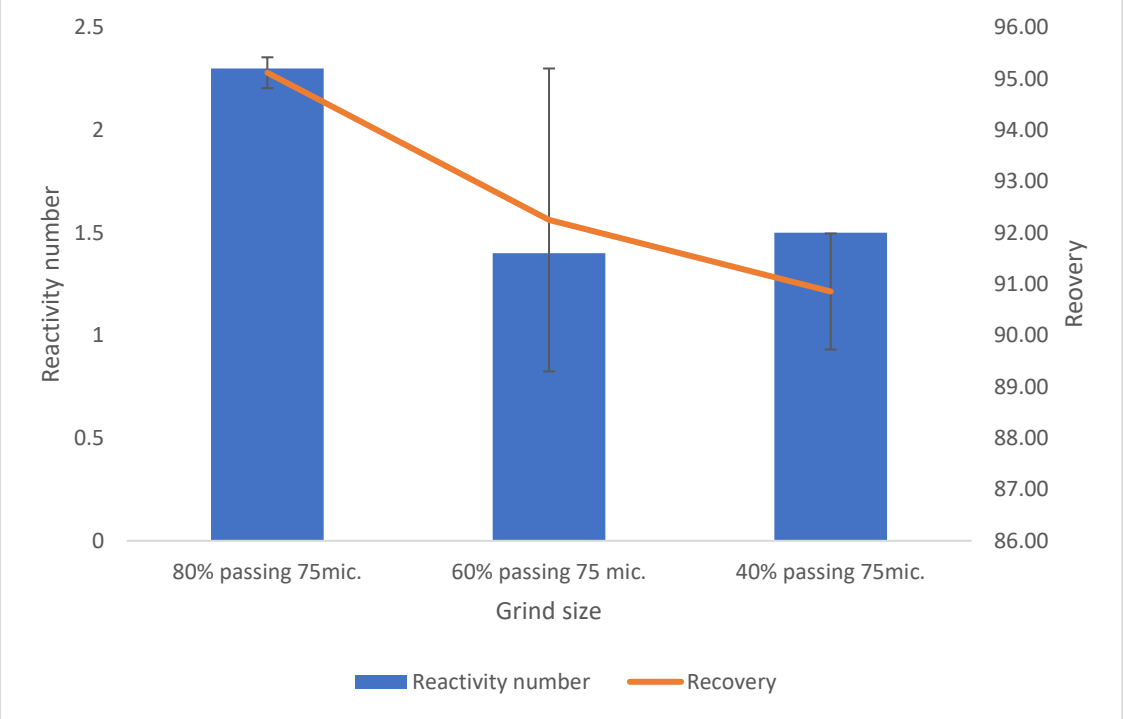

EDTA vs Solids for UG2 Impala (Top) and Kansanshi (Bottom)

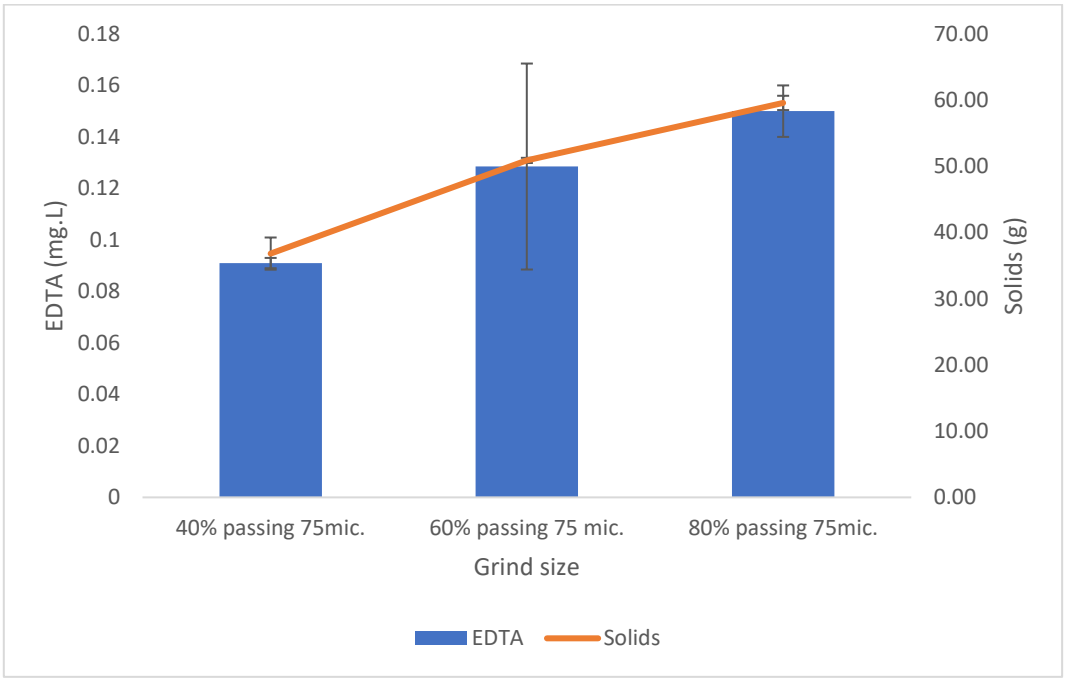

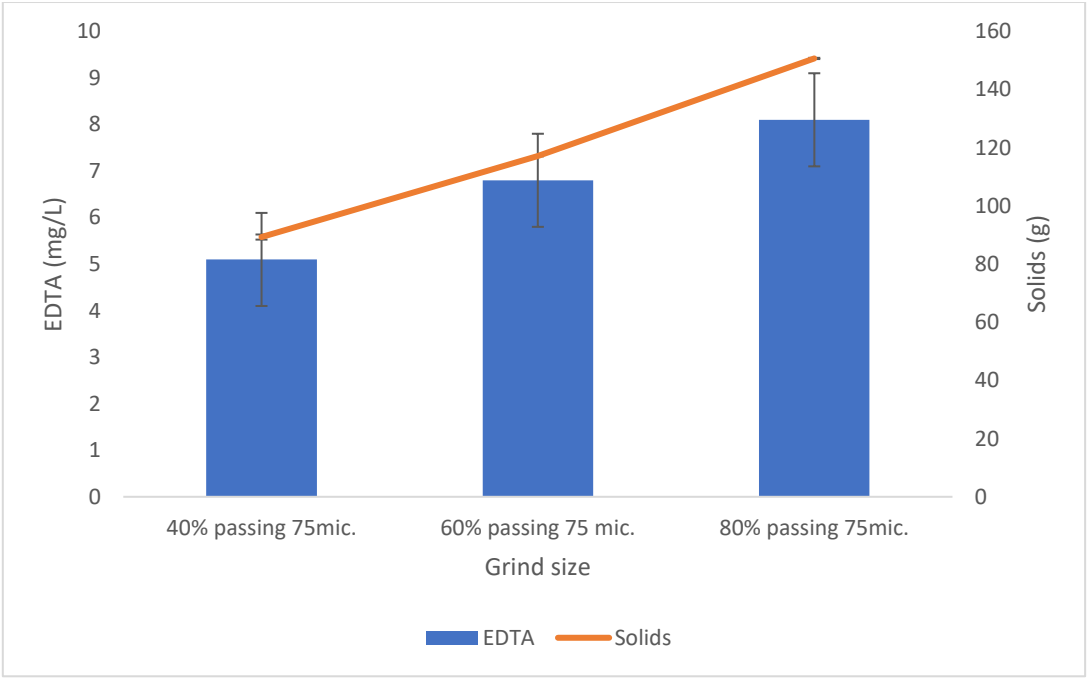

EDTA vs Grade for UG2 Impala (Top) and Kansanshi (Bottom)

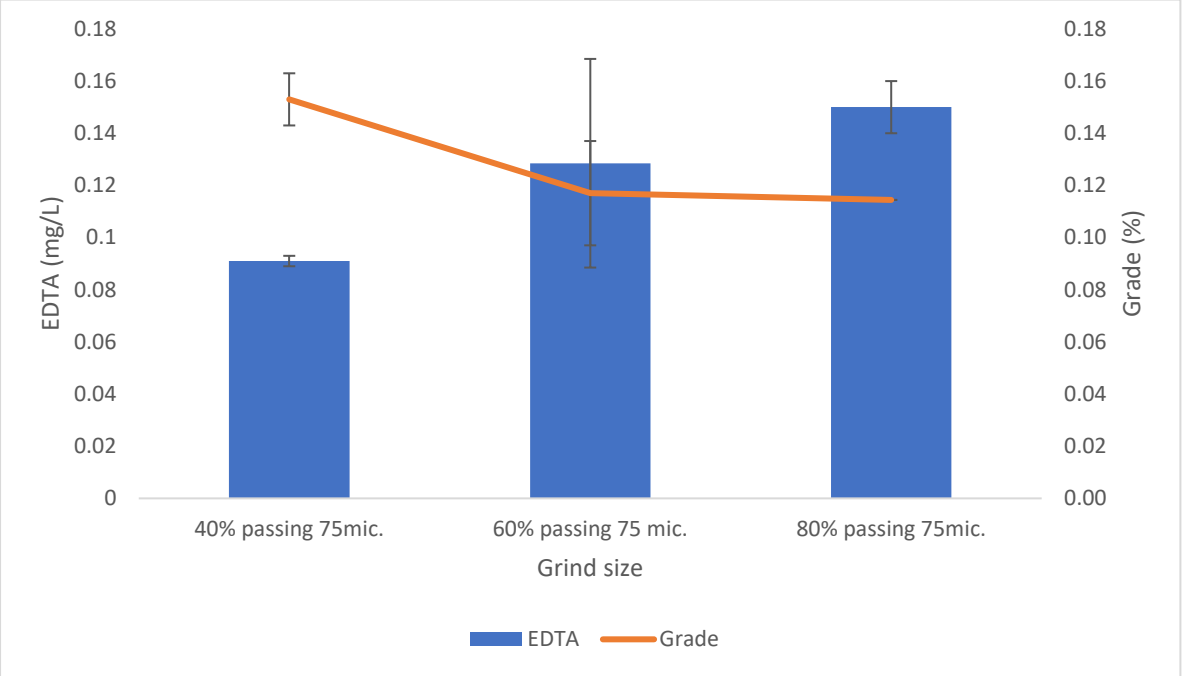

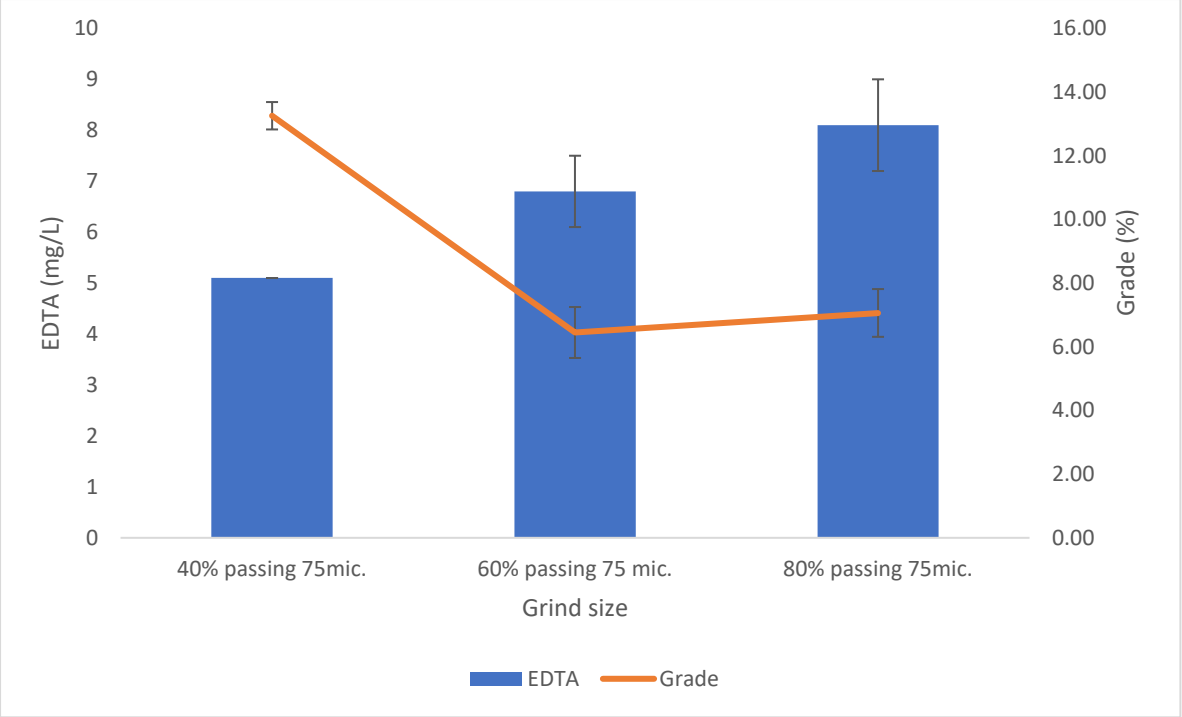

RN vs Grade for UG2 Impala (Top) and Kansanshi (Bottom)

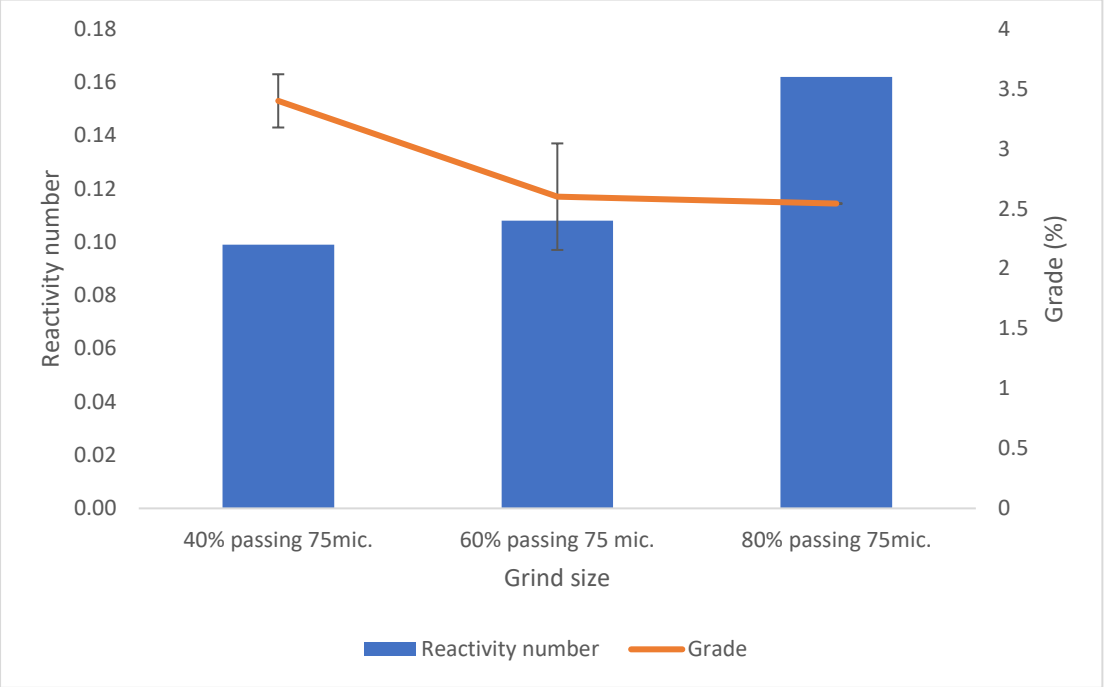

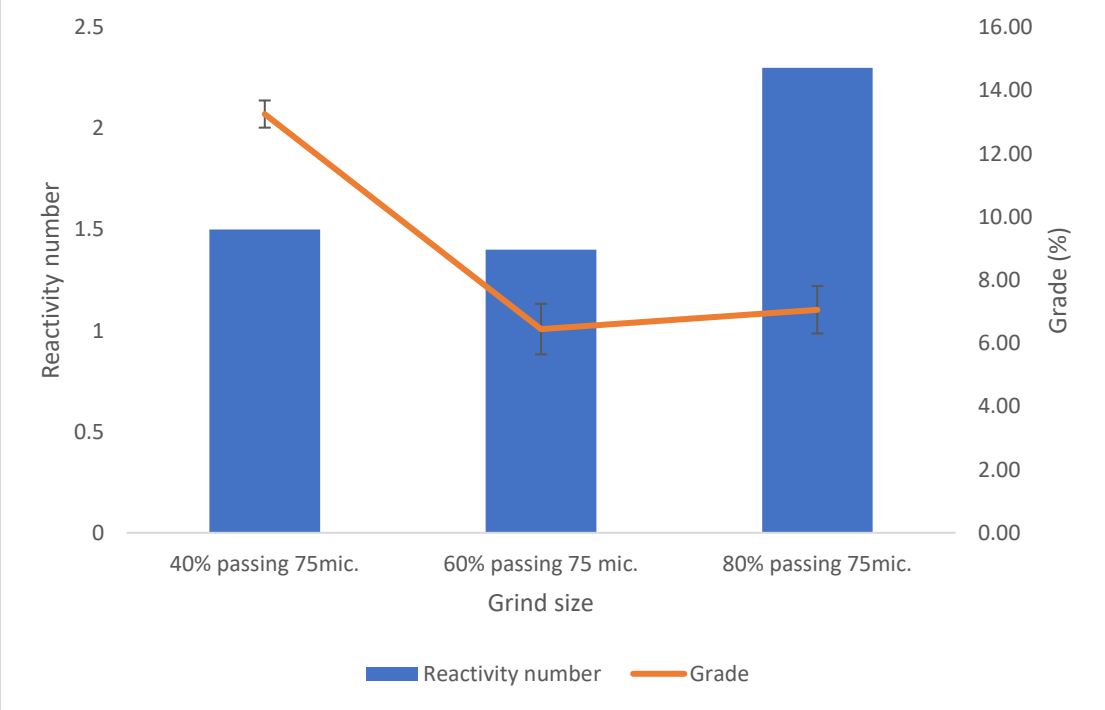

Appendix B: Bulk Minerology (Ore characterisation)

Mineral contents (wt.% in fraction) - BMS ungrouped								
Mineral	**Kansanshi Feed**				**UG2 Feed**			
	Combined	**+53**	**+25**	**-25**	**Combined**	**+53**	**+25**	**-25**
Total Mass	99,97	43,26	22,45	34,26	100,00	46,41	18,10	35,49
Pyrite	1,79	2,65	1,37	0,99	0,02	0,01	0,03	0,03
Chalcopyrite	3,90	5,46	2,53	2,82	0,03	0,00	0,02	0,06
Pyrrhotite	0,54	0,73	0,53	0,32	0,03	0,00	0,05	0,05
Pentandite	0,00	0,00	0,00	0,00	0,03	0,00	0,03	0,06
Other sulfides	0,22	0,19	0,17	0,30	0,18	0,11	0,13	0,32
Quartz	27,33	36,81	25,77	16,41	1,62	1,29	2,11	1,81
K-feldspar	1,40	1,45	0,74	1,77	0,34	0,27	0,37	0,40
Plagioclase	35,15	29,66	46,70	34,53	17,08	16,56	18,33	17,12
Orthopyroxene	0,10	0,11	0,06	0,11	34,75	38,89	33,84	29,81
Clinopyroxene	0,01	0,00	0,00	0,01	4,31	3,96	4,62	4,62
Amphibole	0,07	0,04	0,02	0,15	2,17	1,69	1,74	3,04
Serpentine	0,00	0,00	0,00	0,00	0,67	0,71	0,55	0,68
Talc	0,02	0,02	0,01	0,02	2,60	1,44	1,70	4,58
Chlorite	1,60	1,75	1,43	1,54	2,76	1,37	2,43	4,76
Mica	21,84	14,09	15,70	35,65	0,51	0,43	0,43	0,64
Calcite	2,61	3,36	2,46	1,77	0,19	0,16	0,13	0,26
Chromite	0,20	0,01	0,09	0,52	30,71	31,62	31,86	28,93
Other Fe-Ti oxides	3,05	3,54	2,32	2,92	1,98	1,49	1,64	2,80
Others	0,13	0,12	0,10	0,16	0,01	0,00	0,01	0,02

Mineral	Kansanshi Tails				UG2 Tails			
	Combined	+53	+25	-25	Combined	+53	+25	-25
Total Mass	100	45,93	23,09	30,98	100,00	66,01	15,10	18,89
Pyrite	0,37	0,44	0,28	0,32	0,01	0,00	0,01	0,01
Chalcopyrite	0,86	1,01	0,63	0,80	0,01	0,01	0,00	0,02
Pyrrhotite	0,37	0,58	0,31	0,11	0,01	0,00	0,02	0,03
Pentlandite	0,00	0,00	0,00	0,00	0,01	0,01	0,00	0,03
Other sulfides	0,12	0,16	0,07	0,10	0,11	0,09	0,11	0,15
Quartz	29,01	39,74	26,40	15,03	1,72	1,66	1,99	1,69
K-feldspar	1,48	1,77	0,69	1,63	0,27	0,22	0,31	0,42
Plagioclase	37,28	32,49	48,44	36,05	17,11	16,62	18,52	17,70
Orthopyroxene	0,10	0,12	0,06	0,10	35,59	38,67	32,99	26,93
Clinopyroxene	0,01	0,01	0,00	0,01	4,48	4,33	4,68	4,82
Amphibole	0,07	0,04	0,03	0,15	1,87	1,57	1,60	3,16
Serpentine	0,00	0,00	0,00	0,00	0,63	0,69	0,46	0,58
Talc	0,02	0,02	0,01	0,02	1,85	1,34	1,68	3,78
Chlorite	1,59	1,47	1,61	1,75	2,02	1,39	1,90	4,31
Mica	22,10	14,51	16,03	37,86	0,44	0,39	0,43	0,66
Calcite	3,06	3,85	2,64	2,20	0,15	0,11	0,17	0,30
Chromite	0,20	0,07	0,10	0,48	31,77	31,12	33,50	32,66
Other Fe-Ti oxides	3,24	3,54	2,66	3,21	1,93	1,77	1,63	2,73
Others	0,15	0,17	0,04	0,18	0,01	0,01	0,01	0,01

Liberation Data

Ore			% Passing	Liberated	HG Middling	LG Middling	Locked	% Unliberated
Feed	Kansanshi	40	+53	87,33	7,86	3,02	1,80	12,67
			+25	90,03	5,91	2,98	1,08	9,97
			-25	77,59	16,41	4,41	1,58	22,41
		60	+53	87,48	7,69	3,18	1,65	12,52
			+25	89,08	6,74	3,19	0,99	10,92
			-25	75,05	18,07	4,98	1,89	24,95
		80	+53	86,62	8,75	2,92	1,71	13,38
			+25	92,13	5,24	1,97	0,67	7,87
			-25	77,49	16,87	4,09	1,54	22,51
	UG2	40	+53	41,17	14,96	13,79	30,07	58,83
			+25	59,22	18,41	6,52	15,84	40,78
			-25	58,17	22,18	9,33	10,33	41,83
		60	+53	41,76	9,23	6,36	42,65	58,24
			+25	60,07	13,51	8,02	18,40	39,93
			-25	58,14	22,01	9,31	10,55	41,86
		80	+53	58,86	10,29	6,24	24,60	41,14
			+25	61,46	13,96	5,56	19,02	38,54
			-25	59,59	22,70	8,98	8,73	40,41

Mineral Association (Kansanshi HG)

BMS associations (%)	40% Pass			60% Pass			80% Pass		
	+53	+25	-25	+53	+25	-25	+53	+25	-25
Background	88,24	93,75	89,85	90,74	94,50	89,55	93,76	95,18	90,75
BMS	0,00	0,00	0,00	0,00	0,00	0,00	0,00	0,00	0,00
Quartz	2,48	2,50	6,07	2,19	2,38	6,29	1,29	1,90	5,73
K-feldspar	0,51	0,17	0,18	0,42	0,22	0,19	0,29	0,15	0,15
Plagioclase	1,43	0,47	0,35	0,60	0,33	0,32	0,36	0,27	0,27
Orthopyroxene	0,02	0,01	0,00	0,01	0,01	0,00	0,00	0,00	0,00
Clinopyroxene	0,00	0,00	0,00	0,00	0,00	0,00	0,00	0,00	0,00
Amphibole	0,00	0,01	0,03	0,01	0,00	0,04	0,00	0,00	0,03
Serpentine	0,00	0,00	0,00	0,00	0,00	0,00	0,00	0,00	0,00
Talc	0,01	0,00	0,00	0,00	0,00	0,00	0,00	0,00	0,00
Chlorite	0,49	0,14	0,18	0,17	0,12	0,18	0,08	0,08	0,13
Mica	3,40	1,24	2,50	2,53	0,95	2,60	1,82	0,89	2,18
Calcite	0,24	0,10	0,04	0,23	0,10	0,07	0,08	0,09	0,05
Chromite	0,01	0,04	0,07	0,05	0,04	0,18	0,03	0,06	0,18
Other Fe-Ti oxides	2,85	1,27	0,47	2,71	1,11	0,39	2,02	1,12	0,37
Others	0,33	0,29	0,24	0,34	0,25	0,19	0,26	0,25	0,16
Total - background	11,77	6,24	10,13	9,26	5,51	10,45	6,23	4,81	9,25
Total unlib.	12,67	9,97	22,41	12,52	10,92	24,95	13,38	7,87	22,51

Mineral Association (UG2 Impala)

BMS associations (%)	40% Pass			60% Pass			80% Pass		
	+53	+25	-25	+53	+25	-25	+53	+25	-25
Background	43,84	63,26	79,21	37,45	61,35	79,16	49,33	62,69	81,72
BMS	0,00	0,00	0,00	0,00	0,00	0,00	0,00	0,00	0,00
Quartz	7,60	2,78	3,29	4,08	3,63	3,27	2,78	3,64	2,26
K-feldspar	0,35	0,15	0,07	0,51	0,16	0,07	0,27	0,29	0,07
Plagioclase	4,09	2,16	0,66	7,54	2,61	0,59	4,18	3,04	0,47
Orthopyroxene	11,24	6,31	2,75	16,62	8,88	3,02	13,52	7,98	2,69
Clinopyroxene	1,09	0,64	0,15	2,56	0,72	0,19	1,26	0,65	0,18
Amphibole	1,63	0,90	0,80	1,94	1,05	0,74	1,94	0,84	0,66
Serpentine	3,99	0,94	0,17	3,76	1,03	0,14	4,52	1,28	0,10
Talc	1,33	1,33	1,53	2,03	1,52	1,15	2,04	0,74	1,33
Chlorite	2,59	1,47	0,94	2,32	1,40	0,86	1,03	1,47	0,52
Mica	0,52	0,22	0,08	0,15	0,32	0,09	0,14	0,22	0,04
Calcite	0,26	0,27	0,05	0,40	0,11	0,09	0,32	0,14	0,06
Chromite	6,27	6,29	4,85	7,88	6,59	5,99	8,38	7,60	5,18
Other Fe-Ti oxides	5,99	3,92	3,73	4,63	5,57	3,29	4,28	4,20	3,62
Others	9,21	9,35	1,71	8,13	5,08	1,37	6,03	5,22	1,11
Total - background	56,16	36,73	20,78	62,55	38,67	20,86	50,69	37,31	18,29
Total unlib.	58,83	40,78	41,83	58,24	39,93	41,86	41,14	38,54	40,41

Appendix C: Flotation Data

Rep	C1	C2	C3	C4	FEED	TAILS	TAILS2	TAILS3
C + PAPER	70,27	41,02	32,05	30,10	22,29	815,50	19,94	19,68
PAPER	4,71	4,81	4,78	4,64	4,38	18,40	4,88	4,68
CONC.	65,56	36,21	27,27	25,46	17,91	797,10	15,06	15,00
B + H2O	570,44	575,93	572,81	576,44				
BOTTLE	432,99	220,09	123,22	80,89				
H20	137,45	355,84	449,59	495,55				
D + C + H20	739,87	921,15	980,17	1042,04				
DISH	392,54	369,39	369,20	366,39				
C + H20	347,33	551,76	610,97	675,65				
H20 REC.	144,32	159,71	134,11	154,64				

Kansanshi 80% passing 75 mic.	C1	C2	C3	C4	FEED	TAILS	TAILS2	TAILS3
C + PAPER	70,27	41,02	32,05	30,10	22,29	815,50	19,94	19,68
PAPER	4,71	4,81	4,78	4,64	4,38	18,40	4,88	4,68
CONC.	65,56	36,21	27,27	25,46	17,91	797,10	15,06	15,00
B + H2O	570,44	575,93	572,81	576,44				
BOTTLE	432,99	220,09	123,22	80,89				
H20	137,45	355,84	449,59	495,55				
D + C + H20	739,87	921,15	980,17	1042,04				
DISH	392,54	369,39	369,20	366,39				
C + H20	347,33	551,76	610,97	675,65				
H20 REC.	144,32	159,71	134,11	154,64				

Rep	C1	C2	C3	C4	FEED	TAILS	TAILS2	TAILS3
C + PAPER	48,88	35,71	32,57	24,23	22,13	823,63	20,11	20,03
PAPER	5,32	4,95	5,26	5,22	5,10	15,06	4,80	5,06
CONC.	43,56	30,76	27,31	19,01	17,03	808,57	15,31	14,97
B + H2O	569,91	576,37	572,19	576,83				
BOTTLE	331,49	246,54	148,16	77,17				
H20	238,42	329,83	424,03	499,66				
D + C + H20	717,27	840,56	982,41	1028,11				
DISH	392,54	369,39	369,20	366,39				
C + H20	324,73	471,17	613,21	661,72				
H20 REC.	42,75	110,58	161,87	143,05				

40% P	C1	C2	C3	C4	FEED	TAILS	TAILS2	TAILS3
C + PAPER	49,32	20,47	20,78	17,82	14,82	879,48	16,09	16,89
PAPER	4,24	4,53	4,49	4,35	4,23	17,23	4,24	4,90
CONC.	45,08	15,94	16,29	13,47	10,59	862,25	11,85	11,99
B + H2O	570,65	576,23	572,22	577,17				
BOTTLE	419,18	259,52	127,74	81,38				
H20	151,47	316,71	444,48	495,79				
D + C + H20	645,95	780,55	900,08	1011,89				
DISH	392,54	369,39	369,20	360,51				
C + H20	253,41	411,16	530,88	651,38				
H20 REC.	56,86	78,51	70,11	142,12				

UG2 80% passing 75 mic	C1	C2	C3	C4	FEED	TAILS	TAILS2	TAILS3
C + PAPER	26,45	15,63	17,15	13,49	21,50	949,72	23,33	22,89
PAPER	3,51	3,06	3,08	3,10	2,98	16,46	3,13	3,00
CONC.	22,94	12,57	14,07	10,39	18,52	933,26	20,20	19,89
B + H2O	569,92	575,19	576,23	574,63				
BOTTLE	485,92	330,04	164,69	90,88				
H20	84,00	245,15	411,54	483,75				
D + C + H20	639,19	720,79	935,85	957,44				
DISH	392,54	369,39	396,20	366,39				
C + H20	246,65	351,40	539,65	591,05				
H20 REC.	139,71	93,68	114,04	96,91				

UG2 60% Passing	C1	C2	C3	C4	FEED	TAILS	TAILS2	TAILS3
C + PAPER	25,22	15,37	14,00	11,40	25,54	842,66	27,19	22,85
PAPER	3,88	3,74	4,08	3,06	4,29	15,63	3,27	4,38
CONC.	21,34	11,63	9,92	8,34	21,25	827,03	23,92	18,47
B + H2O	568,76	573,28	574,17	575,46				
BOTTLE	465,89	325,81	154,10	88,18				
H20	102,87	247,47	420,07	487,28				
D + C + H20	632,99	719,61	887,68	952,96				
DISH	392,54	369,39	369,20	366,39				
C + H20	240,45	350,22	518,48	586,57				
H20 REC.	116,24	91,12	88,49	90,95				

UG2 40% passing	C1	C2	C3	C4	FEED	TAILS	TAILS2	TAILS3
C + PAPER	14,00	13,08	12,17	11,35	28,12	821,00	19,65	24,13
PAPER	3,45	3,55	3,18	3,24	3,45	15,78	3,03	3,23
CONC.	10,55	9,53	8,99	8,11	24,67	805,22	16,62	20,90
B + H2O	570,20	574,93	573,83	576,41				
BOTTLE	469,10	340,03	210,99	87,28				
H20	101,10	234,90	362,84	489,13				
D + C + H20	562,73	699,81	841,45	971,57				
DISH	392,54	366,39	369,20	366,39				
C + H20	170,19	333,42	472,25	605,18				
H20 REC.	58,54	88,99	100,42	107,94				